INTER-REGIONAL WMO SEMINAR ON THE INTERPRETATION AND USE OF METEOROLOGICAL SATELLITE DATA

November 27 to December 8, 1964

MESOMETEOROLOGICAL INTERPRETATION OF SATELLITE DATA

Text for Sessions N through Q

by

Tetsuya Fujita

Satellite and Mesometeorology Research Project (SMRP)
Department of the Geophysical Sciences
The University of Chicago
Chicago 37, Illinois, U. S. A.

Tokyo, Japan

SESSIONS N through Q

MESOMETEOROLOGICAL INTERPRETATION OF SATELLITE DATA

by Tetsuya Fujita
The University of Chicago

INTRODUCTION

Since cloud photographs taken by the earth-orbiting satellites became available to our meteorological communities, they have been efficiently used in learning more about our atmosphere. Due to the fact that the resolution of these photographs is much higher than that of cloud patterns constructed by using the existing synoptic reports, we often find very clearly in satellite photographs various nephsystems which previously have not been known to us. It is also true that some clouds located between stations may remain unobserved until they either grow or drift toward the stations.

Horizontal scales of meteorological systems ranging between a few to a few hundred kilometers are called "mesoscale". This scale has been emphasized during recent years since it is the scale applicable to the cloud patterns seen frequently in satellite photographs.

The purpose of these sessions is first to present satellite photographs which include mesoscale cloud systems and then to interpret the cloud systems with the aid of synoptic, aerological, and radar data usually available to forecasters. During these sessions, photographs and charts will be distributed in sequence. Some are printed on translucent sheets to allow direct superimposition on each other. All charts are identified with the session letter (capital letter), the topic letter (small letter), and the chart number. Nb 3, for instance, designates Session N, topic b, and chart number 3.

Selected topics are:

1. Mesoscale convection associated with a typhoon (Na)
2. Mesoscale features of the typhoon cirrus shield (Nb)
3. Convection over Japan in summer (Oa)
4. Tropical land convection over the Philippines (Ob)
5. North Pacific fog (P)
6. Formation of clouds over the Sea of Japan (Qa)
7. Influence of the Japanese Islands upon the winter monsoon clouds (Qb)

Each session will start with a brief introduction regarding the nature of the subjects to be discussed in the session. Participants will then follow the steps of laboratory work until these subjects are fully interpreted. Questions will be entertained at any time during the sessions.

SESSION N

MESOSCALE TYPHOON STRUCT

Topic a

Mesoscale Convection Associated with a Typhoon (Na)

By Tetsuya Fujita, The University of Chicago

Gridding by Say-Yuo Gargard, The University of Chicago and PAA Meteorological Service, Liberia

Meteorological systems discussed herein are (1) the orographic precipitation areas on the windward side of mountains in the outer region of a typhoon and (2) convective clouds along a warm front accompanied by the storm.

Three pictures (Na 1) from TIROS VII Orbit 721 represent clouds over central Honshu, Japan, clouds along a warm front south of Japan, and a view of Typhoon Bess of August 7, 1963. One-degree geographic grid lines are drawn on each picture to permit determination of cloud positions and horizontal dimensions.

A cloud transfer chart (Na 2) has been prepared for use in transferring selected clouds from gridded pictures in Na 1. Participants are asked to make a rough sketch of the orographic clouds over the Tohoku, Kanto, Chubu, and Kinki districts, referring also to the index map which includes geographic regions, topography, and station numbers. It will be found that the mountains above 1000 m are mostly covered with orographic clouds. Areas of overcast cloud cover extend eastward from the mountain ranges which block fresh moisture inflow from the east. To save time in completing the time-consuming transfer, a cloud chart (Na 3) is used.

By superimposing this chart on the cloud transfer chart (Na 2), it will be found that the extensive overcast areas in Kinki cover the land areas east of the central mountains. The surface map (Na 4) reveals that these orographic clouds are mostly towering cumuli with their cloud bases at about 800 m. The western side of the central mountains in Kinki is clear, for the most part, with a few scattered clouds, according to the satellite picture (Na 1). Synoptic reports from Osaka (772), Kyoto (759), and Wakayama (777) reveal that they are cumuli to towering cumuli with their bases at 1200 m, much higher than those on the windward side.

A similar situation dominates the Chubu and Kanto districts. It should be noted that the eastern edge of the extended overcast areas over the Kanto and southeastern Chubu districts is well-defined, forming a long arc extending over 400 km. In central Chubu and Hokuriku where midday convection is taking place, cloud bases are generally high due to low relative humidity on the surface. Even though the synoptic stations located on the valley floor report only one- or two-tenths of cumulus cover, satellite pictures indicate extensive cloud cover over the mountains, thus demonstrating the representativeness of the data from each reported station.

Mt. Fuji (3776 m), the highest mountain in Honshu, is located near the central fiducial mark " + " on frame 18 exposed at 0430.6Z (1330.6 Local Time). Even though the photograph shows overcast in that area, the mountain-top station reported about one-eighth towering cumuli. The peak is evidently above the top of the undercast cloud cover.

Isobaric analysis (Na 5) of the surface map (Na 4) leads us to investigate the phenomena of the pressure drop along the western edges of the extended cloud cover over eastern Tohoku, Kanto, southeastern Chubu, and eastern Kinki districts. There is cloud dissipation along these western edges due to a small scale so-called Föhn phenomenon. This results in dynamical and thermodynamical warming which reduces the hydrostatic pressure at the surface over the clear areas just west of these western edges.

Two lines of the hook-shaped clouds seen along the surface warm front in the isobar chart (Na 5) are rather peculiar in shape. Radar echoes (Na 6) of these clouds south of Kinki are small but solid, suggesting that the clouds are convective in nature. We can count about 20 such clouds very similar in shape; i.e., each of them has a very small hook on its western end. The main body of the cloud is very bright and is accompanied by something like cirrus streamers extending eastward.

The shape of these clouds resembles to a great degree radar pictures of a thunderstorm with a hook. It may be postulated that there exists a zone of large cyclonic vorticity and convergence along the surface warm front analyzed on the surface isobar chart (Na 5). As in the case of tornado cyclones or hook-echo circulations, a rapid stretch along the vertical would concentrate the low-level vorticity into a small area aloft.

Comparison of the cloud chart (Na 3) and the radar echoes (Na 6) permits us to locate convective clouds in the northwest sector of the typhoon near the leading edge of the outflowing cirrus. It is of interest to see that the leading edge extending from Okinawa to the western end of the warm front is characterized by intense echoes most of which are circular cells.

Seen on Frame 23 (Na 1) and the cloud chart (Na 3) are a large number of faint cirrus streamers extending in the direction of the radials of the typhoon. The outer end of each streamer is bent anticyclonically, forming a gentle hook. This feature will be discussed in the succeeding topic, Nb.

Conclusions:

The areas of orographic cloudiness and possible precipitation in the outer region of a typhoon can be identified if there are no cirrus shields extending from the storm center. Tornadoes are frequently observed associated with typhoons and hurricanes. A large number of convective clouds with rotational characteristics can also be identified outside the cirrus shield. The positions of these clouds coincide with the shear zones accompanied by the main storm.

SESSION N

MESOSCALE TYPHOON STRUCTURE

Topic b

Mesoscale Features of the Typhoon Cirrus Shield (Nb)

by Tetsuya Fujita, the University of Chicago

Gridding by James E. Arnold, the University of Chicago

Meteorological systems discussed herein are (1) the vertical structure of outflow from a typhoon, (2) spiral streaks of cirrus outflow, and (3) fine streaks associated with the wind field above the typhoon top.

A cloud photograph (Nb 1) from TIROS VII Orbit 736 was used in making a cloud chart (Nb 2) which fits to the projection and the scale of other synoptic charts used in this session.

In order to study the three-dimensional structure of the storm, upper-air charts for 0000Z, August 8, 1963 were analyzed. The satellite picture (Nb 1) was taken 4 hours and 50 mintues later.

The central pressure of the storm (Typhoon Bess) with her center at 29N 133E was 950 mb. The surface chart (Nb 3) shows that western Japan was under the influence of the easterly winds in the preceeding sector of the typhoon moving north-northwest. There is a warm front to the south of Kanto, but the cloud pattern associated with this front is not visible in the picture due to large nadir angles of view.

Using radar pictures from Naze (909), Tanegashima (837), and Muroto (899), a composite radar echo chart (Nb 4) was constructed. The times of the radar pictures and the cloud chart (Nb 2) differ by only a few minutes so that we may assume that they represent simultaneous observations. Due mainly to the height of the radar beams which overcut the cloud tops, the rainbands near the typhoon center do not appear on radar. In most areas of radar coverage, the echo and the cloud patterns fit extremely well.

The expansion rate of the cirrus shield is obtained by transferring the leading edges of the cirrus shield in two cloud charts (Na 3 and Nb 2) onto the movement of cirrus shield chart (Nb 5). The leading edges of the shield for 1200 and 1800Z, August 7, and 0000Z, August 8 are interpolated in order to determine their positions at these map times and to visualize the movement of the cirrus shield.

When the cloud chart is examined carefully, it will be found that there are several streaks of cirrostratus clouds oriented in the direction of the logarithmic spiral lines similar to those of the rainbands. These streaks are entered on a thickness and shear chart (Nb 6) for 0000Z, August 8 in an attempt to find the directions of the geostrophic wind shear and the streaks. It is seen that the cirrostratus streaks cross the thickness contours at an angle of about 20 degrees. When a geostrophic component of the outflow is taken into consideration, we may postulate that these streaks represent outflows from the tops of the groups of cloud towers inside the typhoon.

To discuss further the distribution of winds along the vertical, cross-sections of the temperature anomaly (Nb 7) and the height anomaly (Nb 8) from Kagoshima (827) were made. Bold letters and italics respectively denote positive and negative anomalies from the mean values for the month of August 1963. By contouring these values, it is seen that the greatest temperature anomaly is at about 300 mb occurring on August 9. The lowest height anomaly, -202 m, is capped by the bulge of the height contour at about the 125-mb surface.

The wind aloft from Kagoshima (Nb 9) reflects this height pattern very well. In order to convert time changes into space changes, the wind directions are rotated clockwise by 90 degrees; that is, the winds are plotted after adding 90 degrees to their measured values. The dashed lines with arrows on the 1000-mb surface represent the direction of the typhoon center from Kagoshima at each observation time. This direction is also rotated by 90 degrees. Now we examine the winds aloft at Kagoshima by using the cross-section chart (Nb 9), the 300-mb chart (Nb 10), and the 200-mb chart (Nb 12). The abrupt change in winds from almost east to west between these pressure surfaces is not an error. Their time changes are clearly seen in the cross-section chart (Nb 9). The easterly winds are part of the outflow as analyzed on the 300-mb chart (Nb 10). The westerlies which extend up to about the 125-mb height represent the flow south of the trough line running between Korea and Kyushu.

If a hydrometeor from the storm is carried along the arrow starting from point 1 at or above the 200-mb surface (Nb 11), it must descend below this surface upon reaching point 2. The path between 2 and 3 is topped by the westerlies. Somehow the hydrometeor reaches point 3 on the leading edge of the cirrus shield indicated by the 'dash-and-two-dots' line. At this point, the hydrometeor is carried back toward the storm by the westerly winds above the outflowing cirrus shield. A tiny hook near the west end of each cirrus streak probably indicates the trajectory when the motion from the east changes to motion from the west.

Similar streaks seen the previous day in the northwest quadrant of Typhoon Bess can also be explained by using the 200-mb chart (Nb 12) for 1200Z, August 7, 1963. In this case the 200-mb trough extends from near station Mo to Kanto without being interrupted by the typhoon outflow which advanced northward considerably during the subsequent 12 hours.

Conclusions:

Two groups of cirrus or cirrostratus streaks of a typhoon outflow were interpreted. One group which is in the direction of the logarithmic spirals corresponds to the thick clouds drawn out from the tops of the convective towers, most of which are found along the rainbands. These towers move in the direction of the middle-level winds which steer them. The plumes, on the other hand, are drawn by the high-level winds which elongate them in the direction of the vertical wind shear between two proper pressure surfaces.

The other group of streaks which points toward the storm is composed of cloud particles caught near the leading edge of the cirrus shield by the winds blowing immediately above the shield.

SESSION O

CONVECTION OVER LAND

Topic a

Convection over Japan in Summer (Oa)

by Tetsuya Fujita, the University of Chicago

Gridding and Infrared Analysis by Peter G. Black, the University of Chicago

Meteorological systems discussed herein are (1) cumulus to cumulonimbus convection over the mountains and (2) the dissipation of stratus and sea fog as they move inland.

Two photographs (Oa 1) from TIROS VII Orbit 692 cover the northeastern half of Honshu and its southwestern half. A cloud transfer map (Oa 2) is used in locating the boundaries of significant clouds on the map. If we pay careful attention to those orographic cumuli or towering cumuli, the boundaries of which more or less follow the topographic contour lines, we can identify cloud systems extending far beyond the orography which probably gave rise to their initial development.

We shall start from the western end of Honshu and work east and northeastward. An irregular mass of clouds over the western tip within the box bounded by 34N, 35N, 131E, and 132E; a large elliptic cloud in the box 35N, 36N, 132E, and 133E; small areas near the southern tip of Kinki, an elongated mass south of the 37N line between 139E and 140E; and a square-looking cloud in Tohoku within the box 39N, 40N, 141E, and 142E will be transferred and examined first.

A cloud chart (Oa 3) of the same scale as the cloud transfer chart (Oa 2) is available for closer examination and comparison. Also available are two surface maps for 0000Z (Oa 4) and 1200Z (Oa 5). The satellite passed over Japan at around 0600Z. We shall now review the synoptic situation based upon these two charts 12 hours apart. As seen in the charts, the western half of Honshu is under the influence of a weak east-southeasterly flow of the extreme outer region of Typhoon Bess located at 22N 137E. A weak cold front is moving southward over the Pacific Ocean off the coast of Tohoku. Due to the cold ocean surface temperature, fog and stratus are rather common along the eastern coast of Tohoku after a frontal passage.

Fair weather mesohighs over central Honshu at 0000Z are the result of the nocturnal radiation cooling accentuated partially by the sea-level reduction of station pressures from the inland stations. Streamline analysis of land breeze inside the mesohighs will reveal the outflow patterns. It is likely that these mesohighs change into thermal lows before local noon or 0300Z. Their remnants are

seen on the 1200Z chart only near Akita (582) and Niigata (604). A mesoscale thunderstorm high probably resulting from afternoon activities may be seen over Central Honshu.

A radiation map (Oa 7) was contoured with isotherms at 2C intervals of the equivalent blackbody temperature of Channel 2 (8-12 micron) medium resolution infrared (MRIR) scanning radiometer data. This map may be superimposed on the cloud transfer map (Oa 2) or the cloud chart (Oa 3) since all are made in the same scale.

For detailed investigation of clouds over Chugoku, local charts (Oa 6) have been prepared. The upper chart summarizes convective activities reported from 10 stations in the area. The arrows pointing from each station represent directions of thunder or thunderstorms. The local times (9 hours plus GMT) of the occurrence of showers and thunder are entered together with the intensity of the activities as specified by the numbers 0, 1, and 2. The areas above a 1000-m height are contoured and stippled.

The lower chart includes cloud distribution at 1425 local time and synoptic reports from each station. One long barb represents 5 knots of surface wind. It is evident that a zone of convergence exists along the north side of the central range of Chugoku. The fact that the southern limit of the clouds is located along the orographic ridge line and that a strong sea breeze is reported along the Japan Sea coast suggests that the moisture is supplied from the north to build up clouds along the northern slope of the central range. We have no way of knowing the exact height of these clouds; however, the equivalent blackbody temperature of the elliptic cloud (double arrow on Oa 3) is less than -10C, which is about 30C colder than its radiation background. It should be mentioned that the half-power area of MRIR when this cloud was scanned was about 90 km in diameter on the earth, suggesting that fair amounts of the background radiant emittance are also included. Two cloud shadows may be seen on the picture.

A small cold area over southern Kinki seems to be a small thunderstorm, since it is characterized by a temperature of only a few degrees lower than that of the environment. The clouds over northern Kanto are fairly cold, -10C or lower. They undoubtedly embody thunderstorms. In fact, the northeastern corner of Kanto is climatologically the area of most frequent thunderstorms because it does not affect the isotherms of equivalent blackbody temperature. It is probably just remnants of stratus or fog in Tohoku.

Faint streaks extending in the direction of surface isobars are a combination of fog and stratus. The western limit of these streaks ends about 10 km inland where sufficient heating and mixing during midday dissipate them.

Even though the photograph does not clearly show the existence of cirrus clouds near or over this fog region, extremely low radiation (-35C) appears

near 37N 144E. The clouds over this area are faint, suggesting a cirrostratus cover. The differentiation of fog and stratus from high clouds is, therefore, rather difficult without adding radiation data which are not available operationally at the present time.

Conclusions:

Through a careful comparison of accurately girdded pictures and local mountain ranges, it is feasible to identify cumulonimbus clouds, the boundaries of which do not follow the contour lines. Thus the early stage of overland thunderstorms can be detected. For the identification of localized fog and stratus, it is necessary to have infrared radiation data.

SESSION O

CONVECTION OVER LAND

Topic b

Tropical Land Convection Over the Philippines (Ob)

by Tetsuya Fujita, the University of Chicago

Gridding by Peter G. Black, the University of Chicago and Data Analysis by Jaima J. Tecson, the University of Chicago and the Philippine Weather Bureau.

Meteorological systems discussed herein are (1) tropical orographic convection and (2) its influence upon the environment.

A cloud photograph (Ob 1) covering most of the Philippines is used for this synoptic interpretation. An already transferred cloud chart (Ob 2) is made to fit to the scale of a surface map (Ob 3) and the surface isobar chart (Ob 4). The time difference between the surface chart and the cloud photograph is only one hour and 40 minutes. Over Luzon, most of the clouds coincide with the Cordillera Central, the Sierra Madre, and other small mountain ranges. Surface station reports reveal that clouds are mostly cumuli and towering cumuli with their bases at about 800 m. As expected, the sea breeze is predominant all around the island north of Manila.

Some stations report the direction of low cloud motion. Since this often represents the direction of geostrophic winds, it is entered on the surface map (Ob 3) as a short arrow by the station.

A very interesting feature of the clouds in the photograph (Ob 1) is a clear circle of about 500 km in diameter located over Luzon and the nearby ocean. There are orographic clouds directly over the mountains inside the circle. As may be seen, however, the area is relatively clear if such orographic clouds are disregarded. The cloud chart (Ob 2) may also be used in identifying the area circled by a line of clouds. Such a clear area surrounding a tropical island is frequently observed in the afternoon when significant sea breeze gives rise to divergent wind fields over the nearby ocean. Meanwhile the convection over the heated island accentuates convergence over land areas. The descending motion over the ocean surrounding the island thus suppresses the development of small clouds within the clear area. A small but similar clear area is seen around Mindoro Island.

Surface isobars (Ob 4) are contoured for every 0.5 mb to show the heat lows accompanied by several islands in the Philippines. The largest low over northern

Luzon indicates about 2 mb deficit pressure. The environmental surface pressure is rather high along the western boundary of the low, since the entire island is under the influence of a very weak southwesterly flow south of the intertropic convergence zone located between the Philippines and Formosa. This flow actually shifted the center of the circle slightly eastward from the geographic center of the heated island.

With the use of the same technique as that used in detecting cumulonimbus clouds over the complicated terrain in Japan (Oa), several thunderstorms over the islands of Masabate, Panay, and Samar can be identified and compared with the station reports (Ob 3). Note that a late-stage thunderstorm between Mindoro and Panay is accompanied by a long cirrus streamer extending west-southwestward.

Conclusions:

The relatively clear and circular areas over a heated island and the nearby ocean have been discussed. When there are no prevailing winds over the island, the circle is centered at the geographic center of the island which is covered with orographic convective clouds. A clear ring surrounding the island is seen on the satellite picture in such a case.

If such a clear area develops over an island with prevailing winds, the center of the circle is displaced toward the downwind side from the geographic center of the heated island. On a midday or afternoon surface chart, a heat low and converging wind fields can be analyzed on each island accompanied by such a clear area.

SESSION P

NORTH PACIFIC FOG

by Tetsuya Fujita, the University of Chicago

Gridding and Data Analysis by Walter A. Lyons, the University of Chicago

Meteorological systems discussed herein are (1) features of fog and low stratus clouds, (2) their blocking by islands, and (3) identification of higher clouds using their shadows and radiation data.

A case of North Pacific fog photographed by TIROS VII in its Orbit 735 is used in studying the three meteorological systems mentioned above. The cloud photographs (P 1) taken with about 30° tilt cover areas of the Aleutian Islands which partially block the southwesterly advection of a mixture of sea fog and low stratus, called simply "fog" in this session.

In an attempt to relate the blocking action with a chain of islands, a cloud transfer chart (P 2) has been prepared. The numbers entered near each island denote the height in feet of the highest mountain on the island. These numbers are used during this session to identify the islands.

The largest cloud band, indicated in the cloud pictures (P 1) by four arrows, is blocked by the western half of island 407, the eastern half of which is rather flat. It is postulated, therefore, that the limited heating by the flat part of the island, about 10 km wide, is not enough to dissipate this cloud band. The western half of the island, with about 120 m elevation, blocked the band completely as if it were cut by a sharp knife. This appearance would indicate that it is a band of fog which is rather thick but does not extend to a high elevation. Even very small islands, such as 402, 1157, and 762, can be clearly identified on the photographs.

Features of the fog, especially when it appears in bands, are very similar to those of cirrostratus bands. A thin, narrow band extending SW to NE through 50N 176E, for instance, looks very much like a band of high clouds because it is rather faint. In order to distinguish sea fog from a band of high clouds, it is necessary to investigate the influence of islands by careful detective work. Unlike tropical islands, the Aleutian chain very often acts as a fog or cloud dissipator rather than as its generator.

The cloud chart (P 3) gives overall patterns of fog which sometimes show small vortices behind the islands. The heights of such vortices are limited to the top of the temperature inversion which forms at a low altitude when warm air travels over the cold sea surface.

The orientation of the fog band is usually parallel to the vertical wind shear between the surface and the fog-top level. Because of the fact that the wind velocity at the surface is theoretically zero, the direction of the shear is very close to that of the geostrophic winds at the surface. A surface map (P 4) analyzed by using additional data outside the map indicates such a relationship between the orientations of the fog bank and the surface isobars.

When we examine Frame 8 (P 1) very carefully, it will be found that a line of clouds along longitudes 172E and 173E is accompanied by distinct shadows. In order to prove that these are definitely shadows, it is necessary to obtain the antisolar point (AS) on successive frames. The antisolar point is a point where the shadow of TIROS would appear if the satellite were large enough. Theoretically a vector connecting a cloud and its shadow on an image plane always directs toward the antisolar point. If a cloud exists at or very close to the antisolar point, its shadow should be hidden behind the cloud. As a result, no shadow can be seen from the satellite. A series of cloud photographs (P 9) reveals the fact that the shadows disappear when the antisolar point approaches them as a result of the orbital motion of the satellite. A dashed circle around the AS denotes a 10° object angle from AS. Two clouds indicated by single and double arrows, respectively, may be followed in each frame to see that their shadows disappear near the antisolar point.

A radiation map (P 8) clearly represents the difference in temperature between these shadow-casting clouds and the underlying fog. The map also shows that the top of the major fog band is a few degrees colder than the ocean surface that is free from fog.

A surface map (P 5) has been made to determine the areas of north Pacific fog from surface synoptic data. Its area corresponds, as expected, to the region where warm air advection over cold sea surface takes place. Photographs show that the major fog band originates at about 175E and 45N. This location, when identified on the surface map, exists on a ridge where the easterly flow changes into a southwesterly flow.

A 500-mb chart (P 6) including a boxed area of the cloud chart (P 3) is used to investigate height and moisture patterns in relation to the positions of the shadow-casting clouds. The analyzed result (P 7) indicates that the cloud lines, "a" and "b" correspond to the leading edge of the moist tongues at 500-mb surface and extend from the troughs "A" and "B" in which rain and drizzle are found on the surface map.

Conclusions:

Identification of an extensive sea fog on satellite photographs is rather difficult. Through careful study of the direction of drift and the blocking effect by islands, however, it is feasible to distinguish it from other types of clouds. Higher cloud cover can be identified either by its shadow-casting on the fog or the equivalent blackbody temperature obtained from the infrared radiation data.

SESSION Q

OROGRAPHIC EFFECTS ON SOME WINTER CLOUDS

Topic a

Formation of Clouds over the Sea of Japan (Qa)

by Tetsuya Fujita, the University of Chicago

Gridding and Radiation Analysis by Say-Yuo Gagard, the University of Chicago, and PAA Meteorological Service, Liberia

Discussion here is concerned with the characteristics of low clouds that form over the Sea of Japan when the winter monsoon prevails.

Three photographs (Qa 1) from TIROS VII Orbit 3085 have been gridded and carefully analyzed in an attempt to study the locations over the Sea of Japan where the low clouds first form as a result of evaporation and subsequent convection inside the mixing layer. Transfer of such locations of initial clouds to a cloud chart (Qa 2) reveals that there is a zone of cloud-free area extending downwindward about 100 km from the coast of Sikhote Alin.

The formation takes place, more or less, at a point from which a long line of cloud streaks extends in the direction of the flow. The streaks are about 20 km apart, but each of them extends several hundred kilometers.

A surface map (Qa 3) includes the synoptic data to be used in constructing the surface isobars and isotherms (Qa 4). It is obvious that the mountains in Sikhote Alin, 1000 to 2000 m high, block the outflow of cold air from the Asiatic continent. Dynamical warming due to the descending motion along the leeward slope of the Khrebet Sikhote Alin results in about a 3 mb pressure drop, while at the same time the descending motion prevents a cumulus formation to the west of the mountains.

When the orientation of the surface isobars (Qa 4) is compared with that of the cloud streaks over the Sea of Japan, we see cross-isobaric orientation everywhere. The 850-mb chart (Qa 5), however, shows the height contours somewhat parallel to the cloud streaks.

As expected, an appreciable subsidence is taking place inside the winter monsoon above the low-level cloud tops. The 700-mb chart (Qa 6) includes the isodrosotherms, the pattern of which suggests strong descending motion over the central portion of the Sea of Japan.

The radiation map (Qa 7) was made by using TIROS medium resolution infrared (MRIR) data from Channel 2 (8-12 microns). It will be found that the cloud-free areas off the coast of Sikhote Alin are characterized by warm areas of about 0C. A patch of faint clouds off the coast of Sikhote Alin near the 45N latitude seems to be rather high because of its orientation and the low equivalent blackbody temperature. The temperature of the Japan Sea clouds west of Hokkaido and Sakhalin is rather uniform, ranging between -24 and -26C. If the clouds were opaque and filled up the radiometer's field of view, their height would be up to about 3 km.

The blocking action of Hokkaido and Sakhalin upon these clouds is appreciable. In the wake of south Sakhalin with 1028 m mountains is a 300-km long clear area. There is tongue of cold equivalent blackbody temperature pushing out eastward over the strait between Hokkaido and Sakhalin.

The convection regime over the southwestern portion of the Sea of Japan is quite different. There the winter monsoon is rather weak and clouds are in irregular shapes rather than in streaks. The vertical extent of these clouds is not very high, because the equivalent blackbody temperature is only about -10C, which corresponds to the free-air temperature at about 1500 m level.

Conclusions:

It is revealed that the low clouds that form over the Sea of Japan during the winter monsoon appear in the form of streaks when the monsoon is strong. The distance between the streaks is about 20 km, and the streaks orient in the direction of the 850-mb flow. The cloud-top height gradually increases to about a 3-km level before reaching the coast of Sakhalin and Hokkaido. Over the sea surface with a weak monsoon, the cloud development takes place in the form of irregular cells which reach only to about an 850-mb surface. Even though these figures were obtained through the analysis of a specific case, they may not be too far from representing the situations during the typical winter monsoon. It is hoped that a few more cases may be investigated in an attempt to generalize the findings.

SESSION Q

OROGRAPHIC EFFECT ON SOME WINTER CLOUDS

Topic b

Influence of the Japanese Islands upon the Winter Monsoon Clouds (Qb)

by Tetsuya Fujita, the University of Chicago

Gridding and Radiation Analysis by Kiyoshi Tsuchiya, the University of Chicago and Japan Meteorological Agency

The subjects to be discussed are (1) the distribution of clouds along the Japan Sea side of Honshu, (2) the influence of orography in Honshu upon precipitation, and (3) the cloud streaks over the Pacific Ocean.

For the purpose of discussing these three subjects, the winter monsoon situation of January 20, 1964 was selected. The cloud photographs (Qb 1) show the areas of the eastern and the western half of Honshu under the influence of a strong winter monsoon.

Participants are asked to transfer significant cloud features from photographs to the cloud transfer charts (Qb 2). A cloud streak extending southeast from a bay between Kinki and Chubu will be transferred first. Then the southeastern boundary of the cloud deck over Kanto and Chubu and the rather insignificant cloud streak over the Sea of Japan will be transferred. It will be found that the orographic clouds over Chubu and Kanto disappear before entering the low-level plains on the Pacific side of Honshu.

A completed cloud chart (Qb 3) clearly indicates several cloud streaks over the Sea of Japan and plume-like cloud streaks over the Pacific Ocean in the wake of Honshu, Shikoku, and Kyushu. When these cloud streaks over the Pacific are traced back to their origins, it is seen that they coincide with either straits or relatively low passes between groups of high mountains.

Plotted surface data (Qb 4) reveal meteorological conditions at each station within 30 minutes after the exposure times of the photographs (Qb 1). Participants are invited to make direct comparison of these station data and the cloud chart (Qb 3) by superimposing the latter on the former.

Radar echoes in the surface isobar chart (Qb 5) and the cloud chart (Qb 3) are then examined by superimposing one on the other. One of the cloud streaks oriented NW to SE passing near Nagoya (436) coincides extremely well with the

line of the echoes. In fact, the pattern of radar echoes gives the impression that they form over Mt. Ibuki (1377 m), located between stations 436 and 631 and drift away toward the Pacific Ocean. From this point of view, the mountain acts as a cloud generator. When we scan over both Kinki and Chubu, we see that there are a large number of mountains much higher and more extensive than this 1377 m peak. Nevertheless, no cloud streaks originate from these mountains. Moreover, a careful examination of the orientation and location of the cloud streaks reveals that there are practically no streaks extending to the rear of high and large mountains.

It is very likely that each of these cloud streaks is located over relatively low-elevation topography averaged over a radius of some 50 km. In other words, a cloud streak is likely to form over a valley of averaged topography in which low-level convergence takes place due to the so-called channel effect. The 1377 m peak is located in the midst of such a valley, thus triggering the cloud formation inside the converging air through this valley.

One of the most interesting features of radar echoes photographed by the Niigata radar is the NW-SE orientation of the echoes in lines north of Niigata (604) and Aikawa (602). The orientation is identical to that of the cloud streaks extending more than 400 km over the Sea of Japan. That is to say, the lines of echoes appearing on the Niigata (604) radarscope are the tail end of the cloud streaks originating over the Sea of Japan some distance away.

Presented on the isotherm chart (Qb 6) are the isotherms of the surface temperatures obtained from both regular and special observation stations. This chart, when combined with the snow depth and present weather chart (Qb 9), permits us to interpret satellite pictures taking local weather and reflection from snow surfaces into consideration.

An isodrosotherm chart (Qb 7) analyzed with the help of the cloud chart (Qb 3) clearly indicates the areas affected by the Föhn phenomenon behind the high mountains. Note that the Tokyo area is extremely dry in such a winter monsoon.

As has been well-known, the orientation of the cloud streaks coincides extremely well with the low-level flow. The direction of the plumes as seen over Tohoku represents, on the other hand, the direction of vertical wind shear between the cloud top and the steering levels. The 850-mb and the thickness contours (Qb 8) have been prepared to study such relationships. Note that the cloud streaks over the Sea of Japan and the Pacific Ocean are parallel to the 850-mb contours, and the plumes from the cells over Tohoku are oriented in the direction of the geostrophic shear between the 400- and 850-mb surfaces as shown by dashed contour lines.

A radiation map (Qb 10) gives some idea of the height of the clouds that are large enough to fill the radiometer's field of view. The cold spot on the west coast of Tohoku gives the equivalent blackbody temperature at about the 5-km

level. The orographic clouds over Hokuriku show about -26C temperature, suggesting that their tops are at about 3 km. The interpretation of the equivalent blackbody temperature of small cloud streaks is rather difficult since a radiometer always includes the background radiation while scanning such small clouds.

The cross-section chart (Qb 11) schematically represents the vertical distribution of air temperatures as well as the in-cloud temperatures computed by lifting an air parcel moist-adiabatically beyond the cloud base. Due to deep snow on the mountains, the shelter temperature does not change too much during the day and may be regarded as very close to the underlying snow-surface temperature. The cross-section chart thus indicates the fact that the mountain surfaces are not acting as heat sources as in the case of heated mountains in summer. There will be very little heat exchange between the orographic clouds and the mountain surfaces. The January 20, 1964 case may be considered as a typical one in which the formation of orographic clouds takes place as a result of simple dynamical lifting. In such a case, the cloud formation can be treated as a function of the strength of the monsoon blowing against the mountains.

Conclusions:

It has been pointed out that the echoes in lines near the Japan Sea coast of Honshu are a result of the convection inside the cloud streaks extending far over the Sea of Japan. A mechanism of the formation of cloud streaks over valleys of the averaged topography was presented in an attempt to explain the origin of the cloud streaks extending over the Pacific Ocean during a typical winter monsoon.

INDEX MAP FOR SESSIONS Na, Nb, Oa, Qa, and Qb

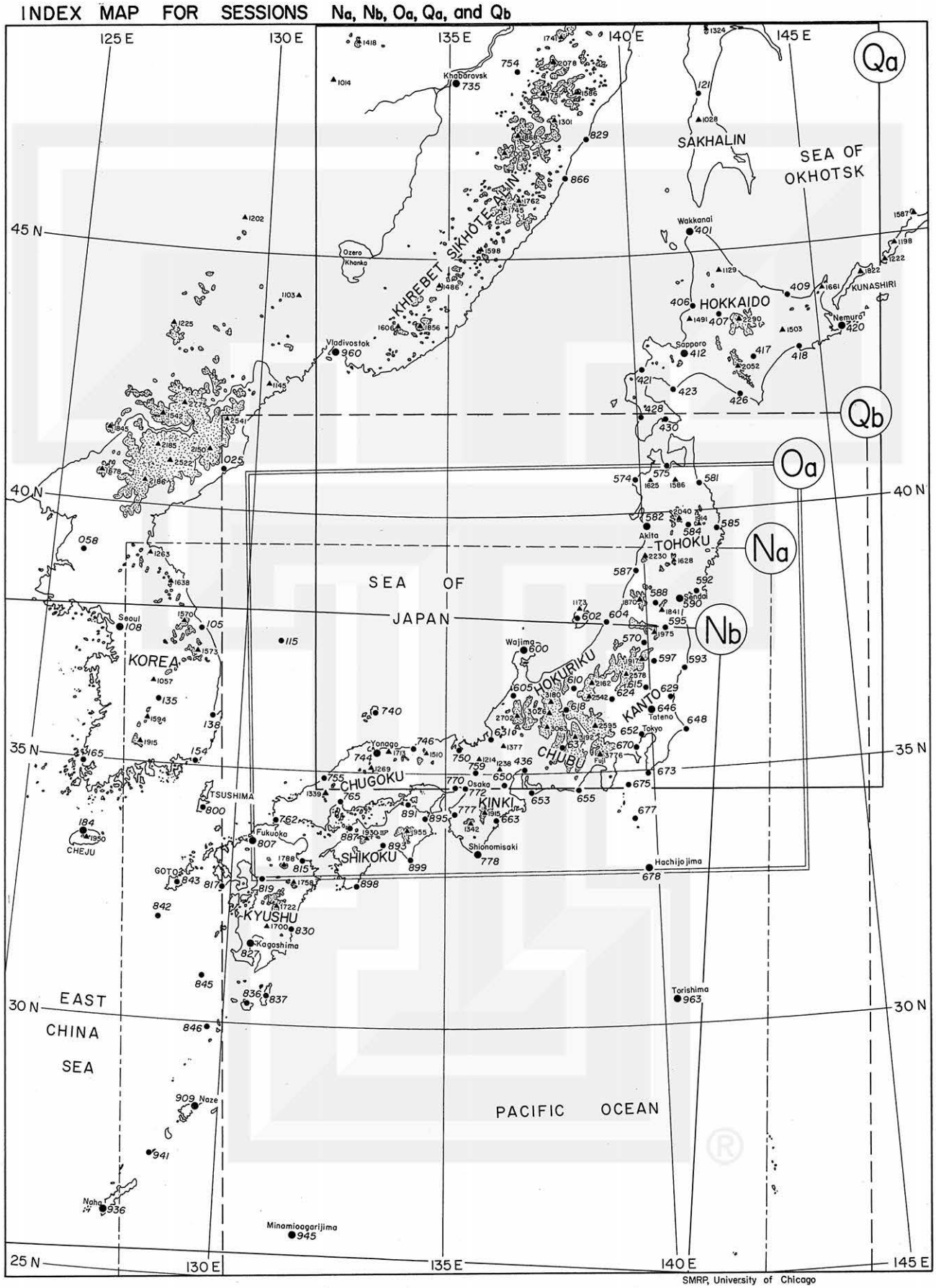

SMRP, University of Chicago

CLOUD PHOTOGRAPHS

Na 1

TIROS 7

A/O 721, R/O 721

TAPE MODE CAMERA 1

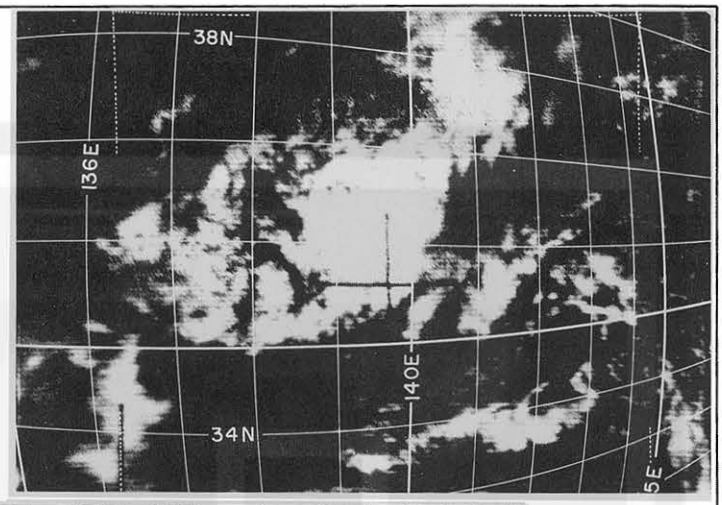

FRAME 18
TIME 0430.6 Z
ϕ^{TSP} = 36.4 N
θ^{TSP} = 137.5 E
H = 627 km
τ = 18.5°
α^{PL} = 107.3°

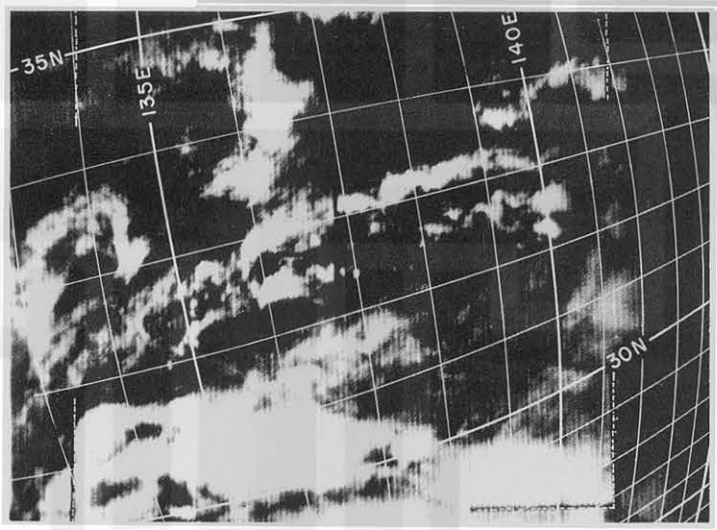

FRAME 20
TIME 0429.6 Z
ϕ^{TSP} = 33.5 N
θ^{TSP} = 134.9 E
H = 627 km
τ = 17.4°
α^{PL} = 116.4°

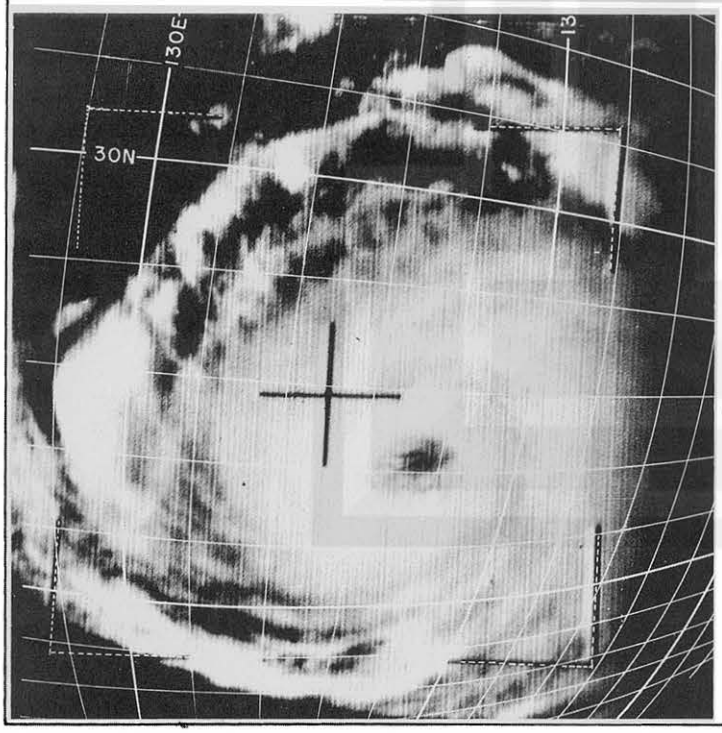

FRAME 23
TIME 0428.1 Z
ϕ^{TSP} = 29.3 N
θ^{TSP} = 131.4 E
H = 627 km
τ = 17.0°
α^{PL} = 132.1°

CLOUD TRANSFER CHART AUG 7, 1963 No 2

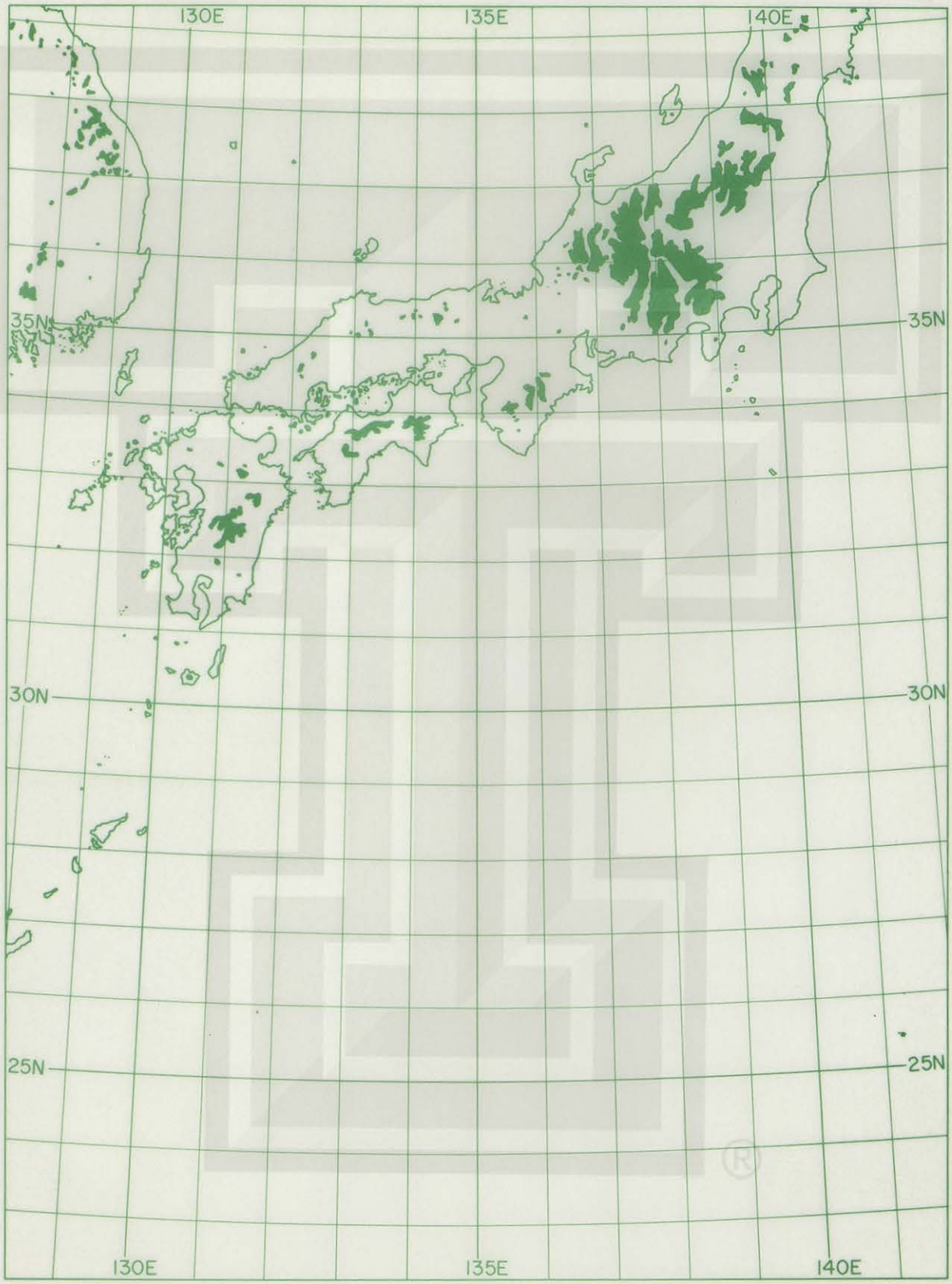

SMRP, University of Chicago

CLOUD CHART 0428 Z AUG 7, 1963 No 3

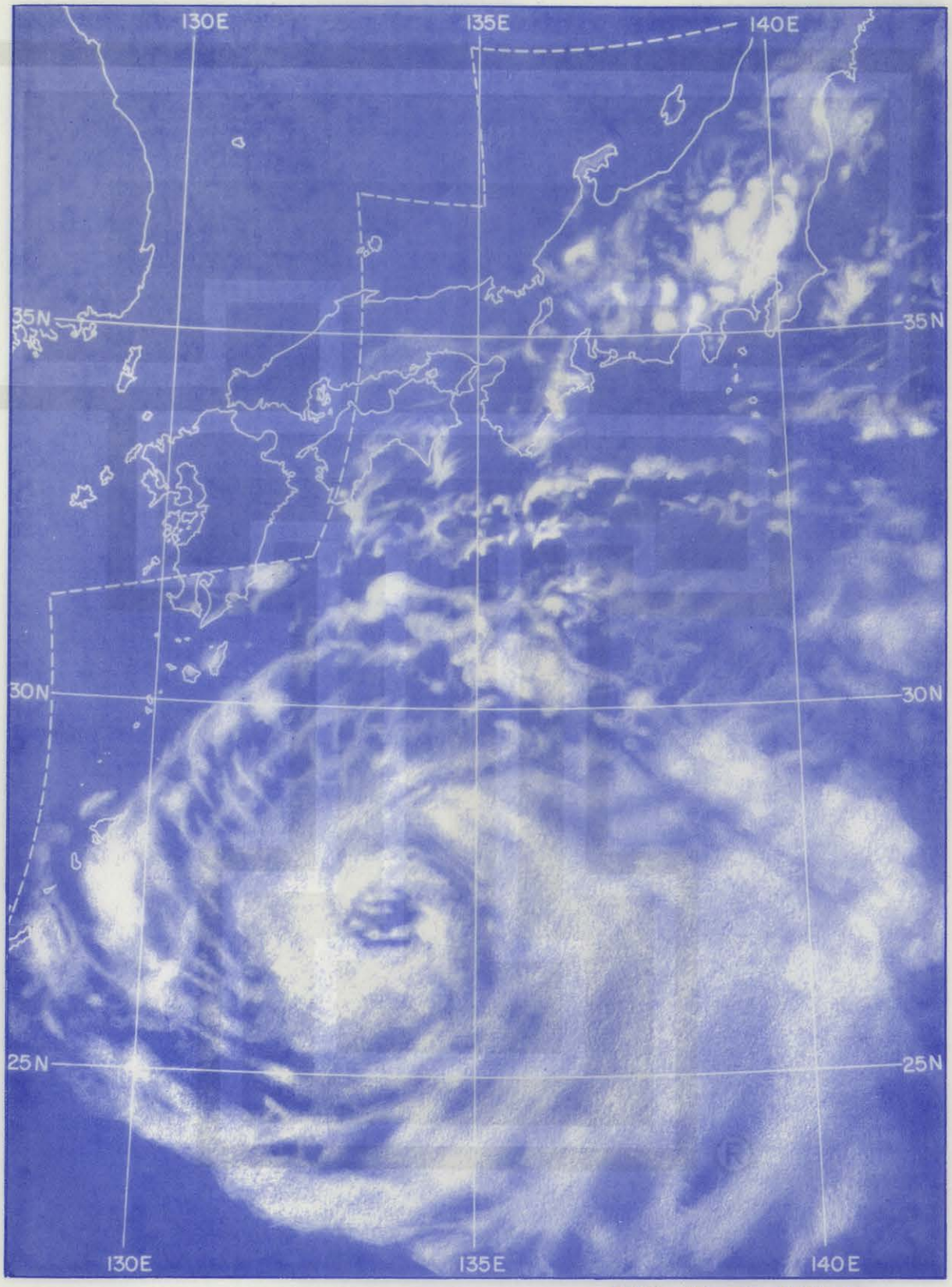

SMRP, University of Chicago

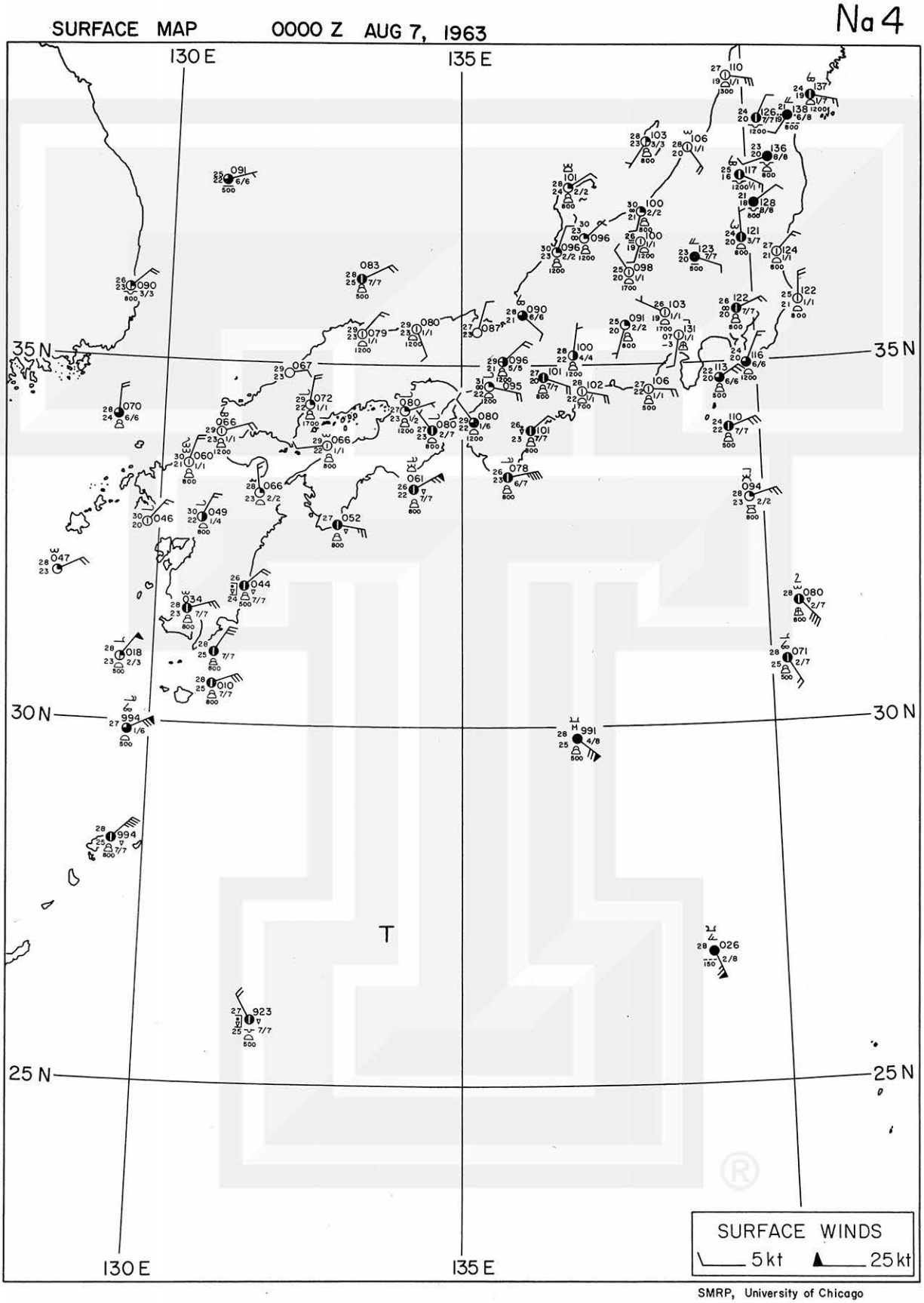
SURFACE MAP 0000 Z AUG 7, 1963
Na 4
130 E
135 E
35 N
30 N
25 N
T
SURFACE WINDS
5 kt
25 kt
SMRP, University of Chicago

SURFACE ANALYSIS 0000 Z AUG 7, 1963 No 5

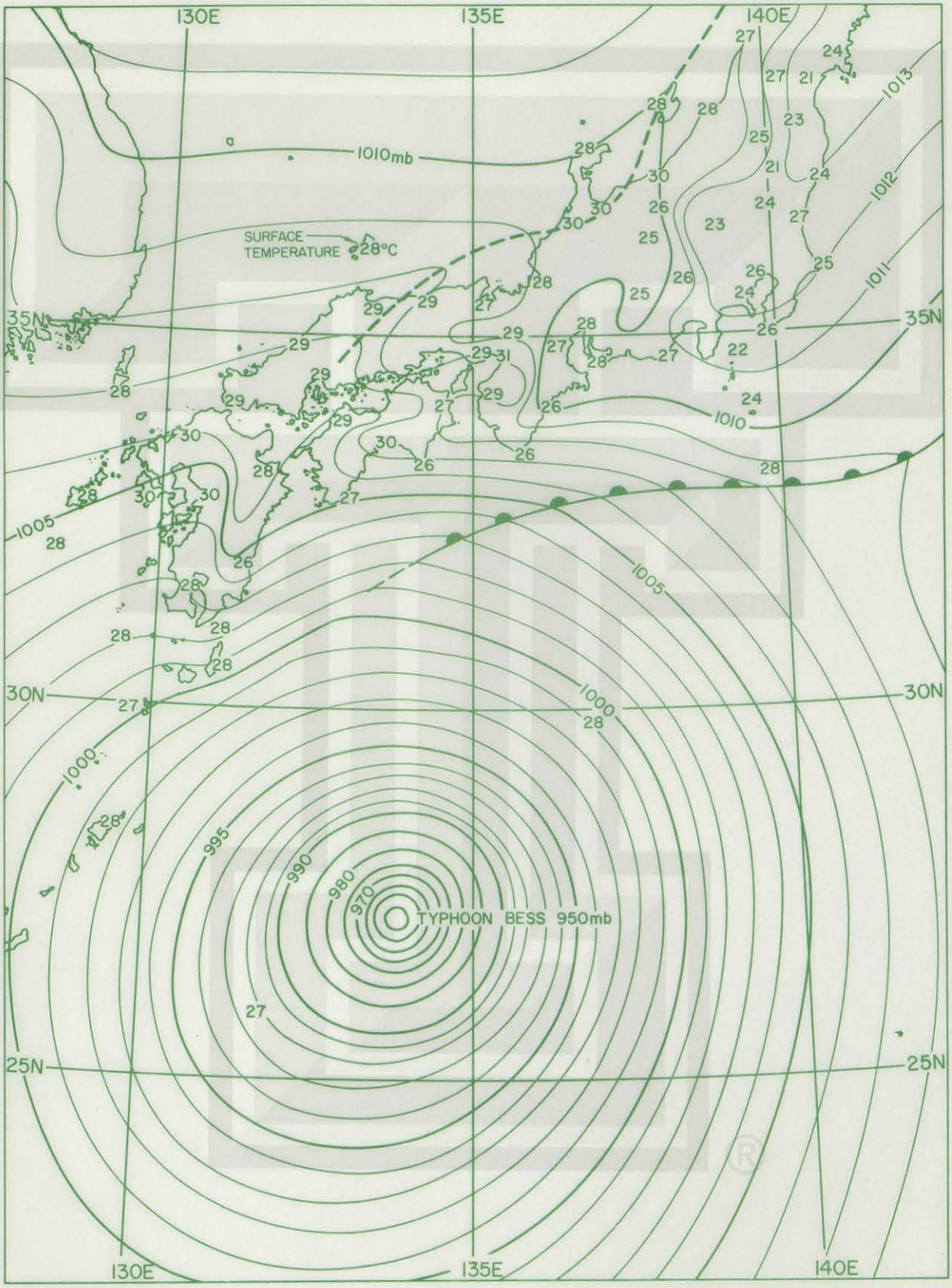

SMRP, University of Chicago

No 6

RADAR ECHOES 0428Z AUG 7, 1963

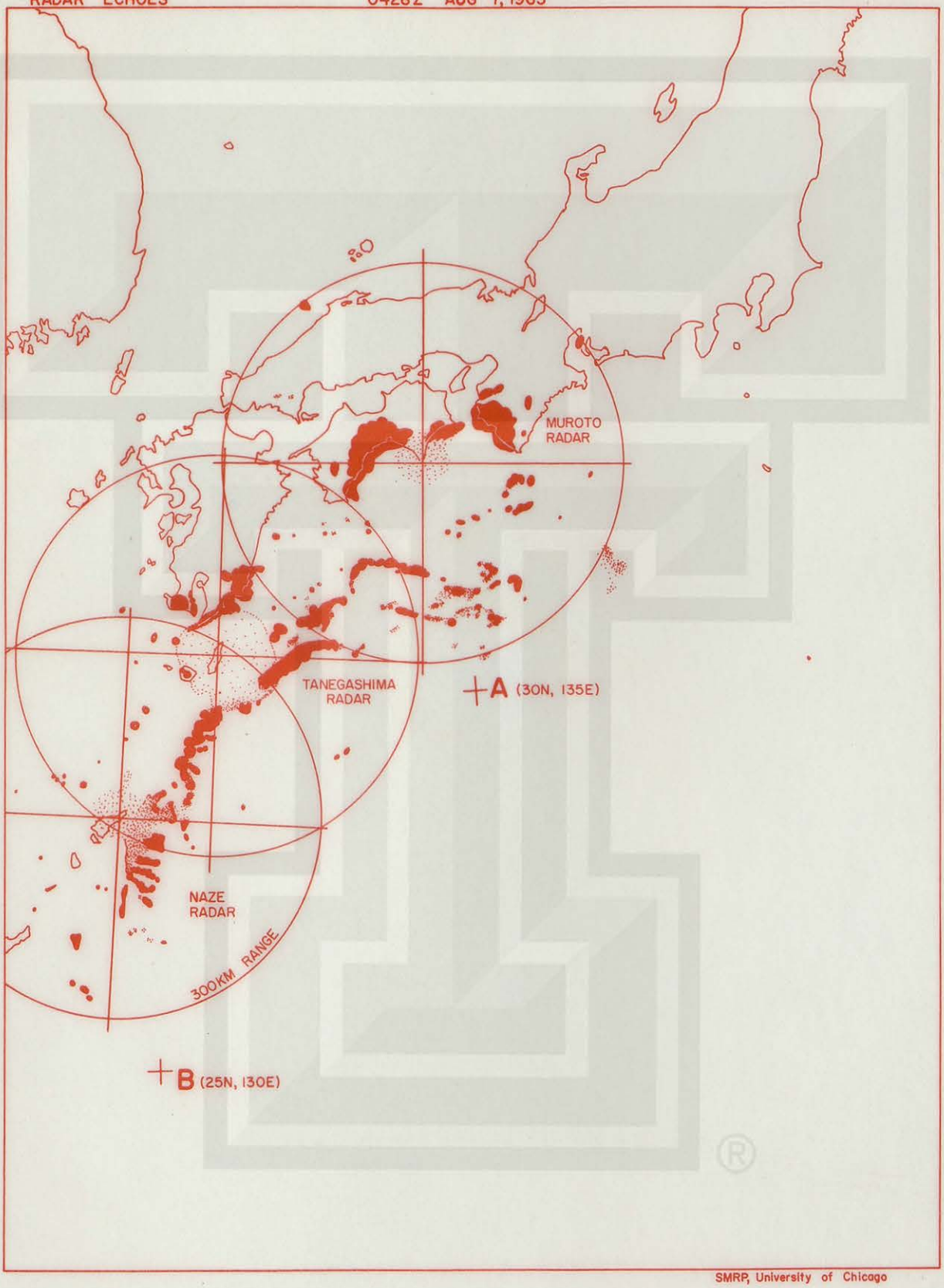

SMRP, University of Chicago

CLOUD PHOTOGRAPH AUG. 8, 1963 Nb1

TIROS VII A/O 736 R/O 736 CAMERA 2, TAPE

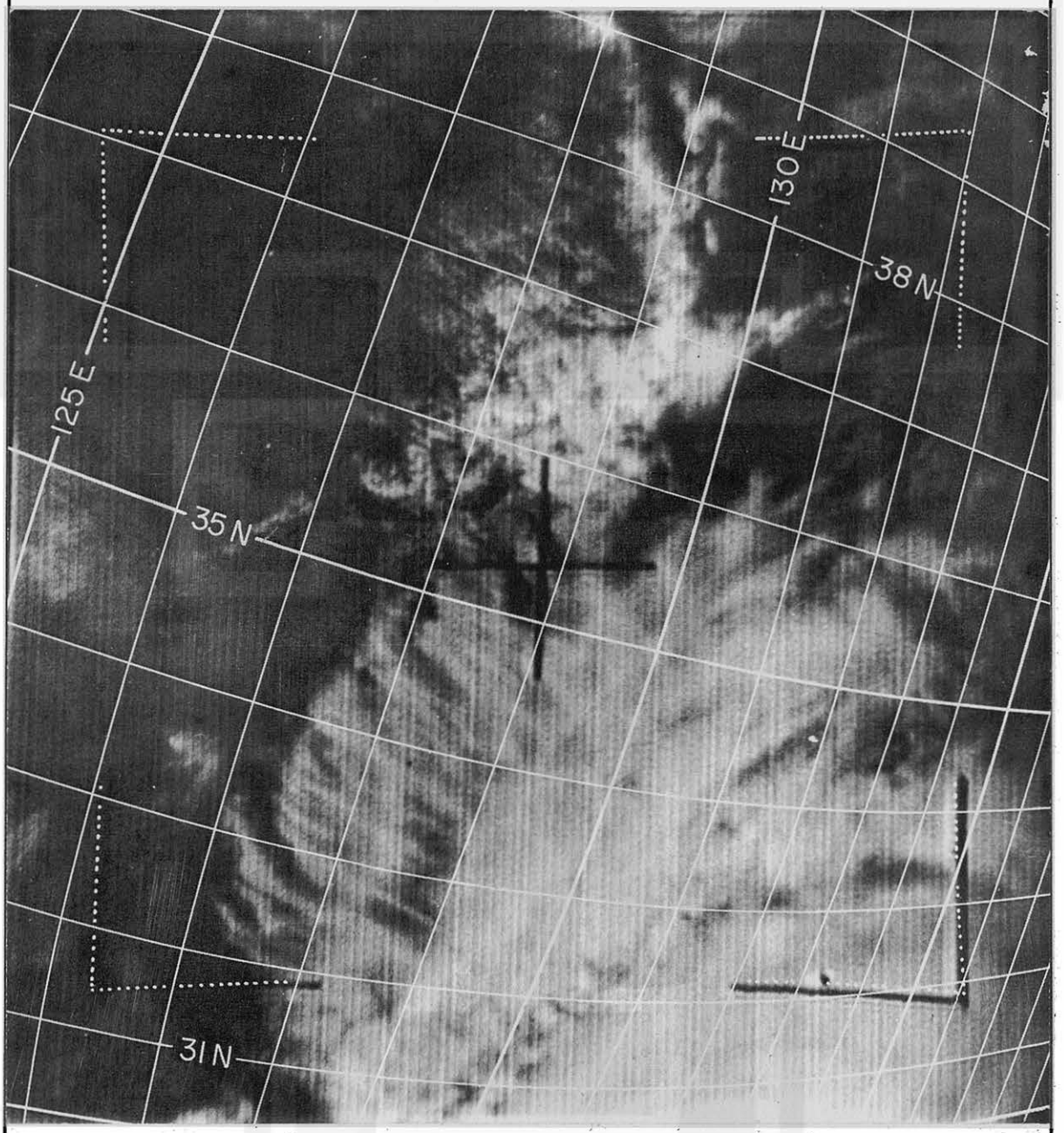

FRAME 20

ϕ^{TSP} = 35.7N

H = 627 km

τ = 15.4°

TIME 0451.4 Z

θ^{TSP} = 126.7E

α^{PL} = 104.0°

SMRP, University of Chicago

CLOUD CHART 0451Z AUG. 8, 1963 Nb 2

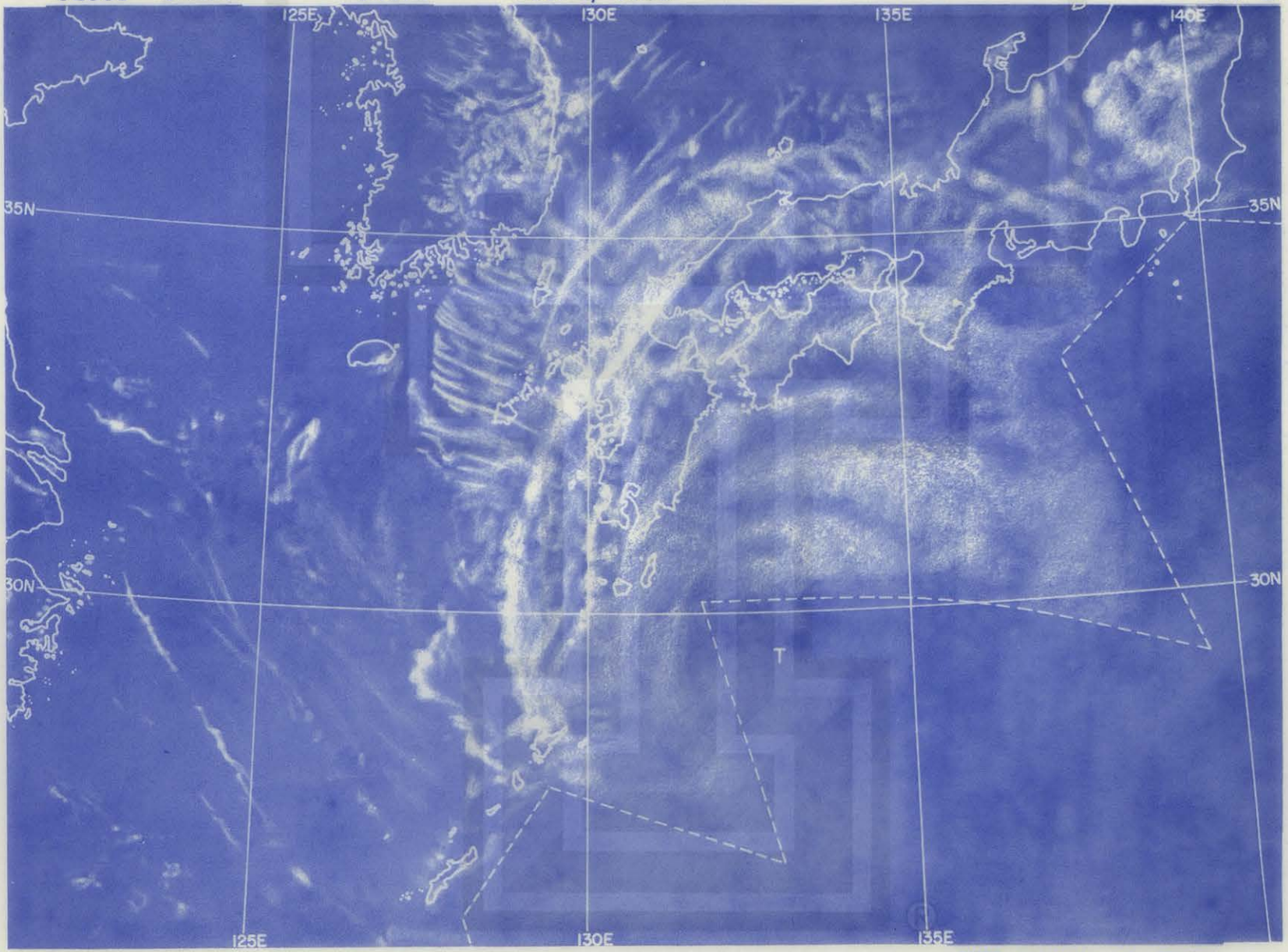

SMRP, University of Chicago

Nb 3

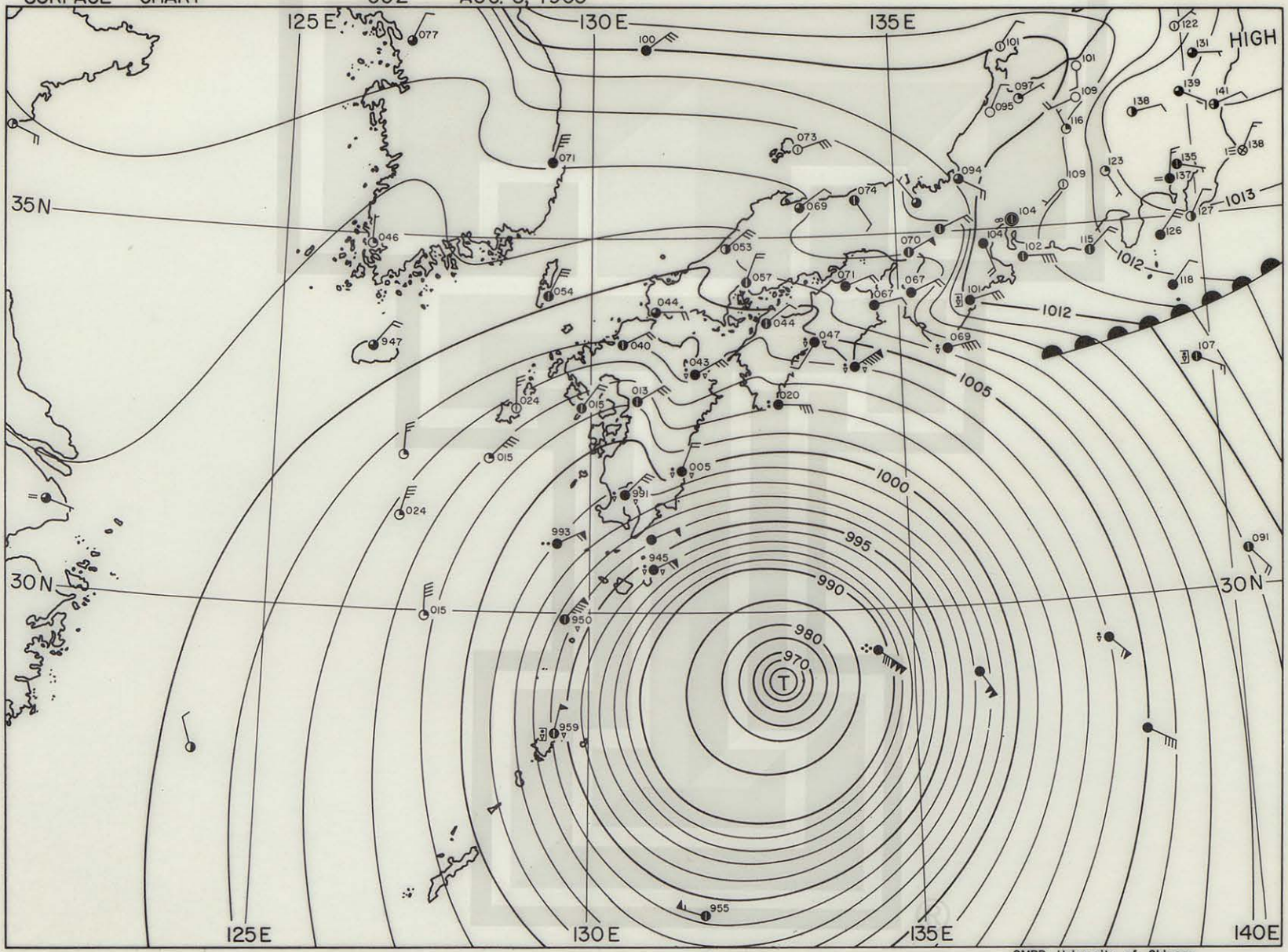
SURFACE CHART 00Z AUG. 8, 1963
125 E
130 E
135 E
140E
35N
30N
HIGH
1013
1012
1012
1005
1000
995
990
980
970
T
SMRP, University of Chicago

Nb 4

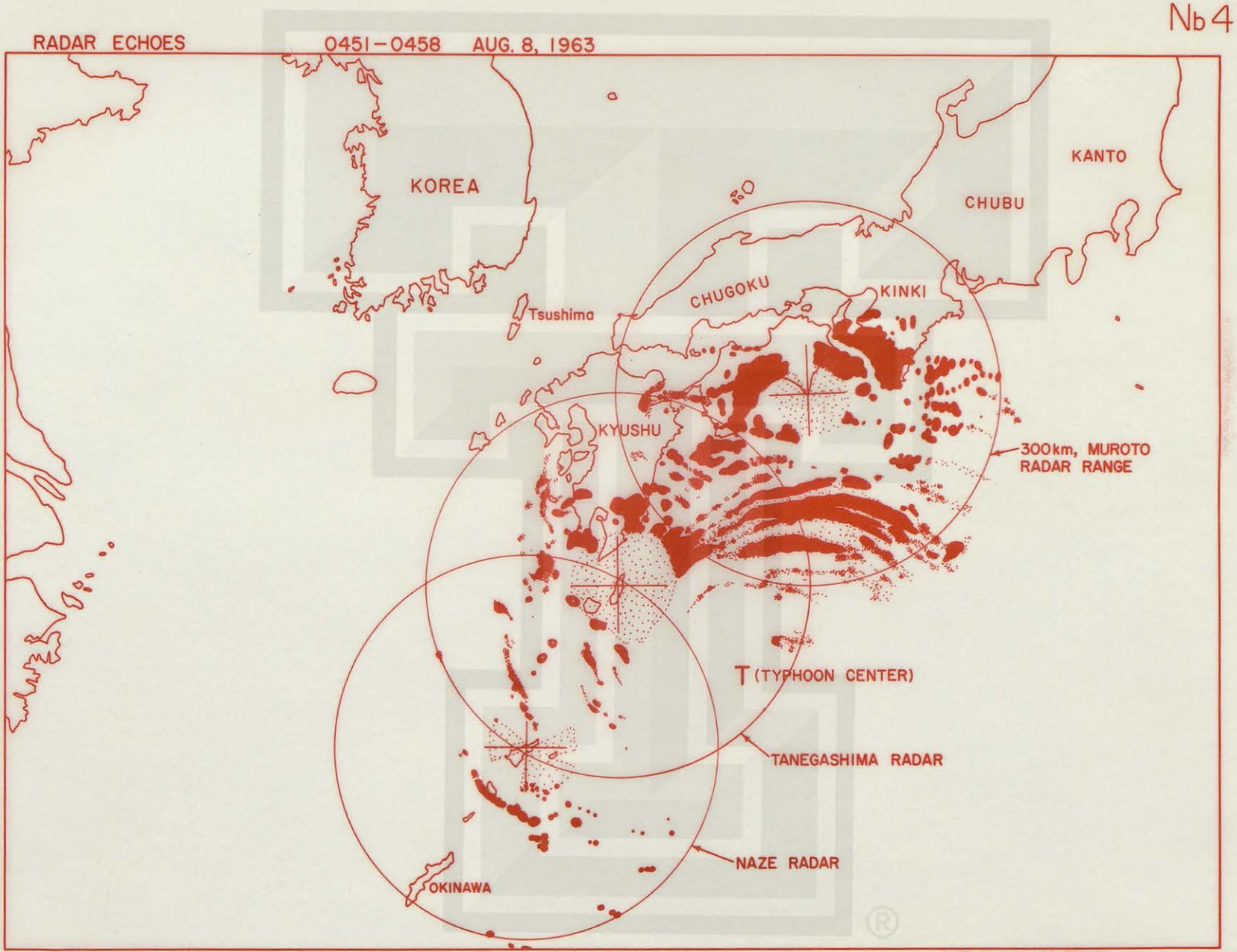
RADAR ECHOES
0451-0458 AUG. 8, 1963
KOREA
Tsushima
CHUGOKU
KINKI
CHUBU
KANTO
KYUSHU
300km, MUROTO
RADAR RANGE
T (TYPHOON CENTER)
TANEGASHIMA RADAR
NAZE RADAR
OKINAWA
SMRP, University of Chicago

Nb 5

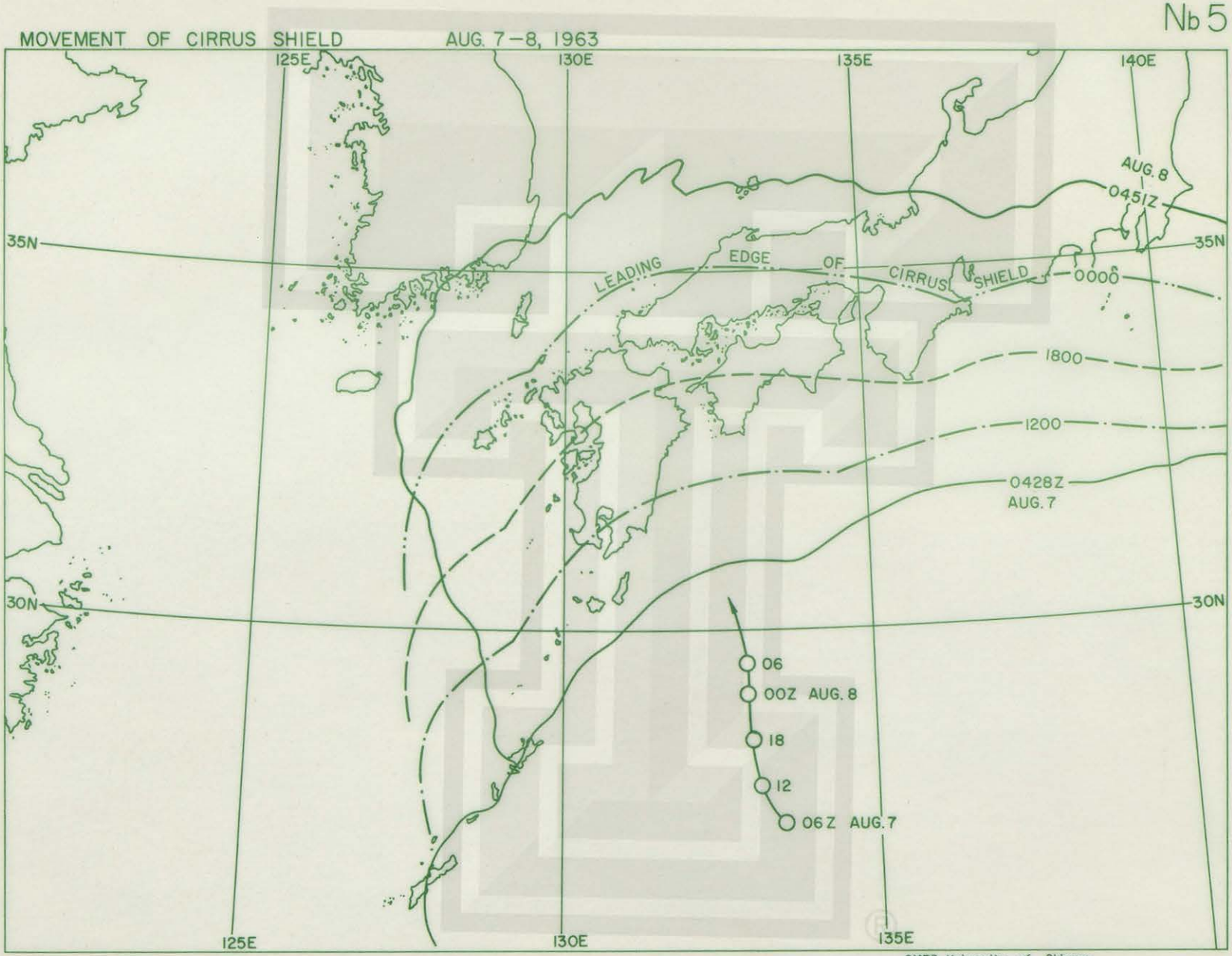
MOVEMENT OF CIRRUS SHIELD
AUG. 7–8, 1963
125E
130E
135E
140E
35N
30N
AUG. 8
0451Z
LEADING EDGE OF CIRRUS SHIELD
0000
1800
1200
0428Z
AUG. 7
06
00Z AUG. 8
18
12
06Z AUG. 7
SMRP, University of Chicago

Nb 6

THICKNESS AND SHEAR 00 Z AUG 8, 1963

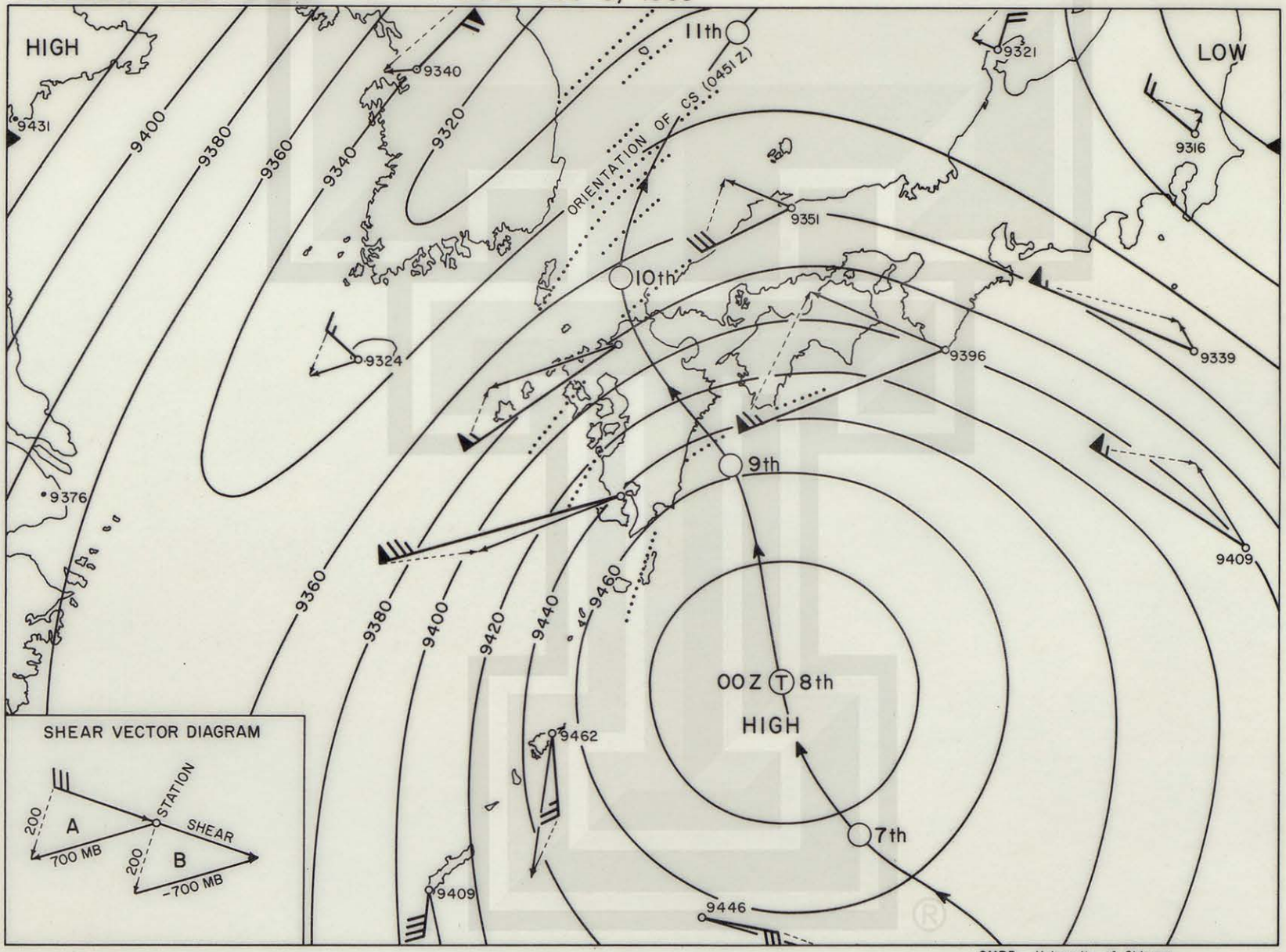

SMRP, University of Chicago

KAGOSHIMA 47827 31°38'N, 130°36'E TEMPERATURE ANOMALY IN 0.1°C Nb 7

MB															
	-44	-27	-15	-09	-10	-14	-18	27	39	20	08	06	10	33	05
100	-78	-25	-83	-13	-18	-50	-24	03	0	26	19	-06	-19	21	29	39
	-09	18	05	06	32	18	-08	0	-06	35	05	20	02	11	36	26
	11	21	78	26	47	58	12	19	11	28	22	45	03	0	-11	-03
	10	25	20	34	48	47	25	11	25	25	37	15	08	07	-23	-17
200	23	34	37	53	71	47	50	22	43	24	37	20	24	-01	-30	-29
	35	29	36	47	62	59	66	33	33	29	29	32	13	-11	-07	-27
300	25	42	37	33	75	70	55	37	42	42	07	16	01	11	0	-23
	-02	12	28	31	74	51	55	34	39	40	03	16	-02	10	01	-24
400	-06	-02	22	25	71	50	51	23	25	32	11	05	05	-02	02	-22
500	-06	23	0	20	32	27	45	22	20	08	11	15	15	-06	-04	-24
	14	02	02	06	33	50	32	20	22	04	(42)	11	16	-05	05	-30
700	08	-03	-15	07	10	25	14	-14	07	-02	-17	-06	11	-10	-17	-30
	04	-02	-02	04		35		-06		-27		-13	-01	-04	12	-24
1000	13	05	-03	-13		0		0		-26		-11	10	-05	17	-03

AUG 1963	10	9	8	7	6	5

SMRP, University of Chicago

KAGOSHIMA 47827 31° 38' N, 130° 36' E HEIGHT ANOMALY IN METERS Nb 8

	-9	42	7	-1	47	27	2	39	85	33	35	1	-22	15	-55
MB 100	32	69	28	23	87	57	38	-3	16	57	11	29	-7	-45	-9	-85
	44	74	30	31	94	66	49	6	22	43	9	33	-5	-43	-36	-108
	41	65	23	21	30	48	47	2	12	27	4	13	-5	-42	-38	-116
	38	56	2	8	48	27	40	-3	13	15	8	4	-6	-42	-32	-112
200	31	44	1	-9	25	8	26	-10	0	7	-23	-3	-13	-45	-22	-104
	13	22	-21	-45	-17	-27	-12	-29	-26	-14	-46	-21	-23	-40	-14	-82
300	-04	5	-41	-66	-51	-61	-42	-48	-45	-32	-55	-33	-28	-33	-11	-68
	-8	-7	-57	-82	-85	-89	-69	-65	-63	-50	-57	-42	-28	-33	-9	-58
400	-8	-10	-69	-96	-115	-110	-91	-79	-77	-65	-59	-46	-28	-36	-9	50
500	-8	-23	-76	-115	-152	-140	-124	-99	-93	-82	-58	-51	-34	-35	-11	-35
	-11	-28	-76	-125	-170	-159	-148	-116	-103	-86	-73	-62	-35	-31	-13	-20
700	-11	-29	-74	-130	-181	-181	-162	-119	-112	-89	-78	-63	-39	-25	-9	-5
	-14	-33	-66	-135	-187	-192	-166	-116	-103	-85	-70	-62	-42	-23	-8	10
1000	-18	-35	-67	-133	-190	-202	-171	-118	-105	-93	-70	-57	-45	-18	-6	19

AUG 1963	10	9	8	7	6	5

SMRP, University of Chicago

KAGOSHIMA 47827 31°38'N, 130°36'E WINDS ALOFT Nb 9

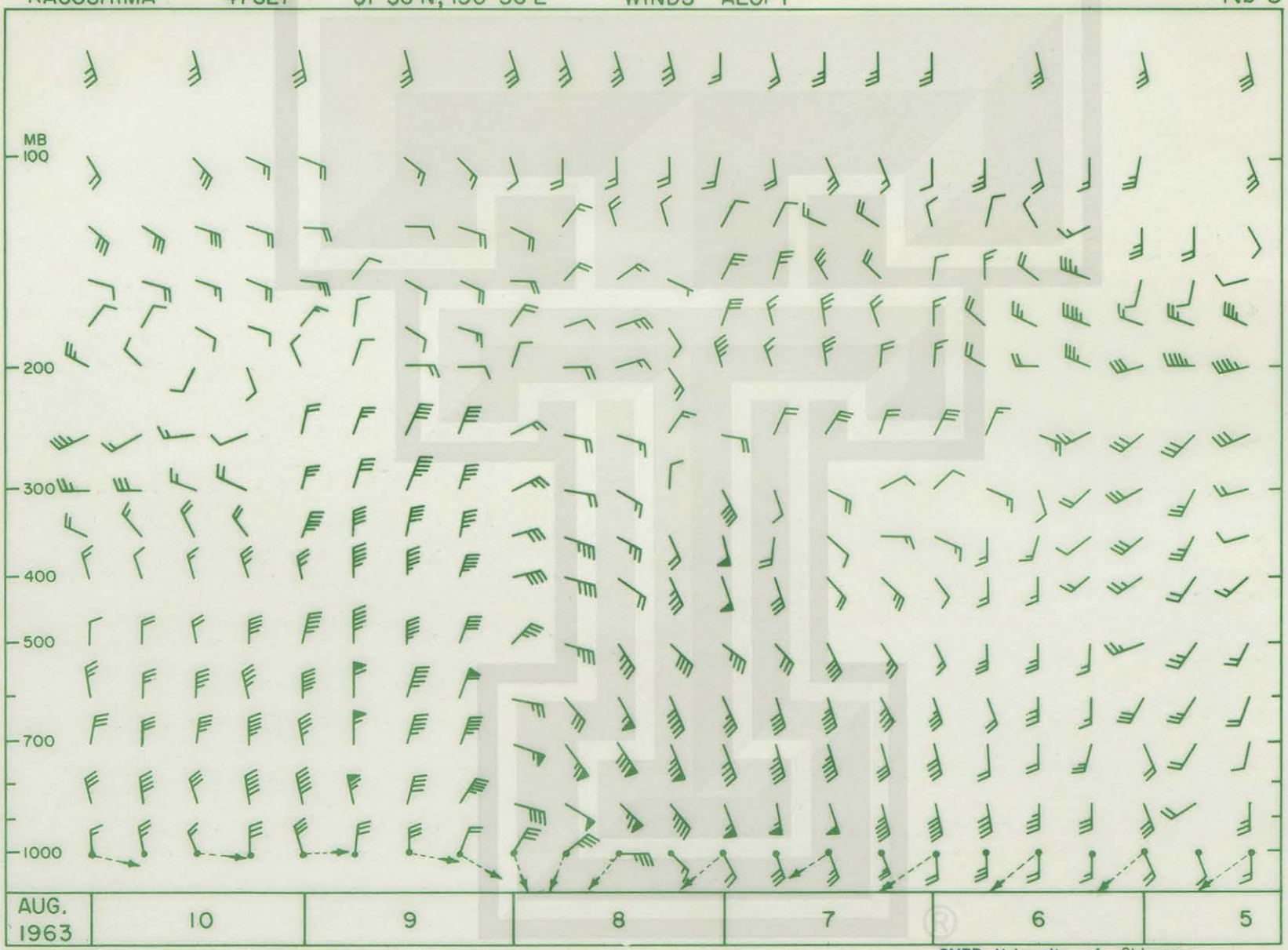

SMRP, University of Chicago

Nb 10

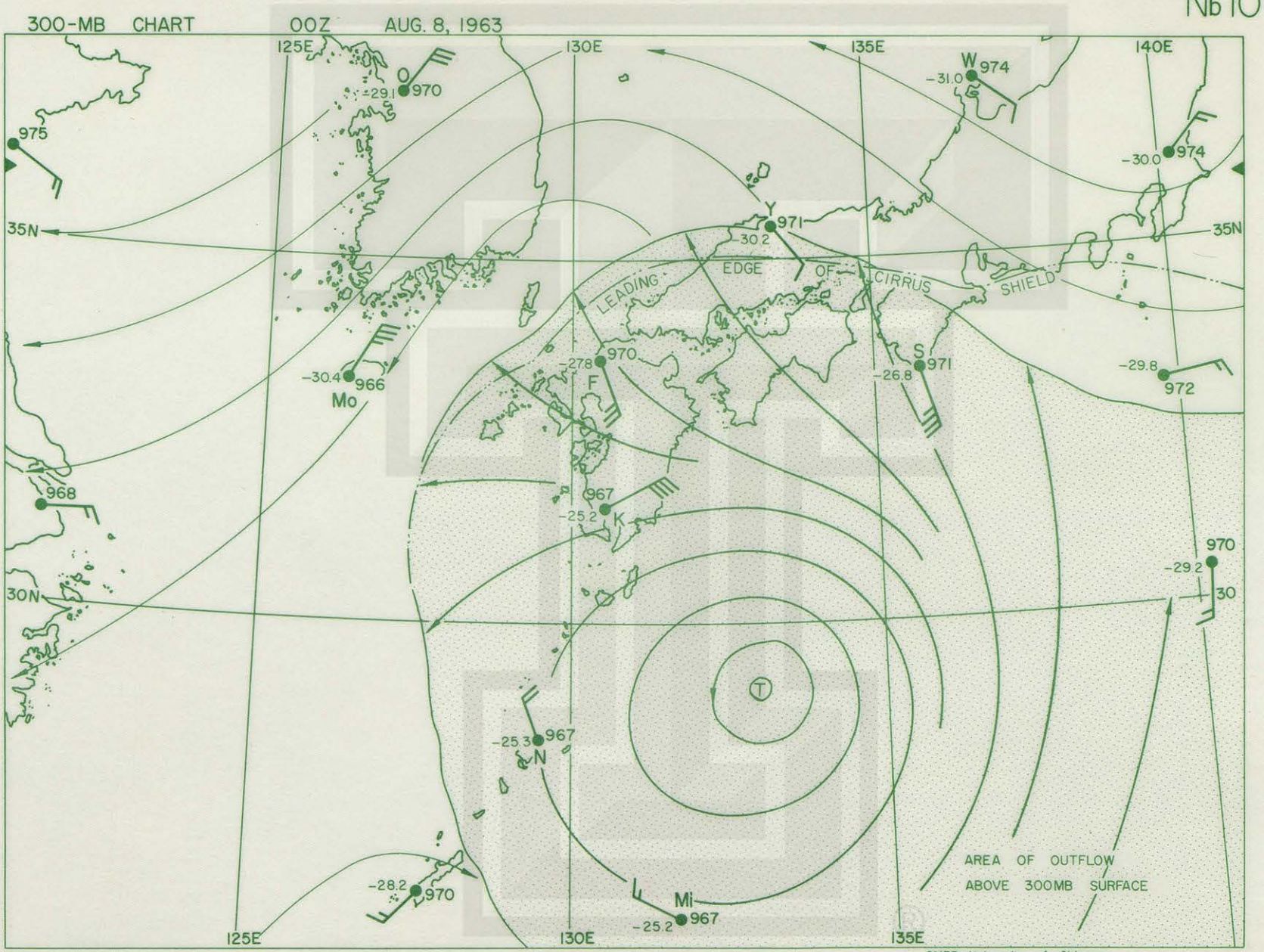

SMRP, University of Chicago

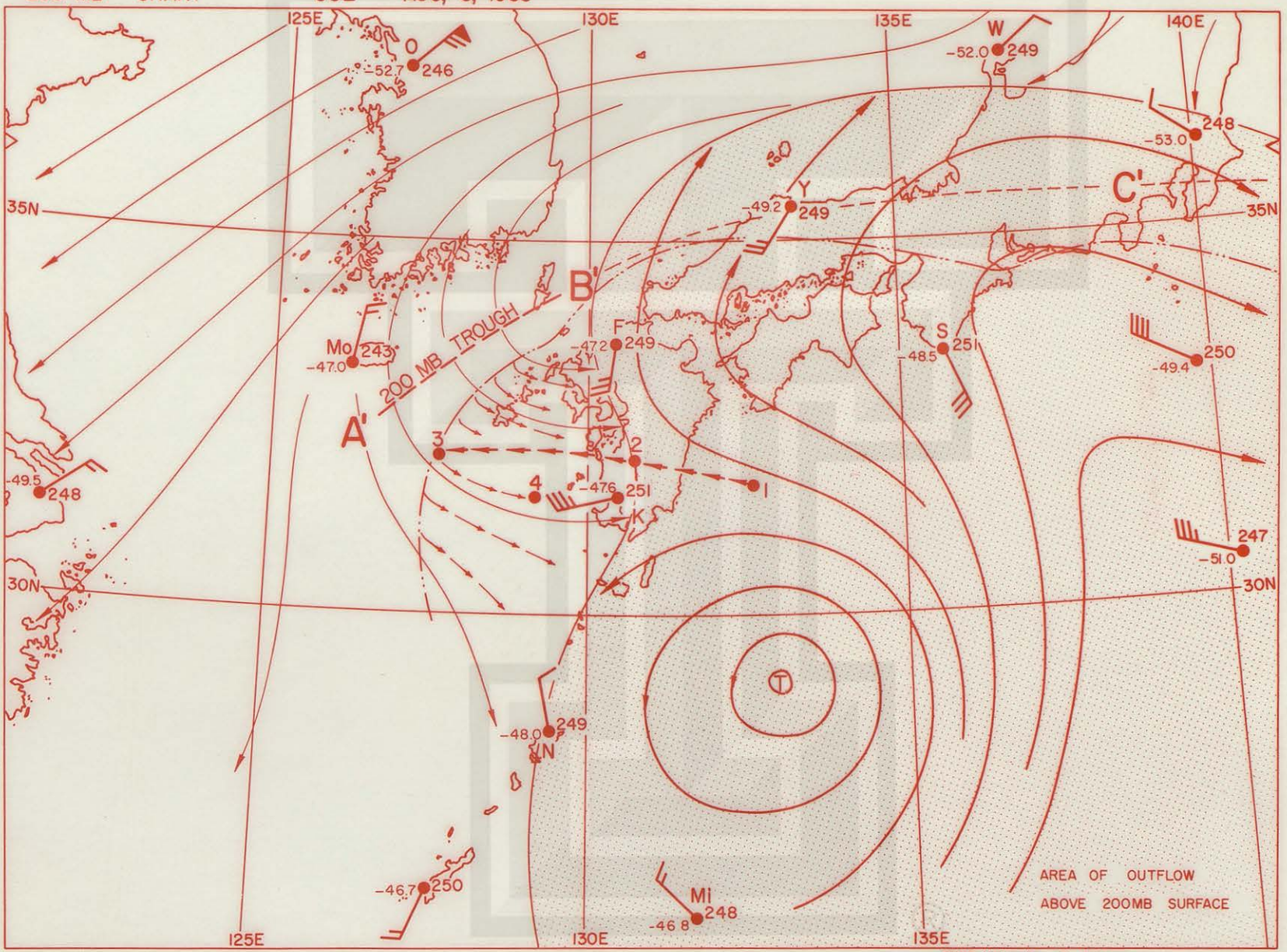
200-MB CHART 00Z AUG, 8, 1963
Nb 11
125E
130E
135E
140E
35N
30N
O
-52.7
246
W
-52.0
249
248
-53.0
Y
-49.2
249
C'
B'
F
-47.2
249
Mo
243
-47.0
200 MB TROUGH
A'
S
251
-48.5
250
-49.4
-49.5
248
3
2
4
-47.6
251
1
K
247
-51.0
-48.0
249
N
-46.7
250
MI
248
-46.8
AREA OF OUTFLOW
ABOVE 200MB SURFACE
SMRP, University of Chicago

Nb 12

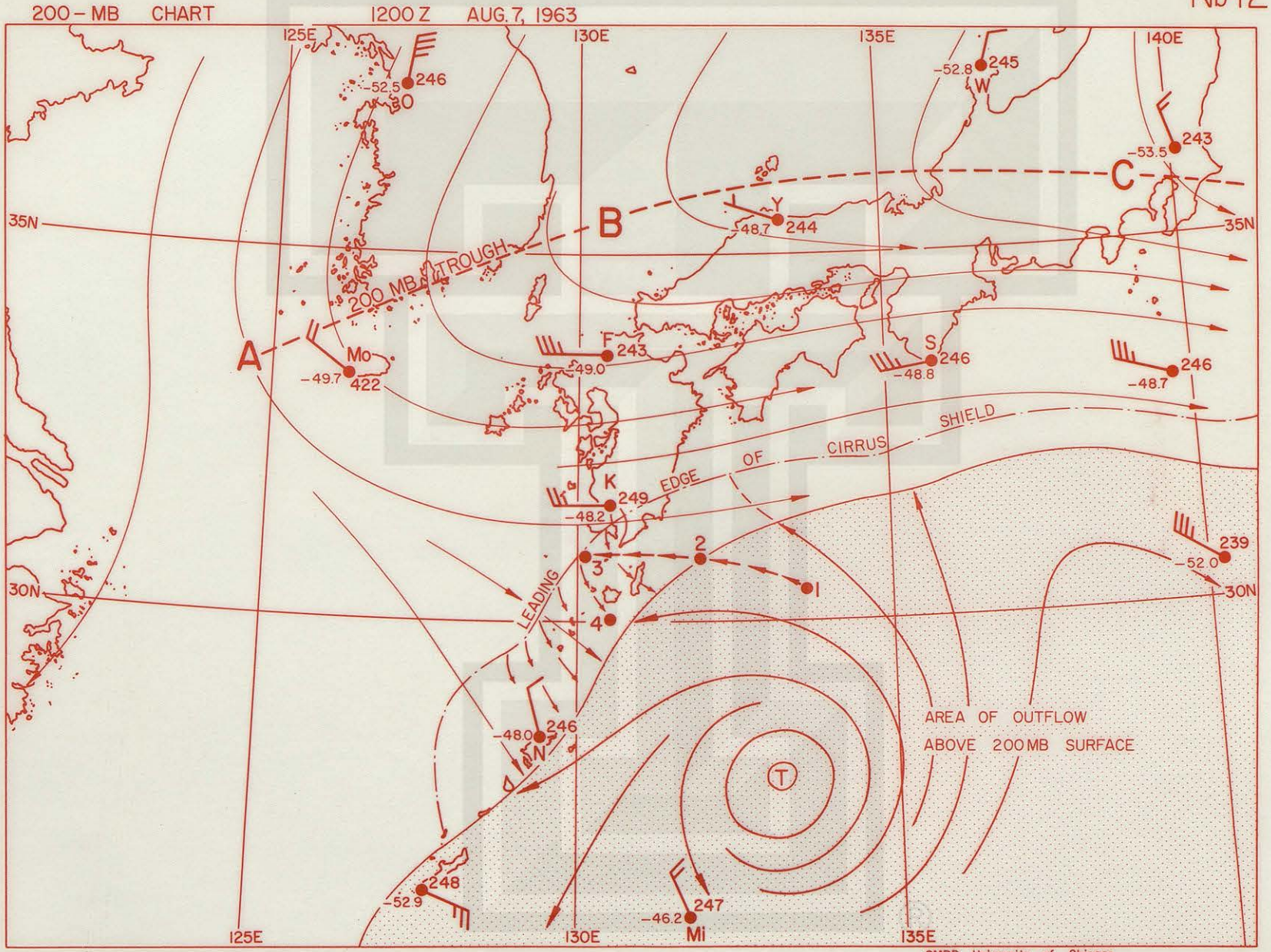
200 – MB CHART
1200 Z AUG. 7, 1963
125E
130E
135E
140E
35N
30N
-52.5 246
30
-52.8 245
W
-53.5 243
C
B
Y
-48.7 244
200 MB TROUGH
A
Mo
-49.7 422
F 243
-49.0
S 246
-48.8
246
-48.7
SHIELD
CIRRUS
OF
EDGE
K 249
-48.2
2
3
1
LEADING
4
239
-52.0
-48.0 246
N
AREA OF OUTFLOW
ABOVE 200 MB SURFACE
T
248
-52.9
247
-46.2
Mi
SMRP, University of Chicago

CLOUD PHOTOGRAPHS AUG 5, 1963

TIROS VII
A/O 692
R/O 692
CAMERA 1

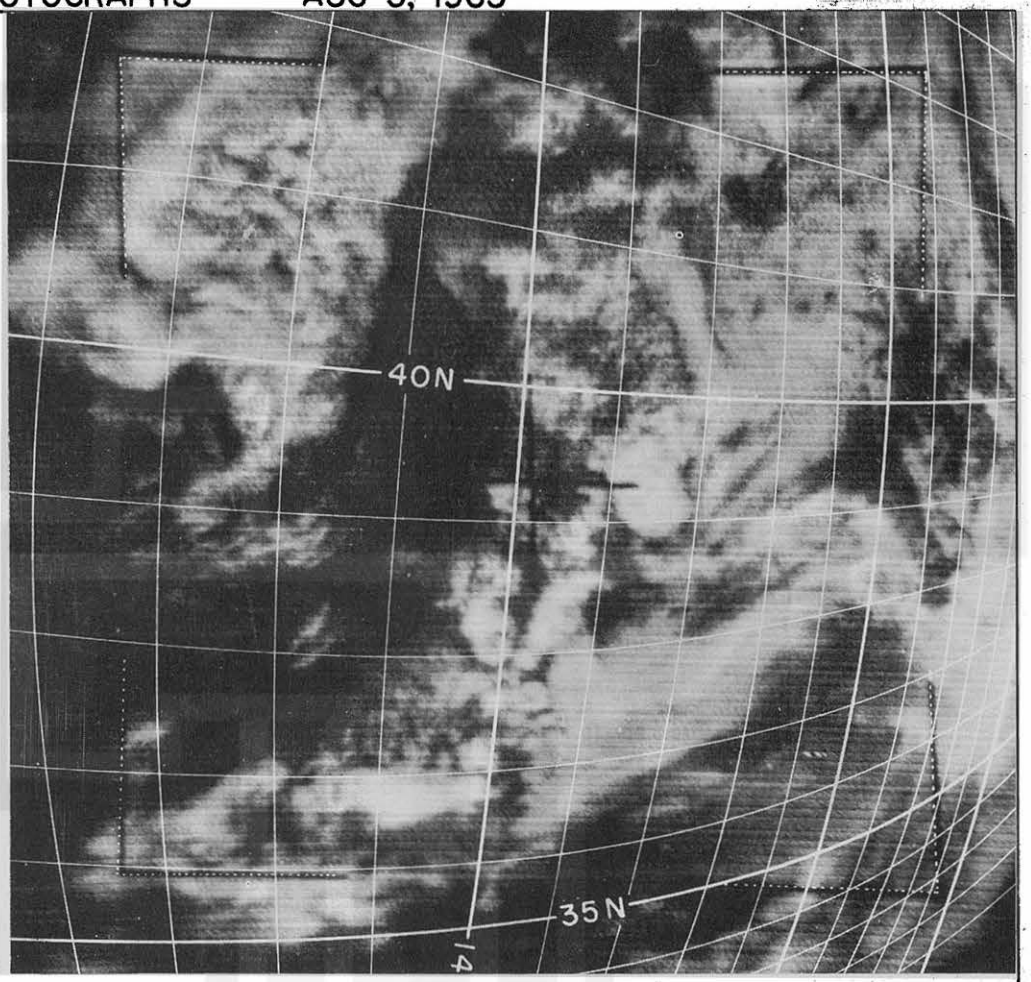

FRAME 5T
TIME 0527.0
ϕ^{TSP} = 40.2N
θ^{TSP} = 137.0E
H = 627 Km
τ = 25.6°
α^{PL} = 108.1°

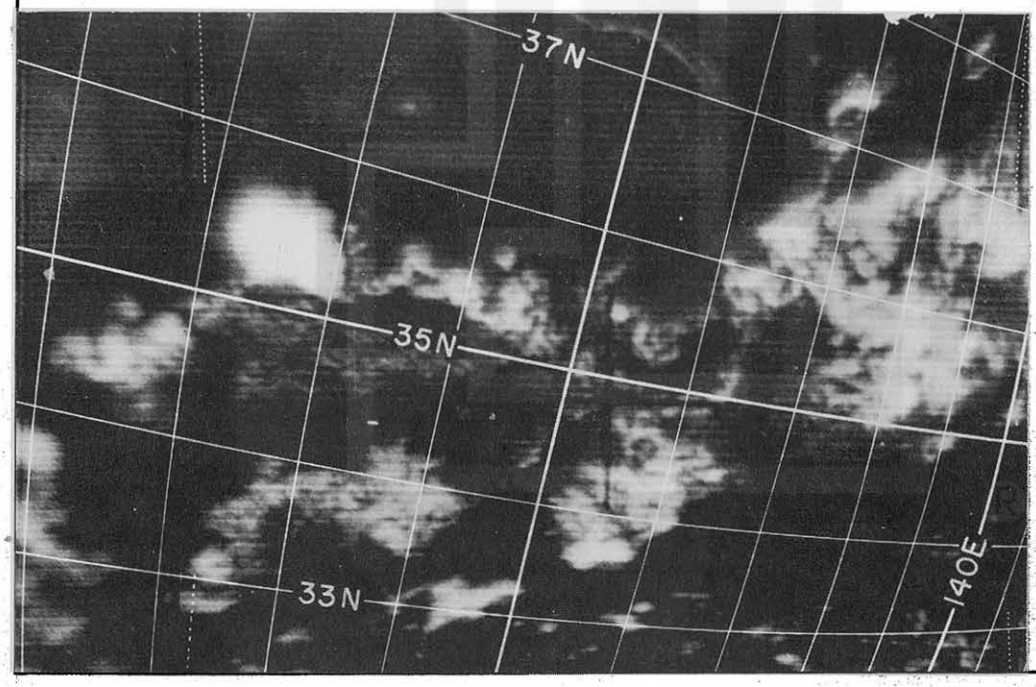

FRAME 8T
TIME 0525.5
ϕ^{TSP} = 36.0N
θ^{TSP} = 132.7E
H = 627 Km
τ = 23.8°
α^{PL} = 116.7°

Oa 2

CLOUD TRANSFER MAP AUG. 5, 1963

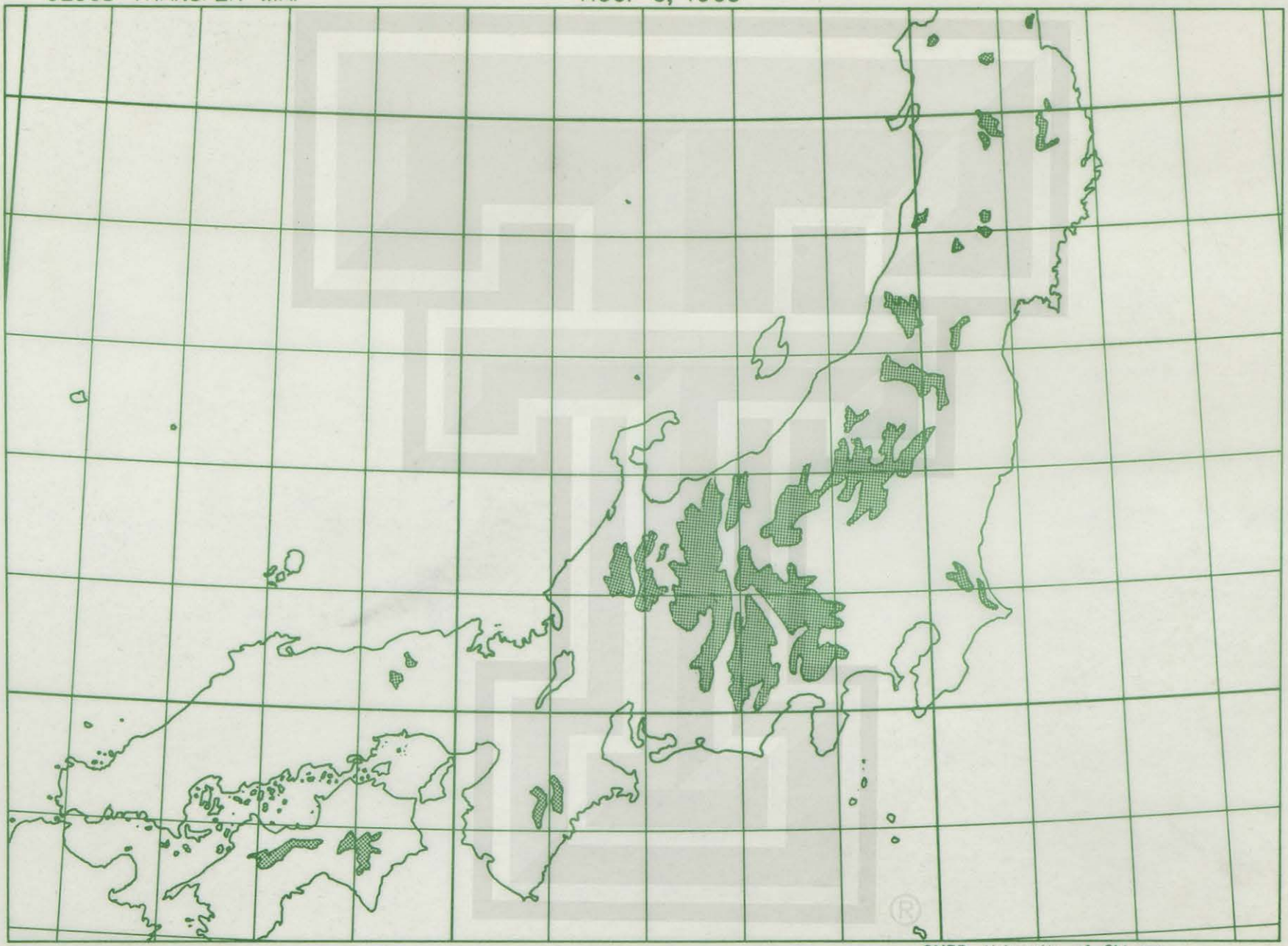

SMRP, University of Chicago

CLOUD CHART 0526 Z AUG 5, 1963 0a 3

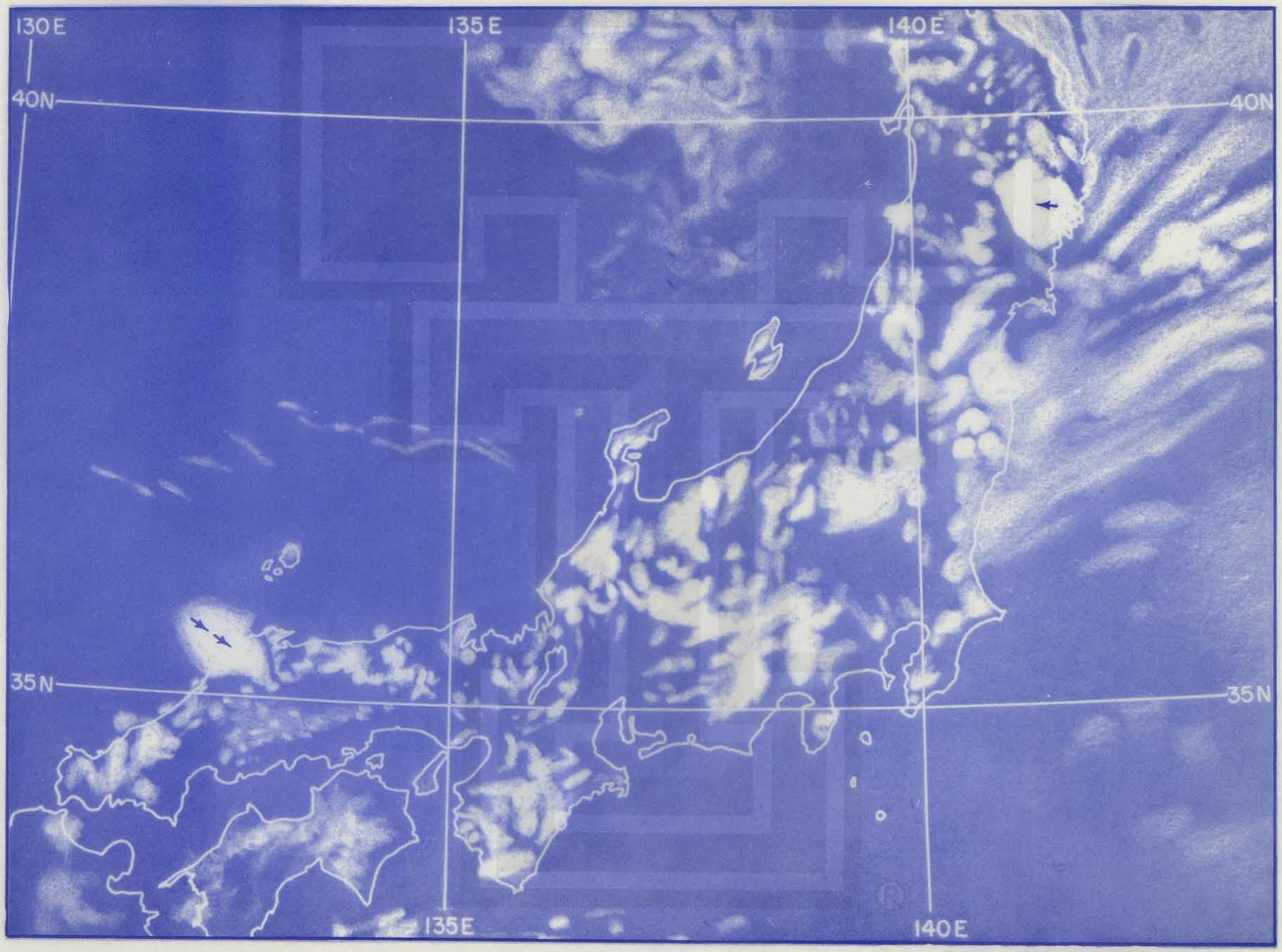

SMRP, University of Chicago

SURFACE MAP 0000 Z AUG 5, 1963 Oa 4

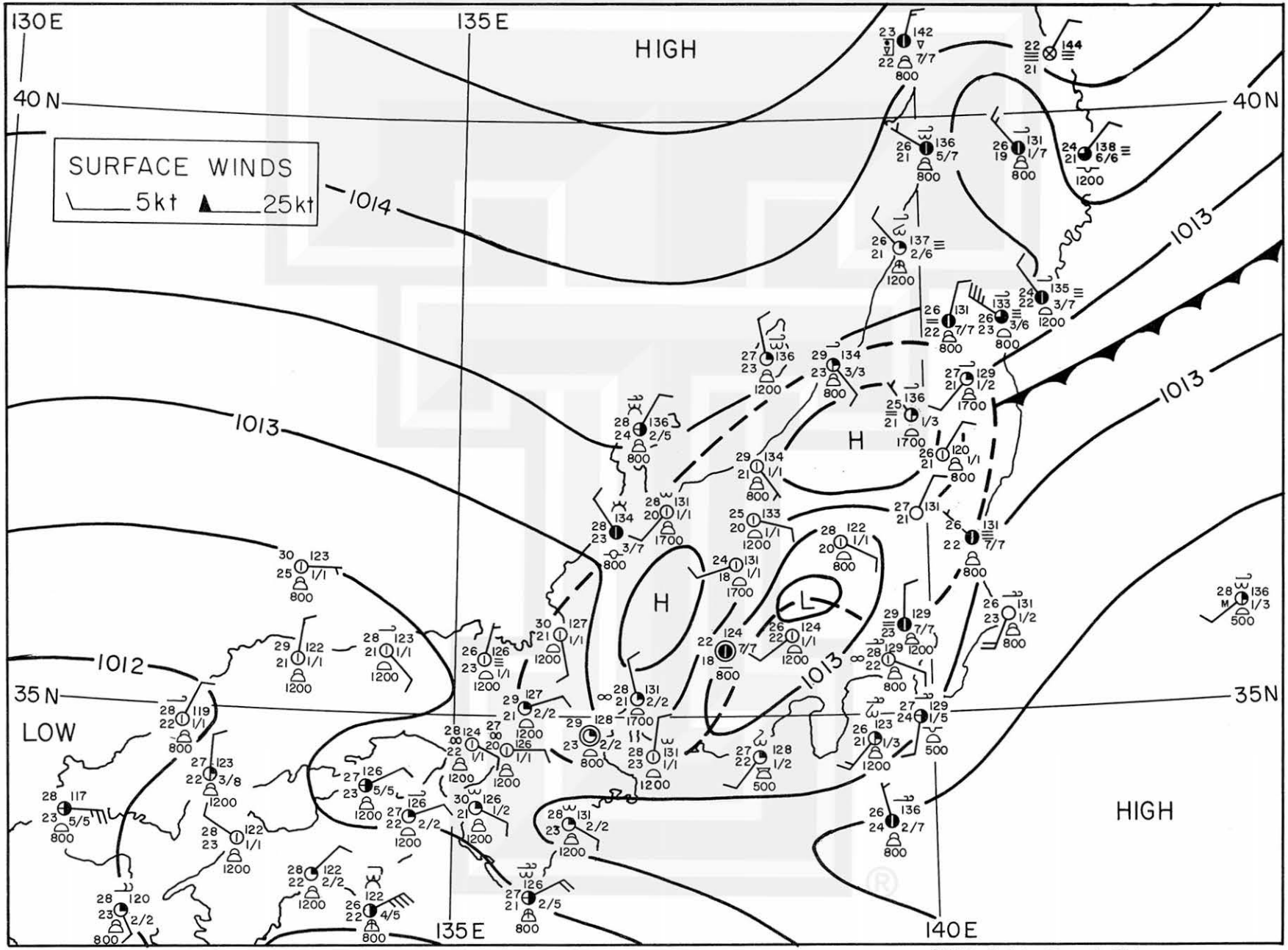

SMRP, University of Chicago

SURFACE MAP 1200 Z AUG 5, 1963 Oa 5

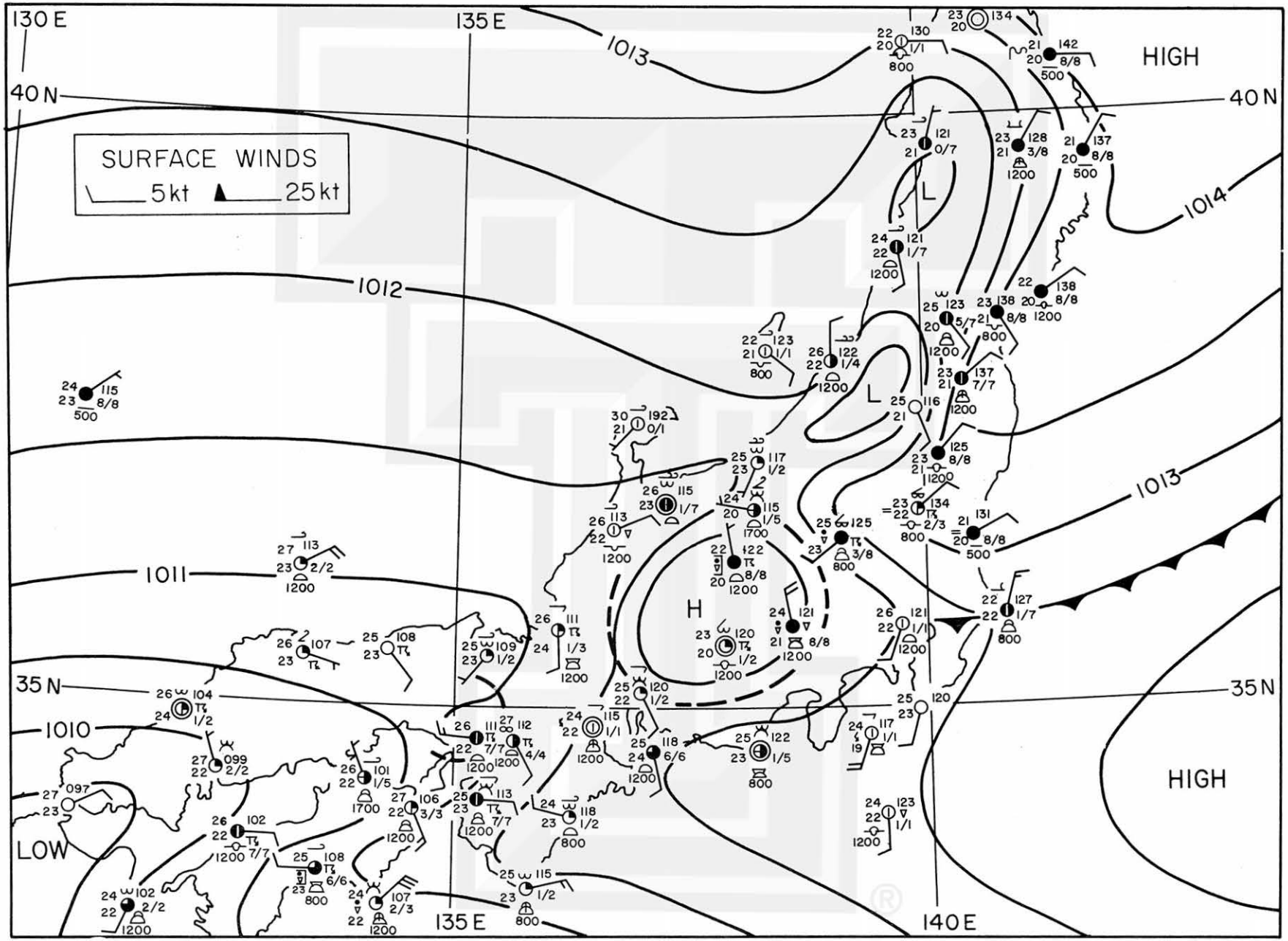

SMRP, University of Chicago

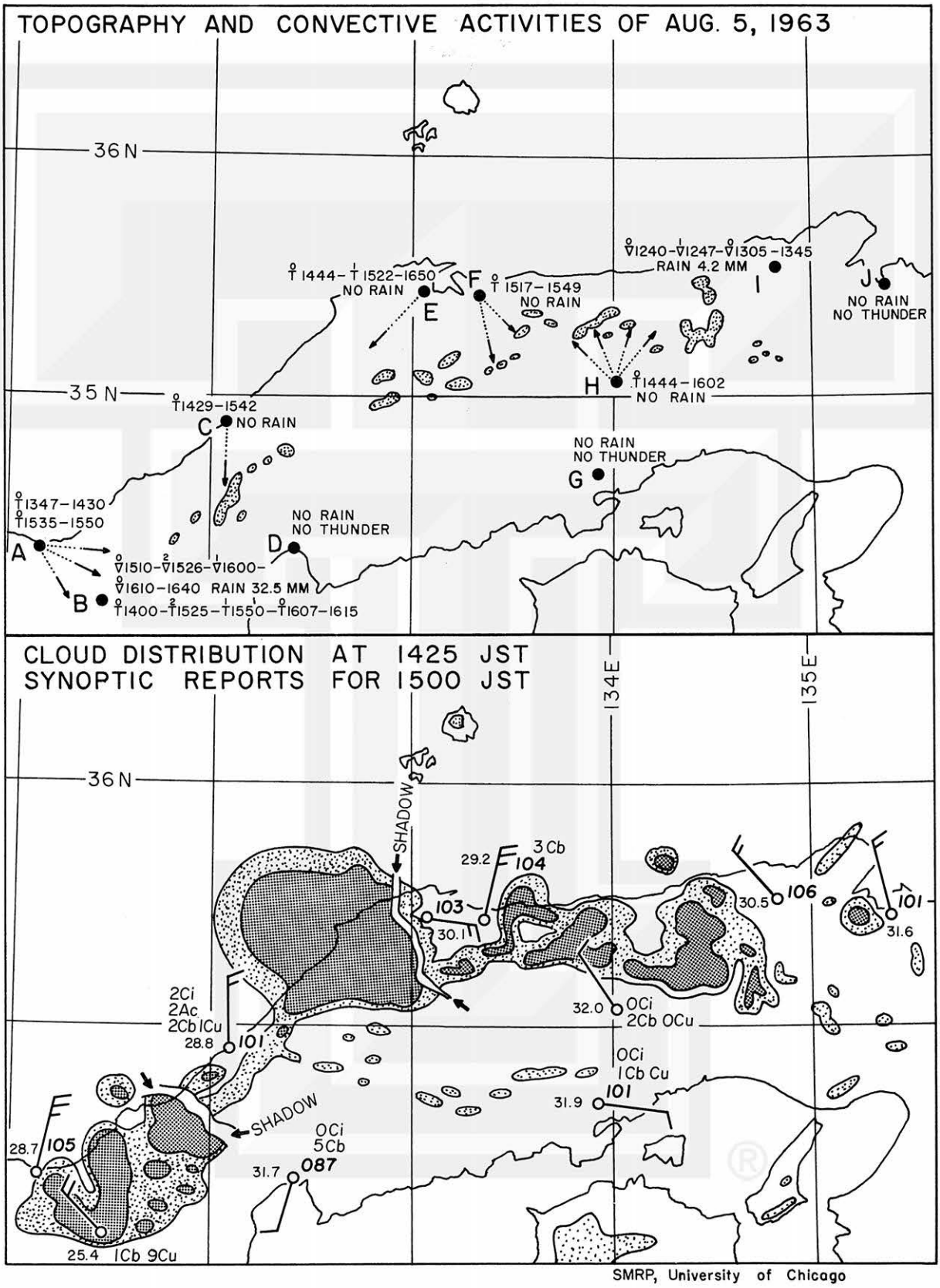
TOPOGRAPHY AND CONVECTIVE ACTIVITIES OF AUG. 5, 1963
36 N
35 N
♀V1240-V1247-♀V1305-1345
RAIN 4.2 MM
I
J
NO RAIN
NO THUNDER
♀T 1444-T 1522-1650
NO RAIN
E
F
♀T 1517-1549
NO RAIN
H
♀T1444-1602
NO RAIN
♀T1429-1542
C
NO RAIN
NO RAIN
NO THUNDER
G
♀T1347-1430
♀T1535-1550
A
NO RAIN
NO THUNDER
D
♀V1510-2V1526-1V1600-
♀V1610-1640 RAIN 32.5 MM
B
♀T1400-2T1525-1T1550-♀T1607-1615
CLOUD DISTRIBUTION AT 1425 JST
SYNOPTIC REPORTS FOR 1500 JST
134E
135E
36 N
SHADOW
29.2
F
104
3Cb
103
30.11
30.5
106
101
31.6
2Ci
2Ac
2Cb ICu
28.8
101
32.0
OCi
2Cb OCu
OCi
ICb Cu
31.9
101
SHADOW
28.7
F
105
OCi
5Cb
31.7
087
25.4 ICb 9Cu
SMRP, University of Chicago

Oa 7

RADIATION MAP 0524 Z AUG 5, 1963

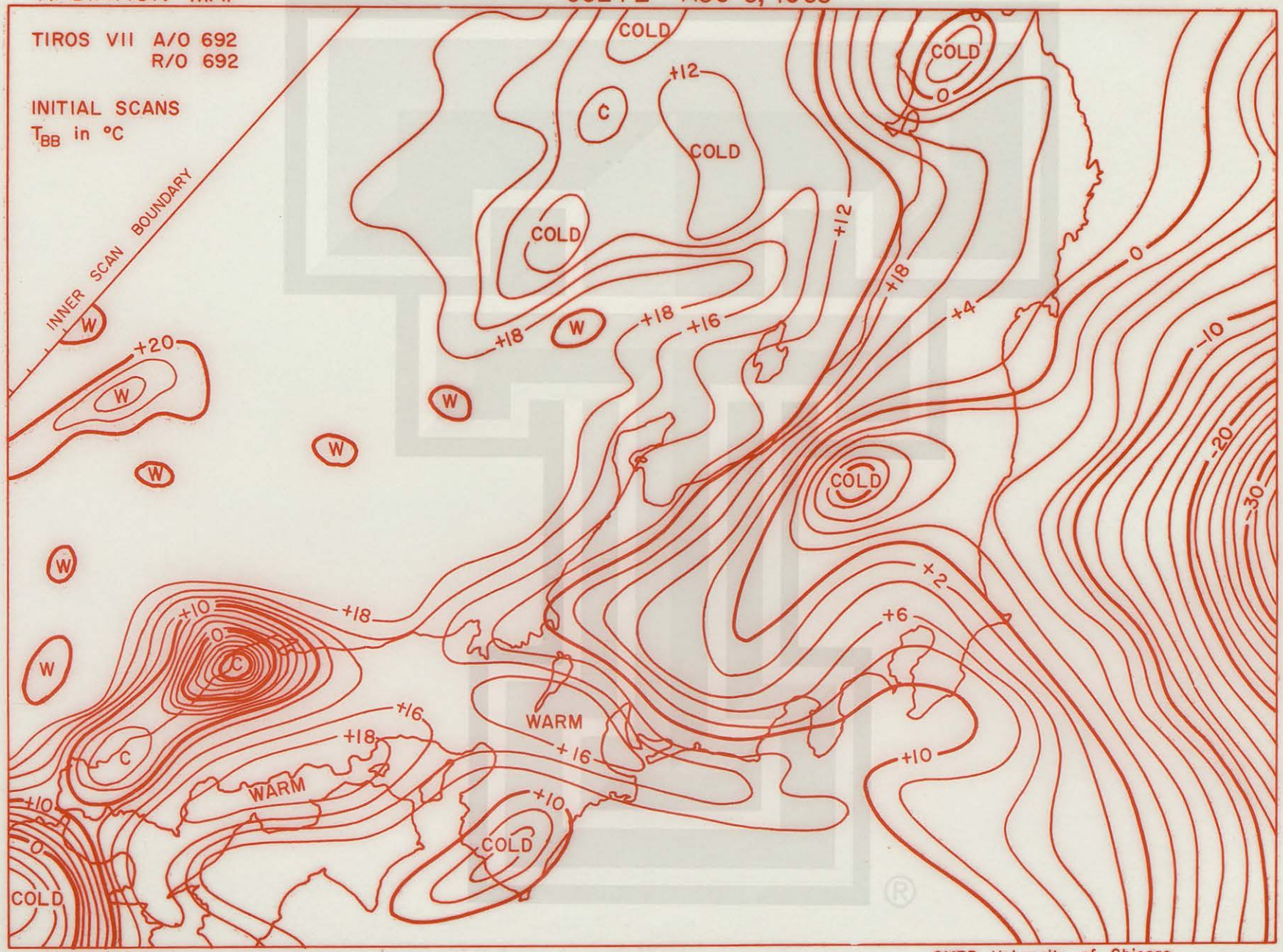

SMRP, University of Chicago

Ob 1

CLOUD PHOTOGRAPH 0520 Z AUG 5, 1963

TIROS VII A/O 962 R/O 962

TAPE CAMERA 1

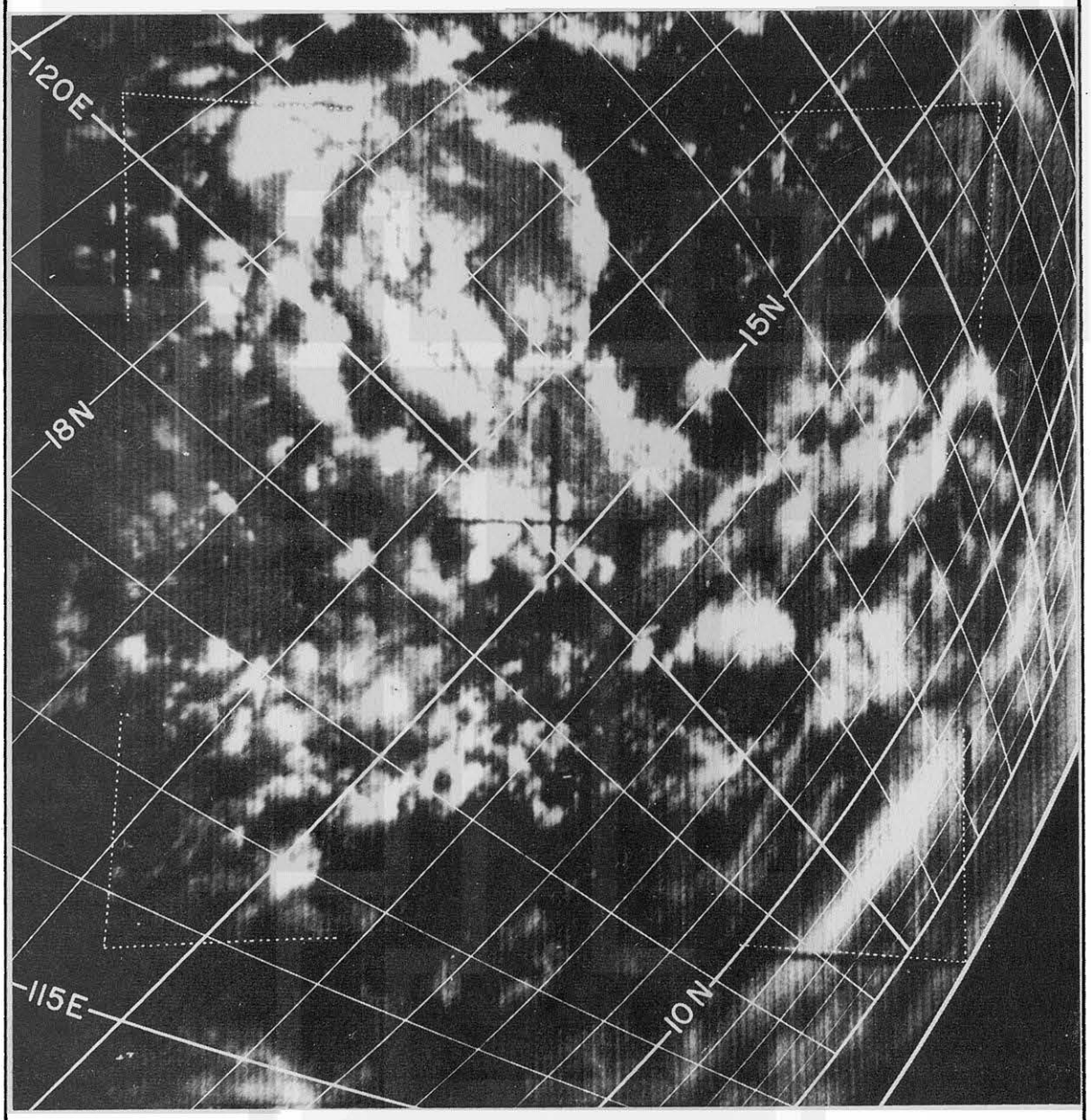

FRAME 20 TIME 0519.5 Z

ϕ^{TSP} = 18.1 N θ^{TSP} = 119.2 E H = 626 km

τ = 27.9° α^{PL} = 156.9°

SMRP, University of Chicago

CLOUD CHART 0520 Z AUG 5, 1963

Ob 2

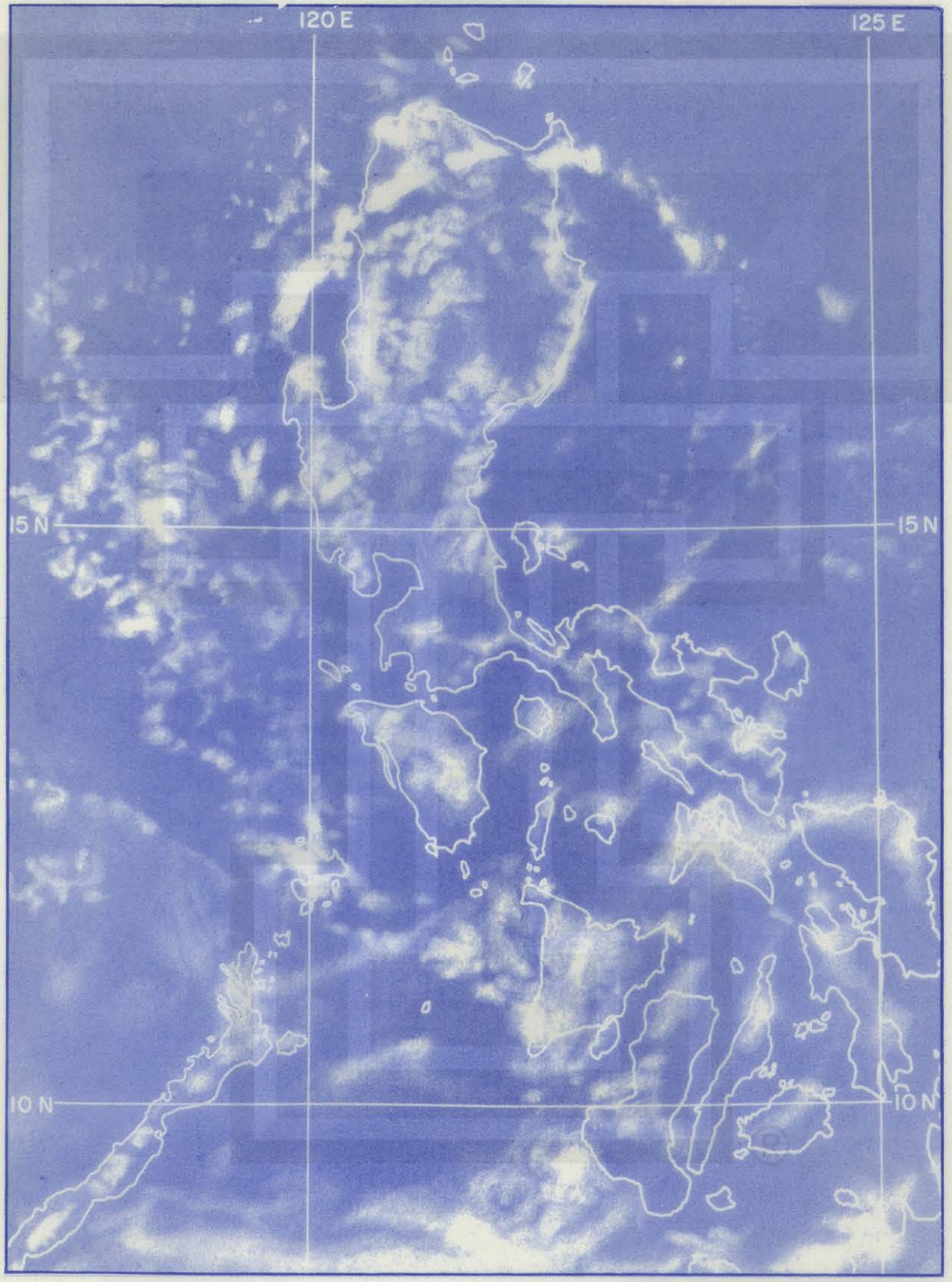

SMRP, University of Chicago

Ob 3

SURFACE MAP 0600 Z AUG 5, 1963

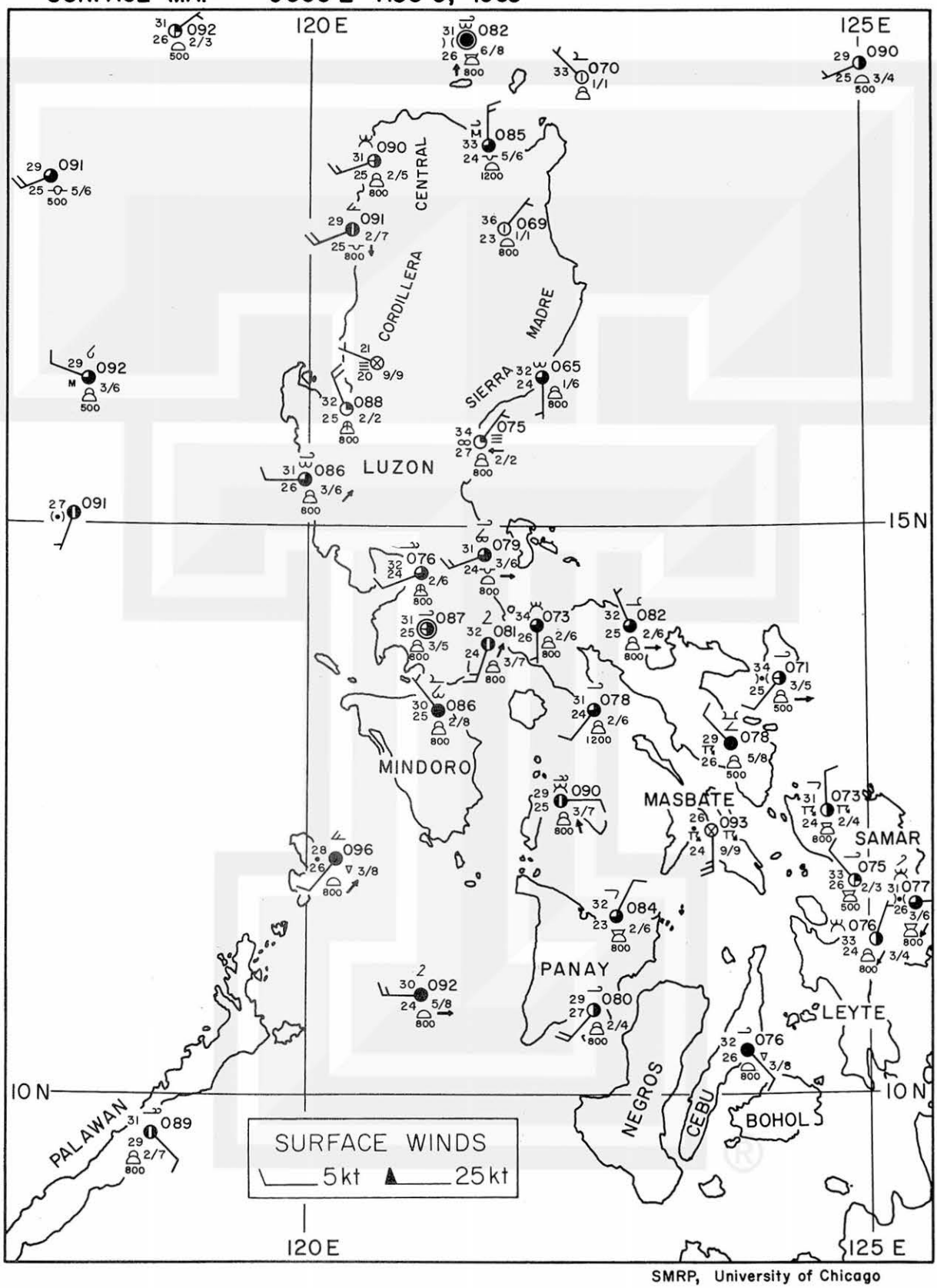

SMRP, University of Chicago

Ob 4

SURFACE ISOBARS 0600Z AUG 5, 1963

SMRP, University of Chicago

CLOUD PHOTOGRAPHS AUG 8, 1963

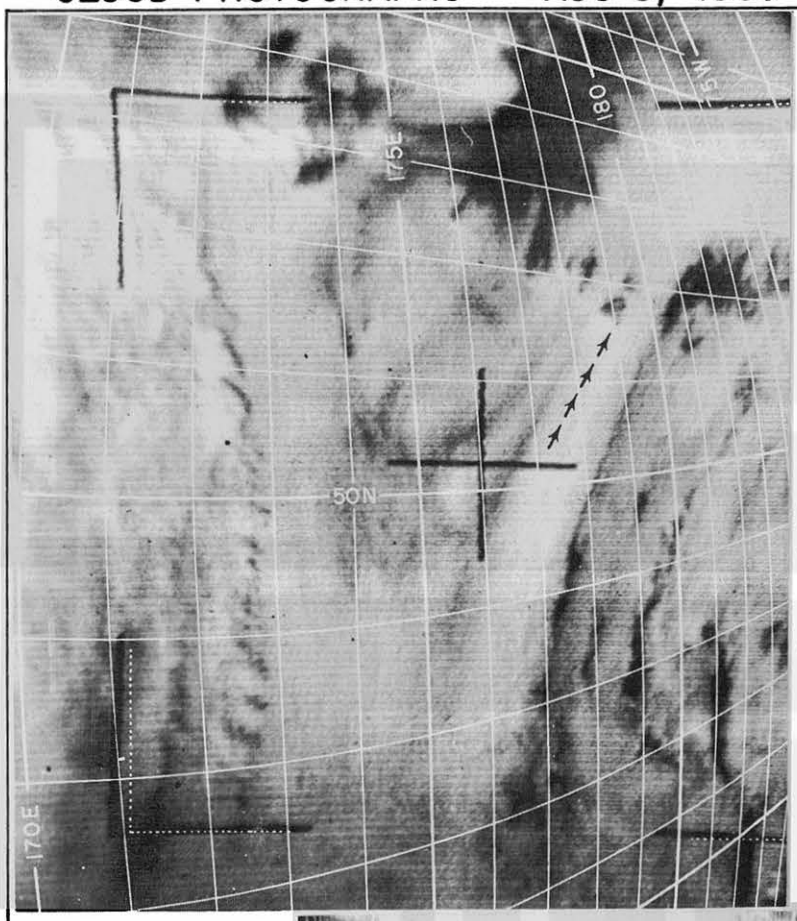

TIROS VII
A/O 735 R/O 735
TAPE CAMERA 2

FRAME 8
TIME 0319.5 Z
ϕ^{TSP} = 49.8 N
θ^{TSP} = 170.5 E
H = 628 km
τ = 30.1°
α^{PL} = 87.4°

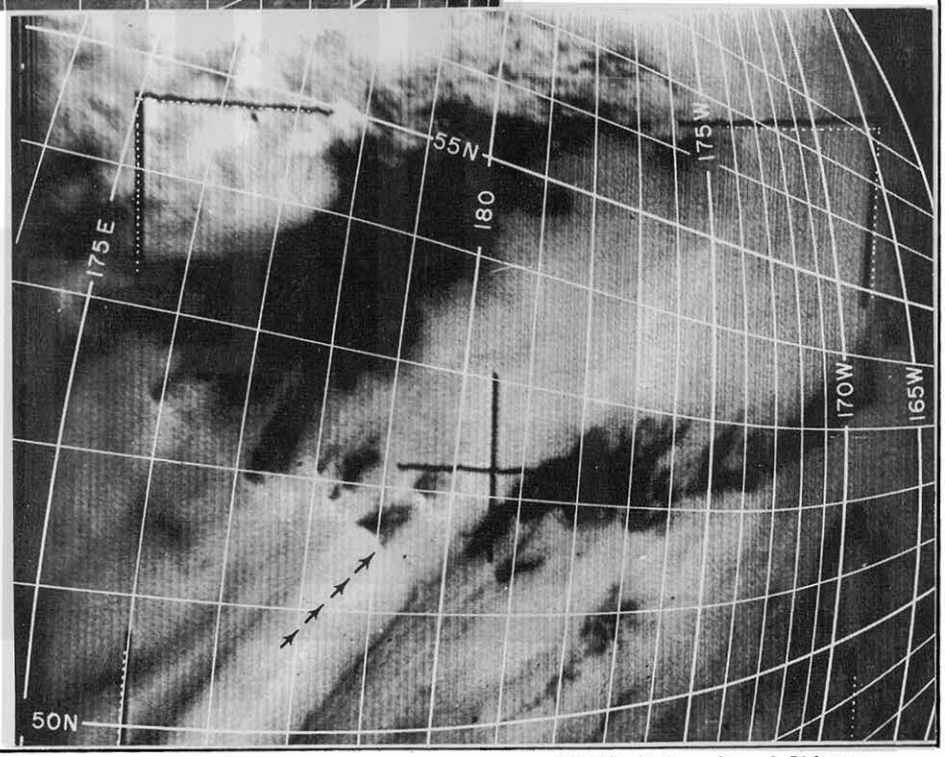

FRAME 6
TIME 0320.5 Z
ϕ^{TSP} = 51.8 N
θ^{TSP} = 175.1 E
H = 628 km
τ = 33.3°
α^{PL} = 88.1°

SMRP, University of Chicago

CLOUD CHART 0320Z AUG 8, 1963 P2

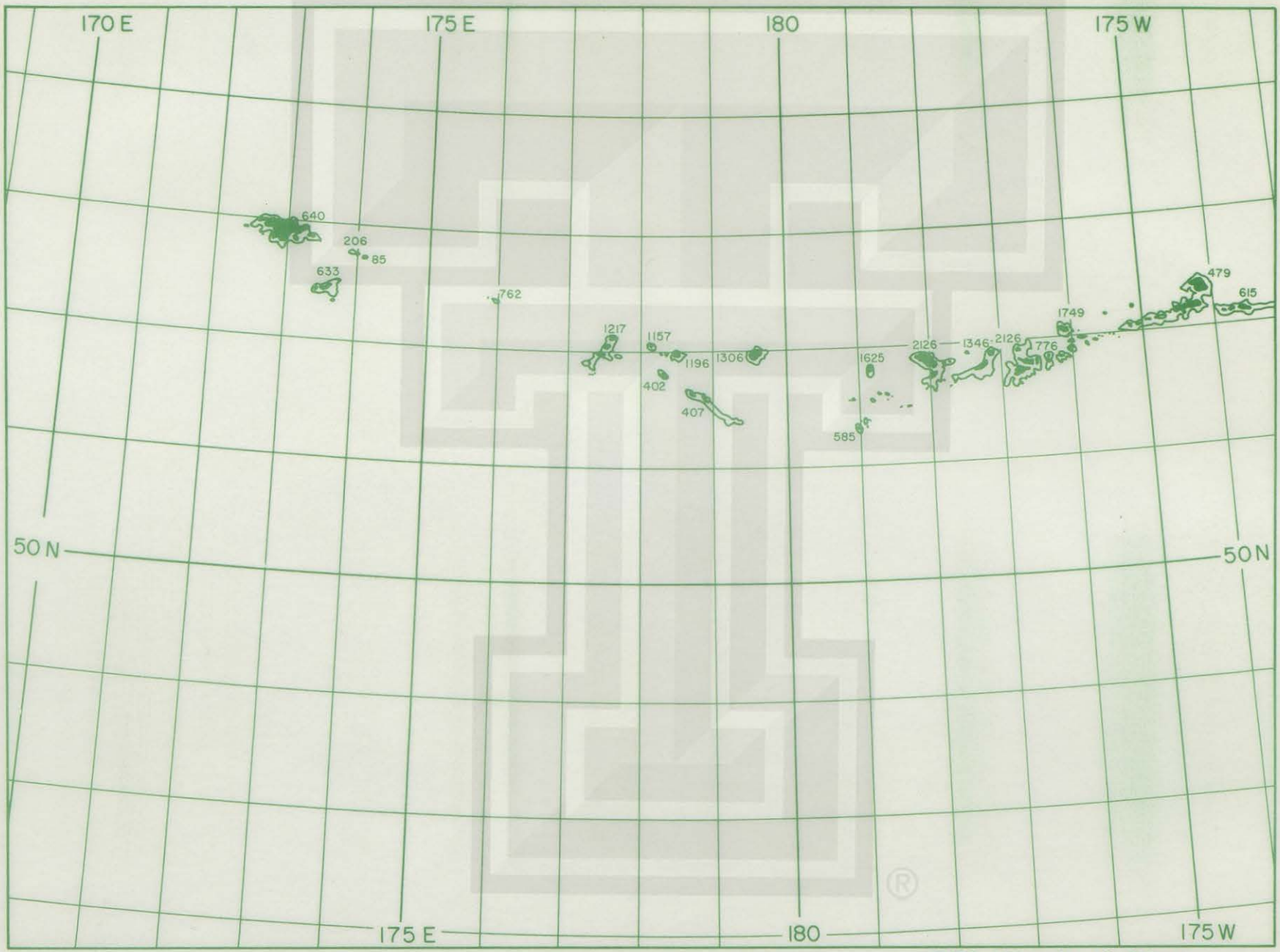

SMRP, University of Chicago

CLOUD CHART 0320 Z AUG 8, 1963 P 3

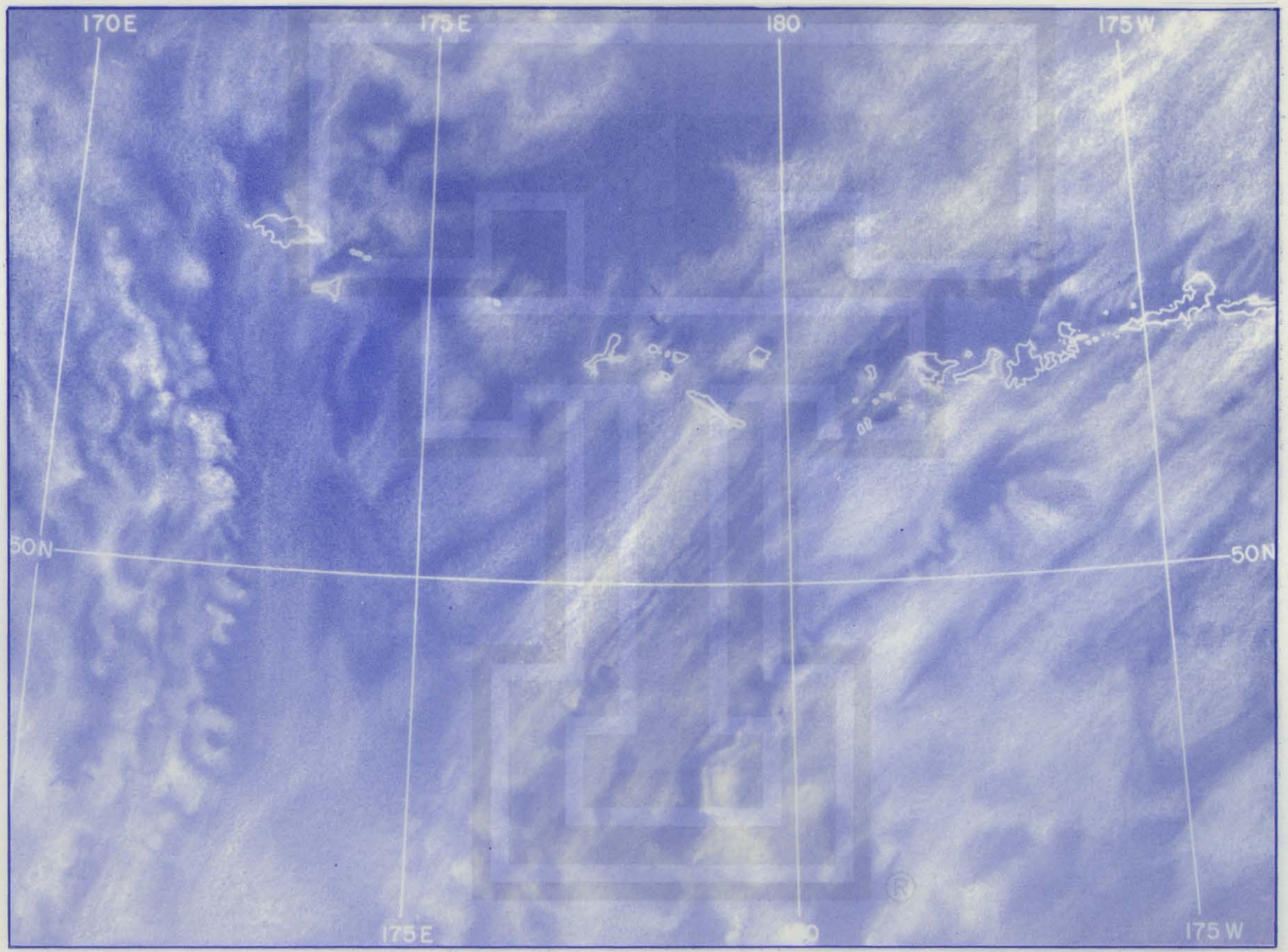

SMRP, University of Chicago

P 4

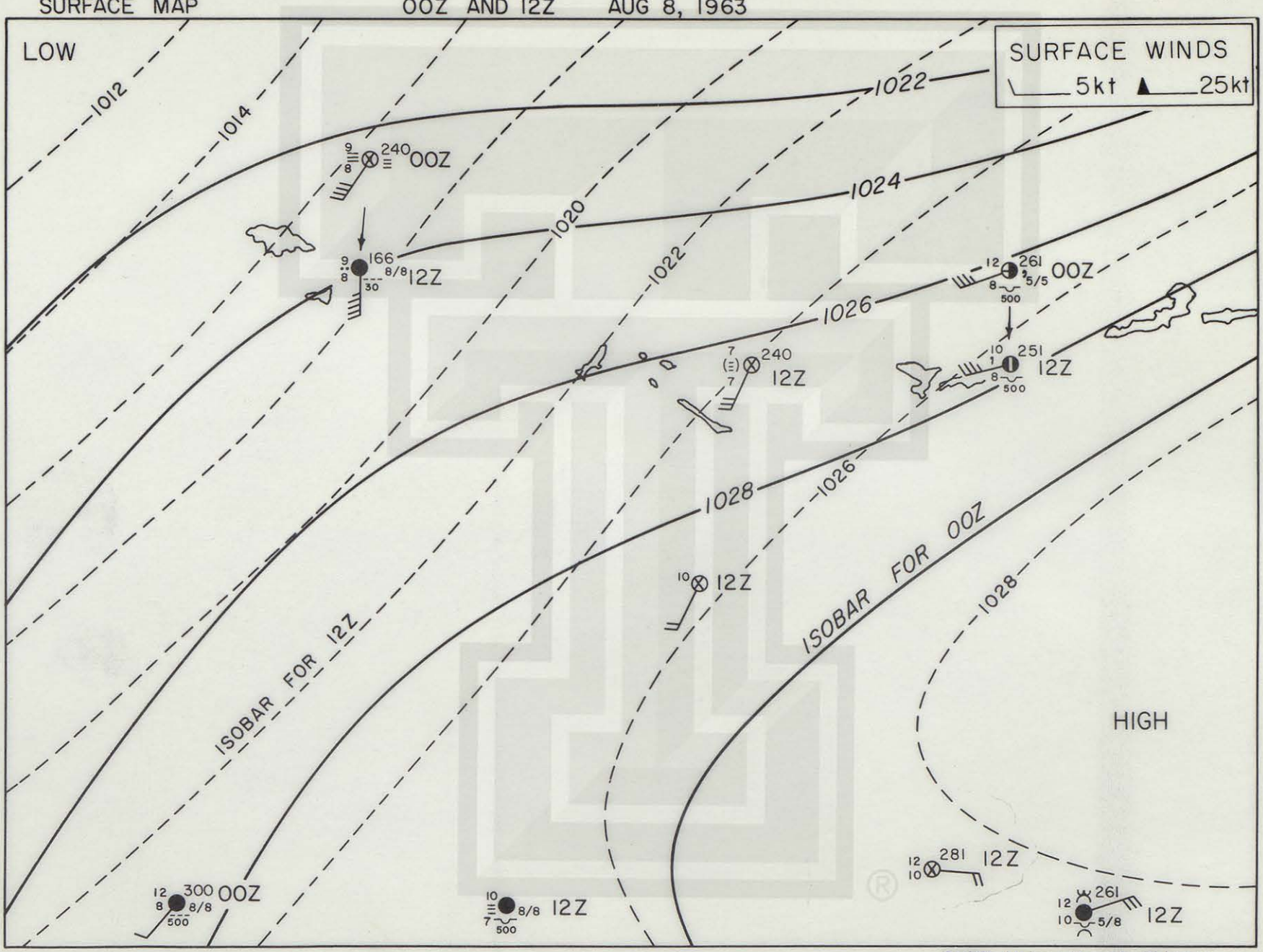

SMRP, University of Chicago

SURFACE MAP 0000 Z AUG 8, 1963 P5

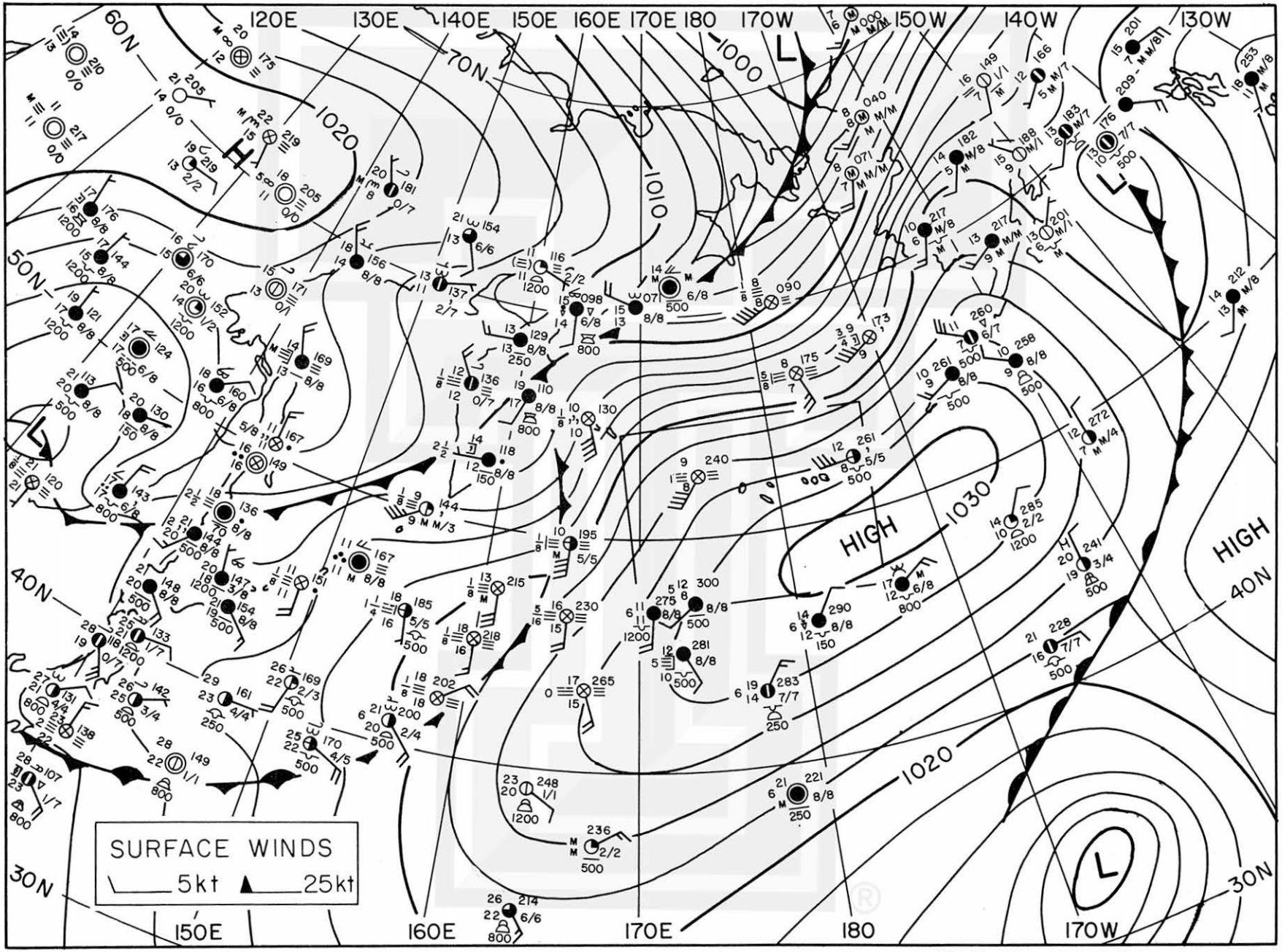

SMRP, University of Chicago

500 MB CHART 0000 Z AUG 8, 1963

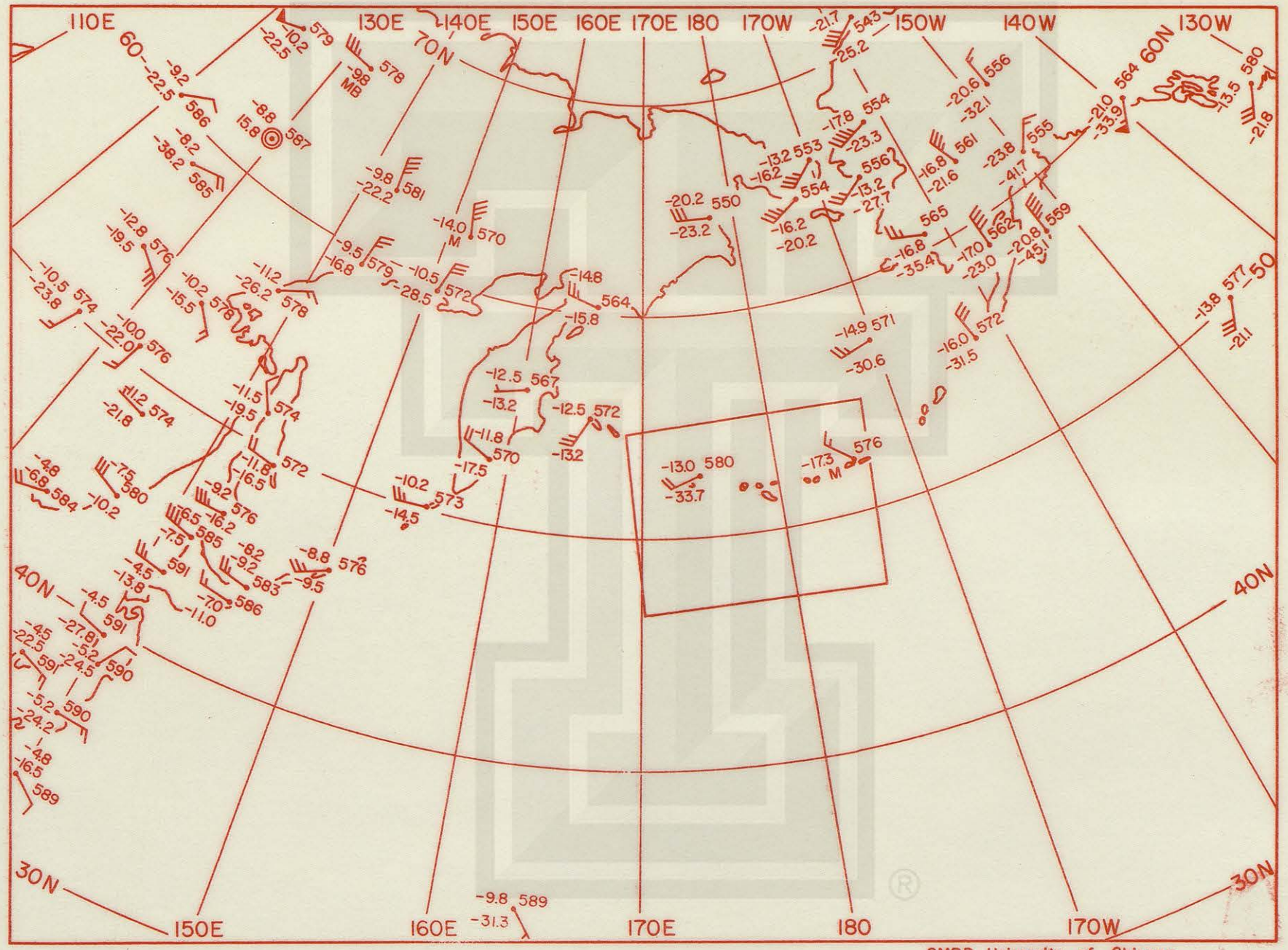

P 7

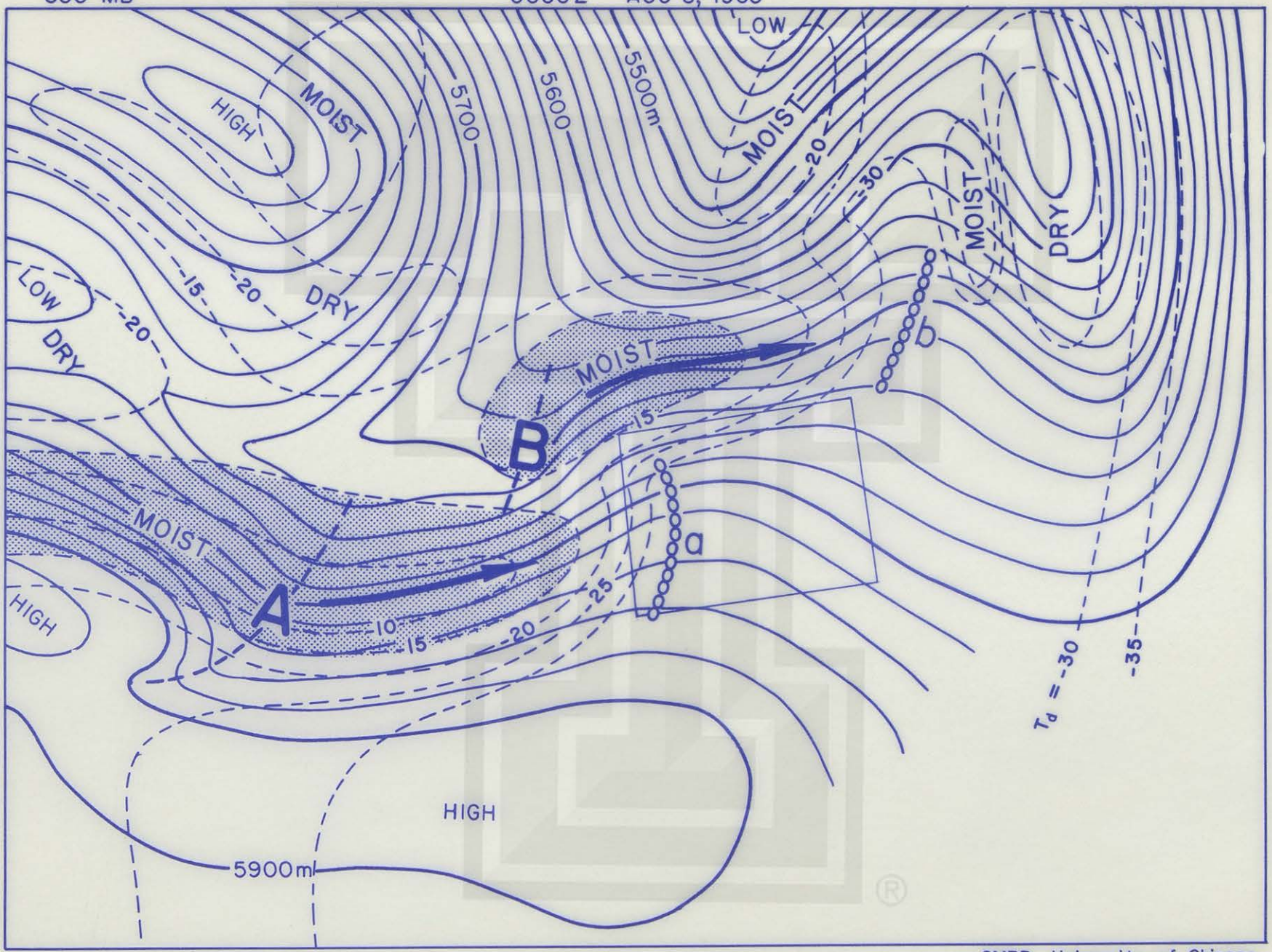

SMRP, University of Chicago

P8

RADIATION MAP 0320–0322Z AUG 8, 1963

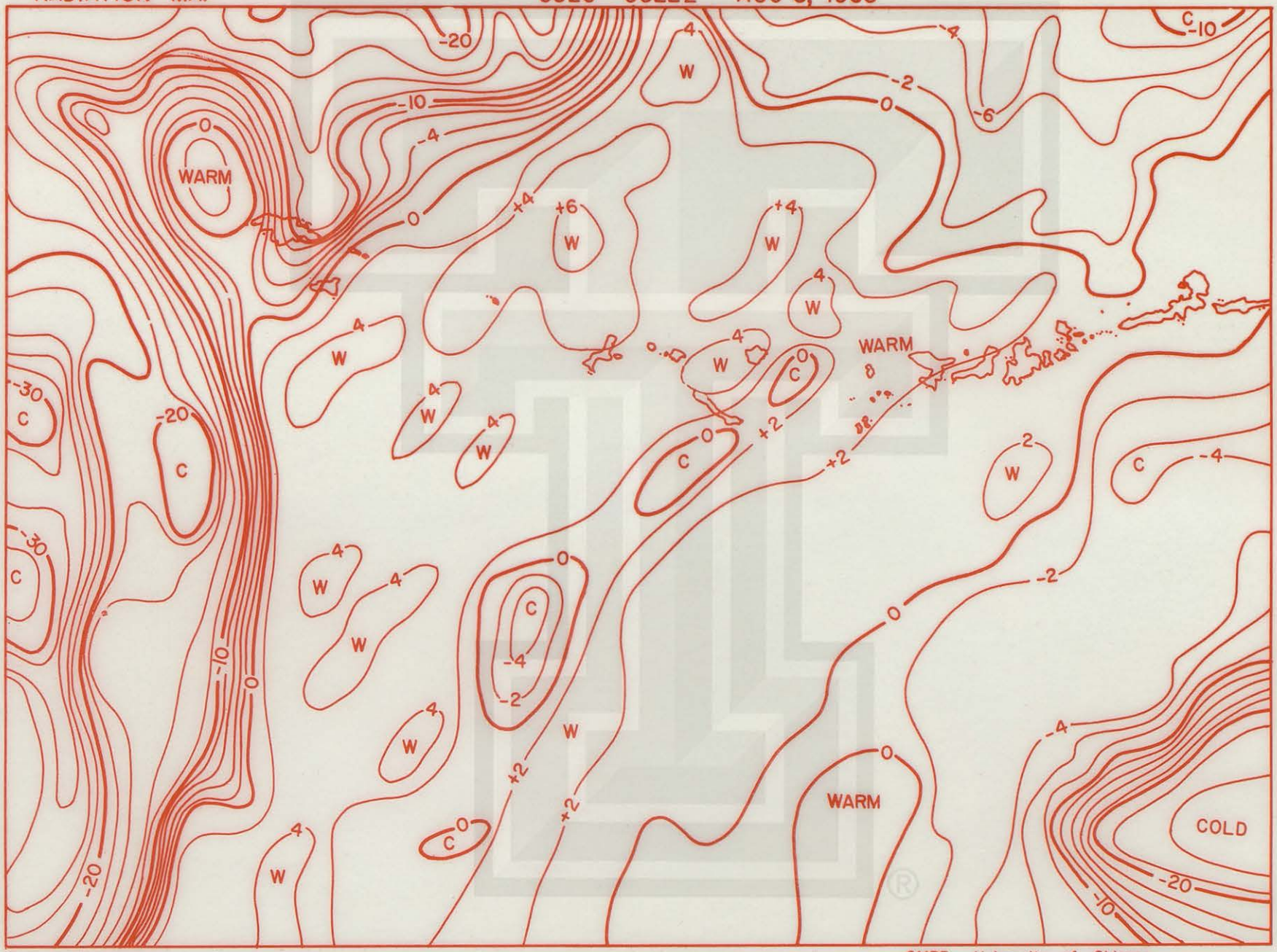

SMRP, University of Chicago

TIROS VII A/O 735 R/O 735

FRAME 8T
t = 0319.5 Z
θ^{TSP} = 170.5 E
τ = 30.1°
ϕ^{TSP} = 49.8 N
H = 628 km
α^{PL} = 87.4°

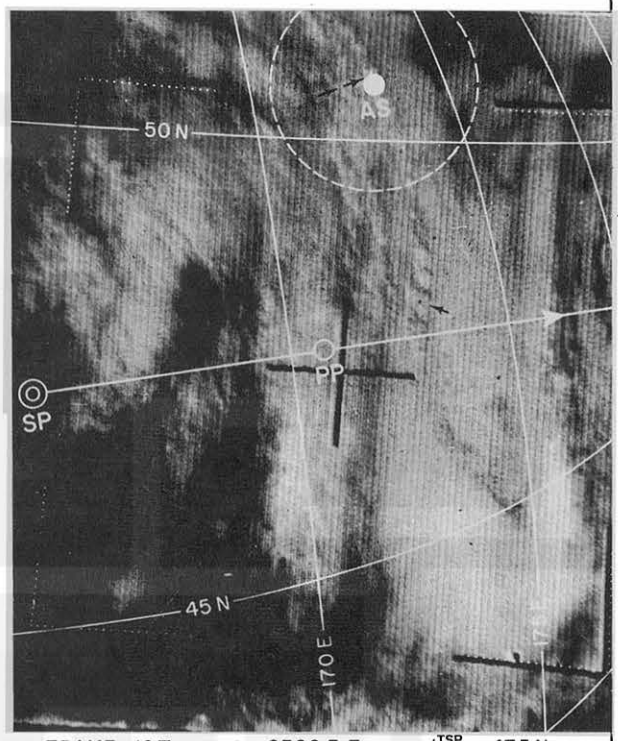

FRAME 10T
t = 0320.5 Z
θ^{TSP} = 166.3 E
τ = 27.1°
ϕ^{TSP} = 47.5 N
H = 628 km
α^{PL} = 88.0°

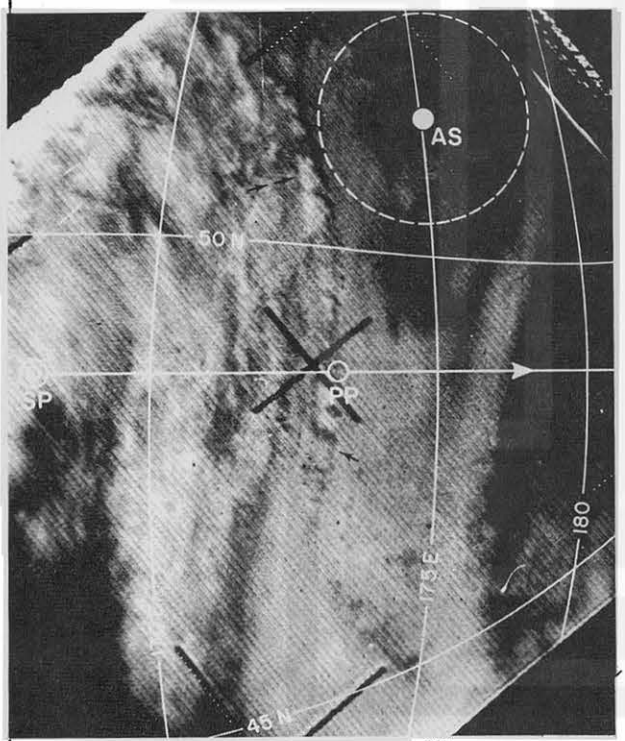

FRAME 9T
t = 0320.0 Z
θ^{TSP} = 168.3 E
τ = 28.6°
ϕ^{TSP} = 48.7 N
H = 628 km
α^{PL} = 87.4°

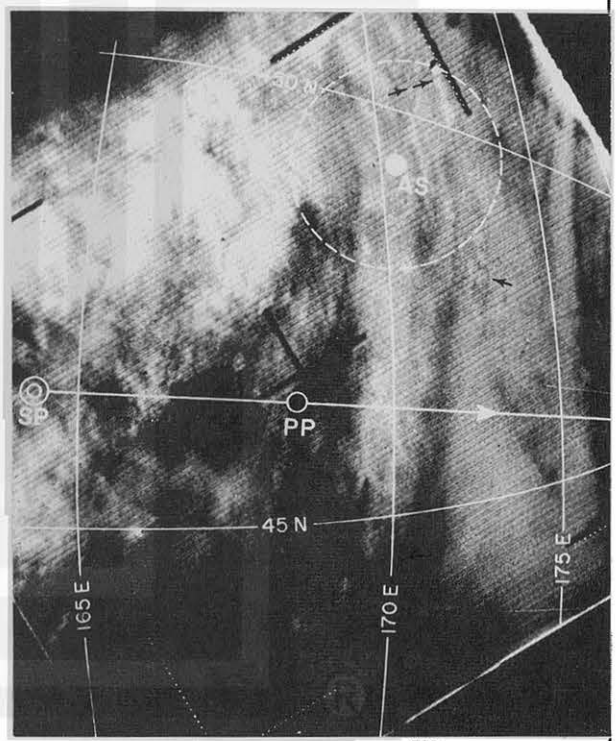

FRAME 11T
t = 0321.0 Z
θ^{TSP} = 164.3 E
τ = 25.6°
ϕ^{TSP} = 46.3 N
H = 628 km
α^{PL} = 88.8°

SMRP, University of Chicago

Qa 1

CLOUD PHOTOGRAPHS JAN 14, 1964

TIROS VII
A/O 3085 R/O 3085
TAPE CAMERA 2

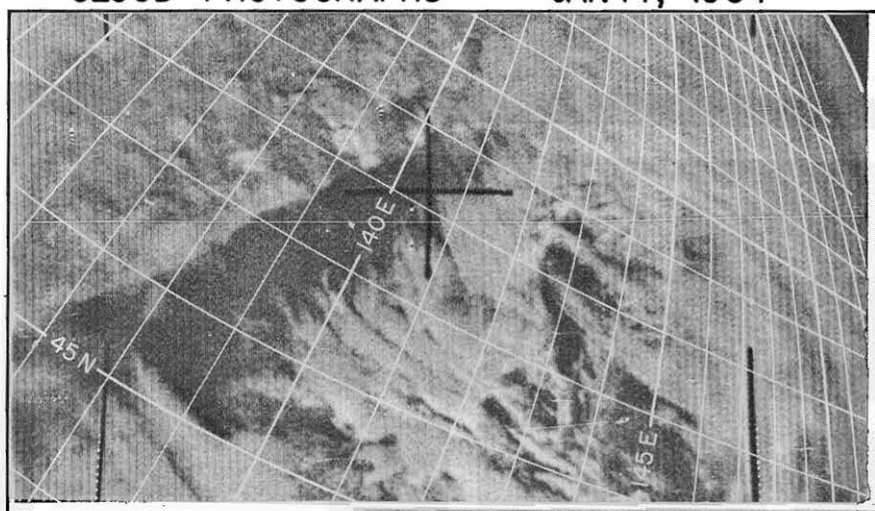

FRAME 6
TIME 0226.0 Z
ϕ^{TSP} = 44.2 N
θ^{TSP} = 139.5 E
H = 642 km
τ = 34.0°
α^{PL} = 2.6°

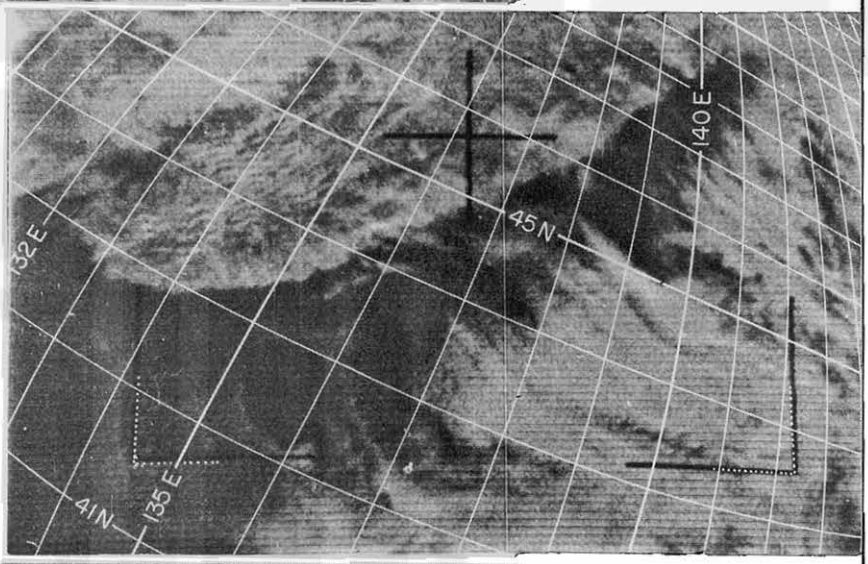

FRAME 8
TIME 0225.0 Z
ϕ^{TSP} = 46.1 N
θ^{TSP} = 136.1 E
H = 642 km
τ = 31.5°
α^{PL} = 355.9°

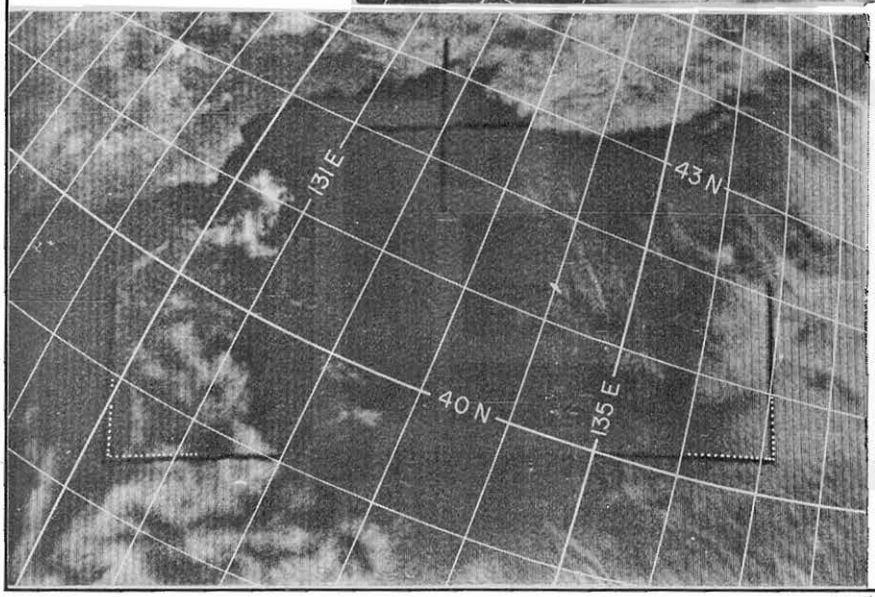

FRAME 10
TIME 0224.0 Z
ϕ^{TSP} = 39.0 N
θ^{TSP} = 133.0 E
H = 641 km
τ = 29.2°
α^{PL} = 348.9°

SMRP, University of Chicago

CLOUD CHART 0224 - 0226 Z JAN 14, 1964 Qa 2

SMRP, University of Chicago

Qa 3

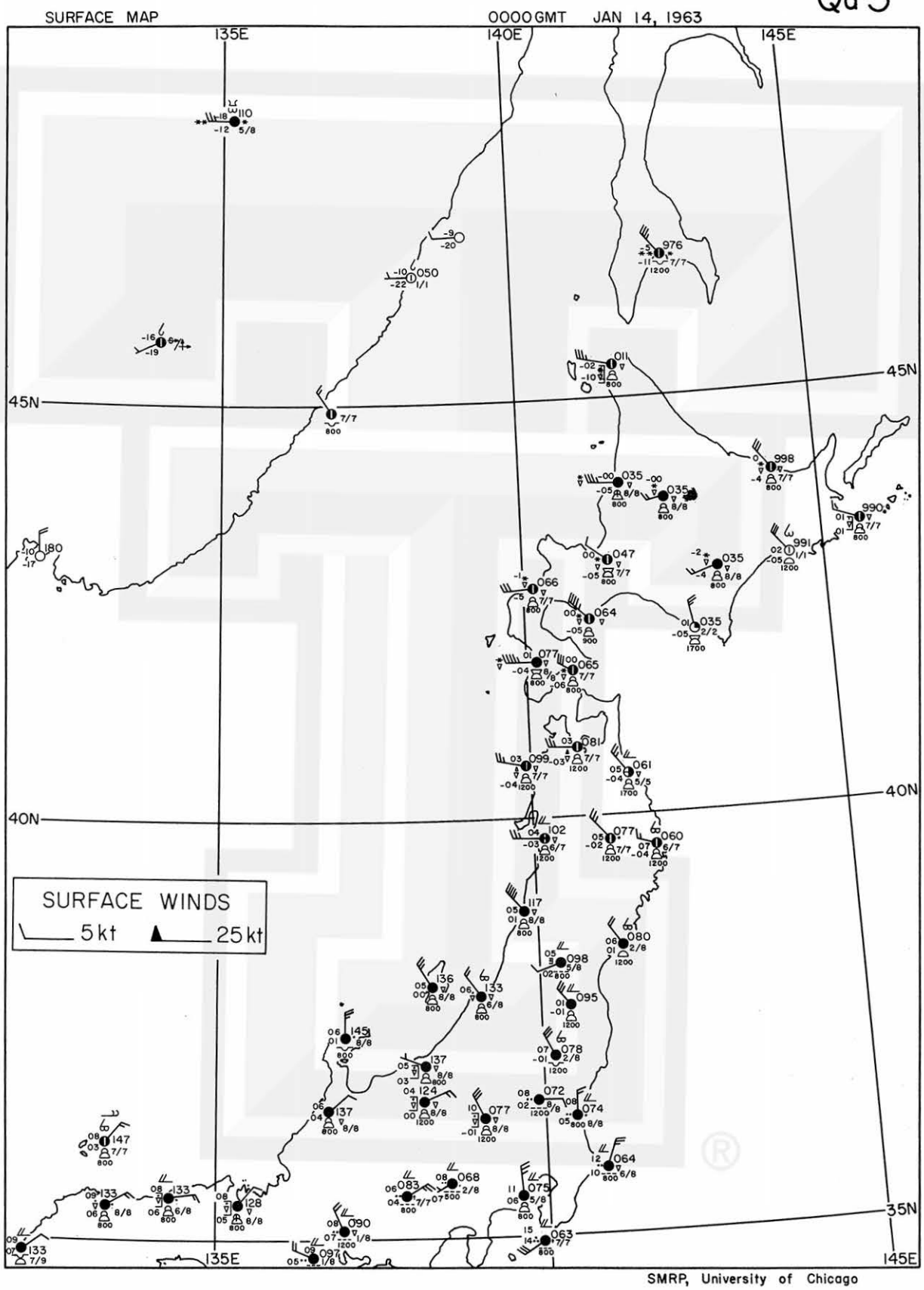
SURFACE MAP
0000 GMT JAN 14, 1963
135E
140E
145E
45N
40N
35N
SURFACE WINDS
5 kt
25 kt
SMRP, University of Chicago

SURFACE ISOBARS & ISOTHERMS 0000 GMT JAN 14, 1964 Qa 4

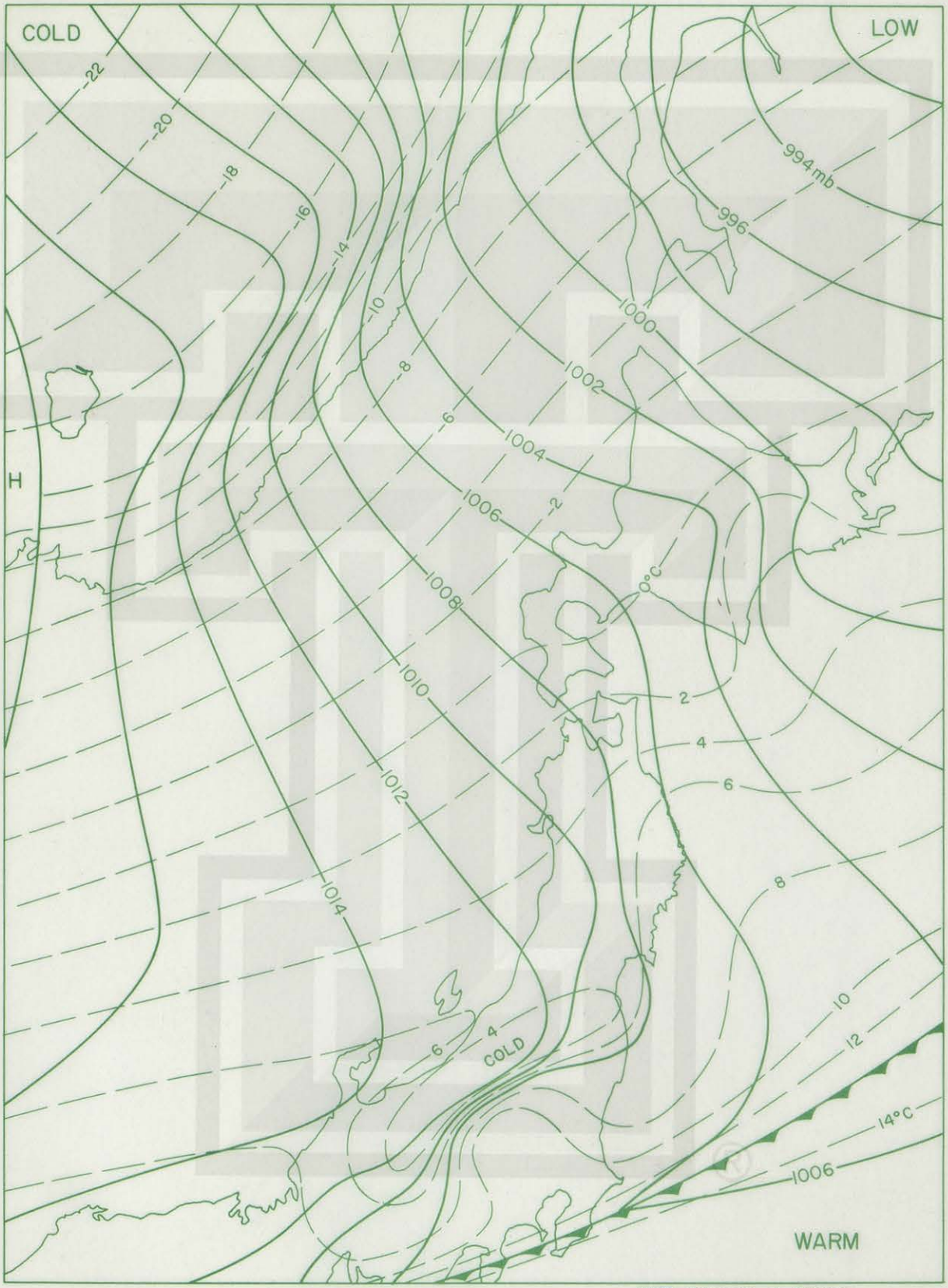

SMRP, University of Chicago

850 MB CHART 0000 GMT JAN 14, 1964 Qa5

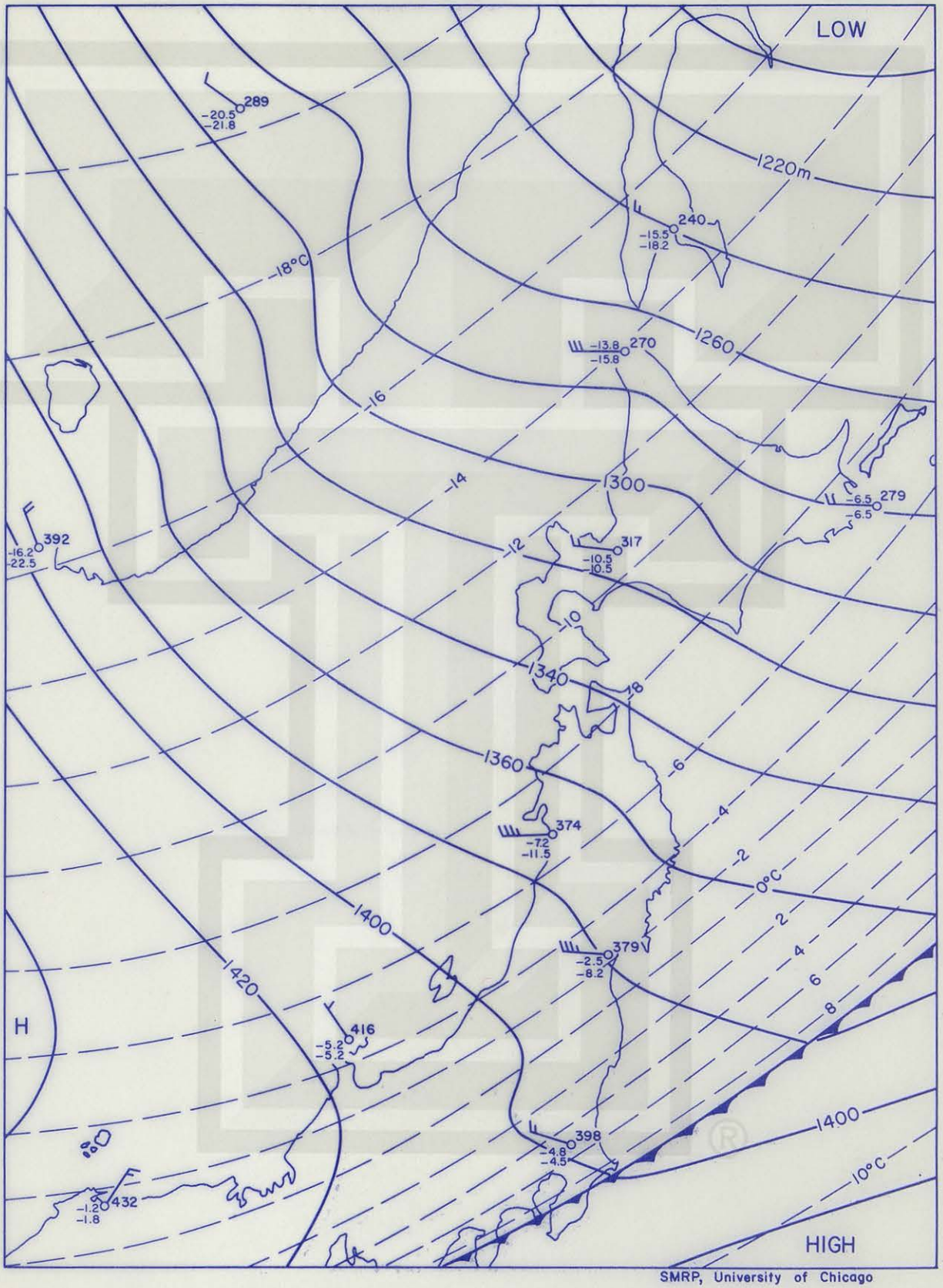

SMRP, University of Chicago

700 MB CHART 0000 GMT JAN 14, 1964 Qa 6

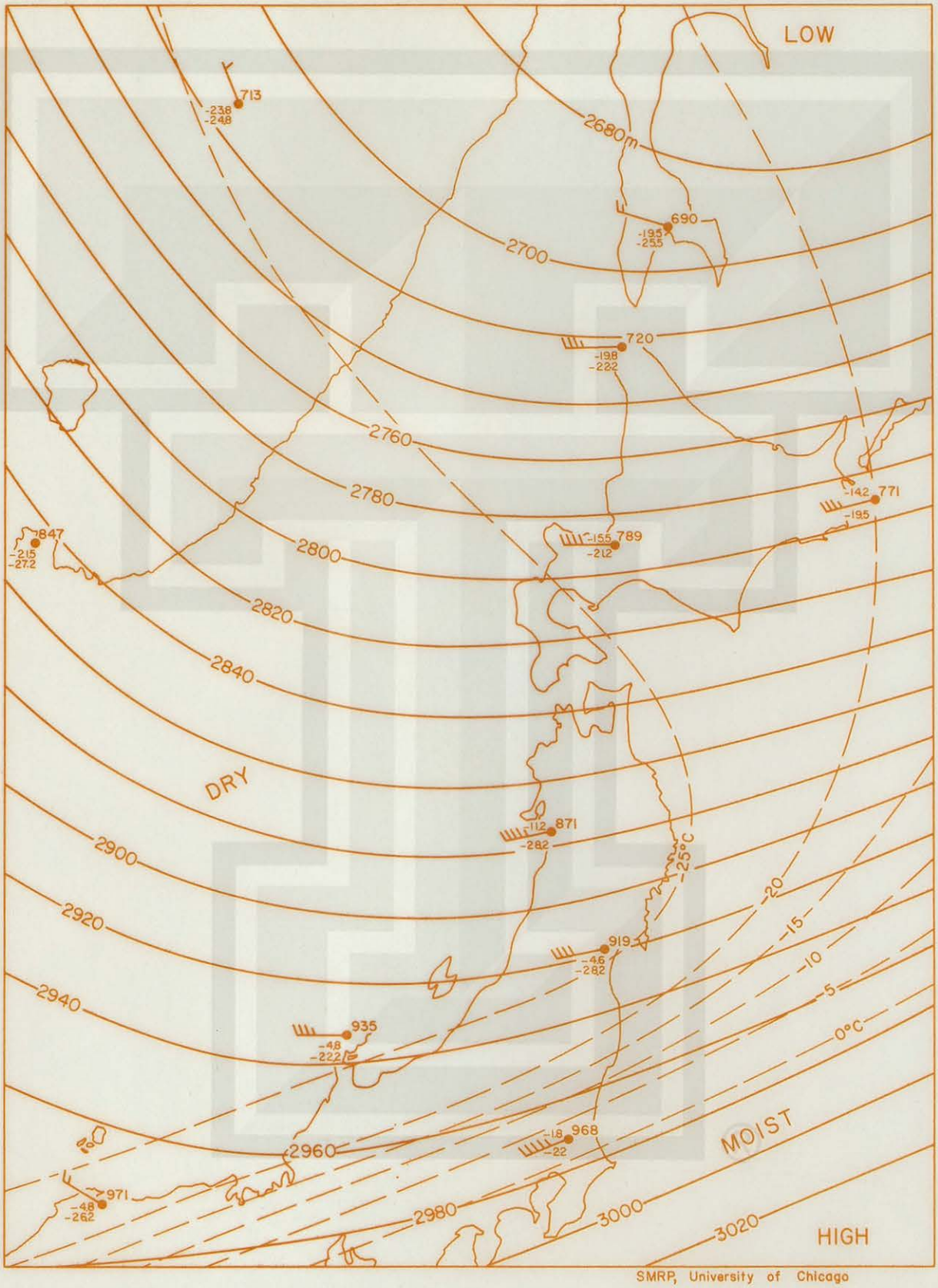

SMRP, University of Chicago

Qa 7

SMRP, University of Chicago

Qb1

CLOUD PHOTOGRAPHS JAN 20, 1964

TIROS VII A/O 3172 R/O 3172

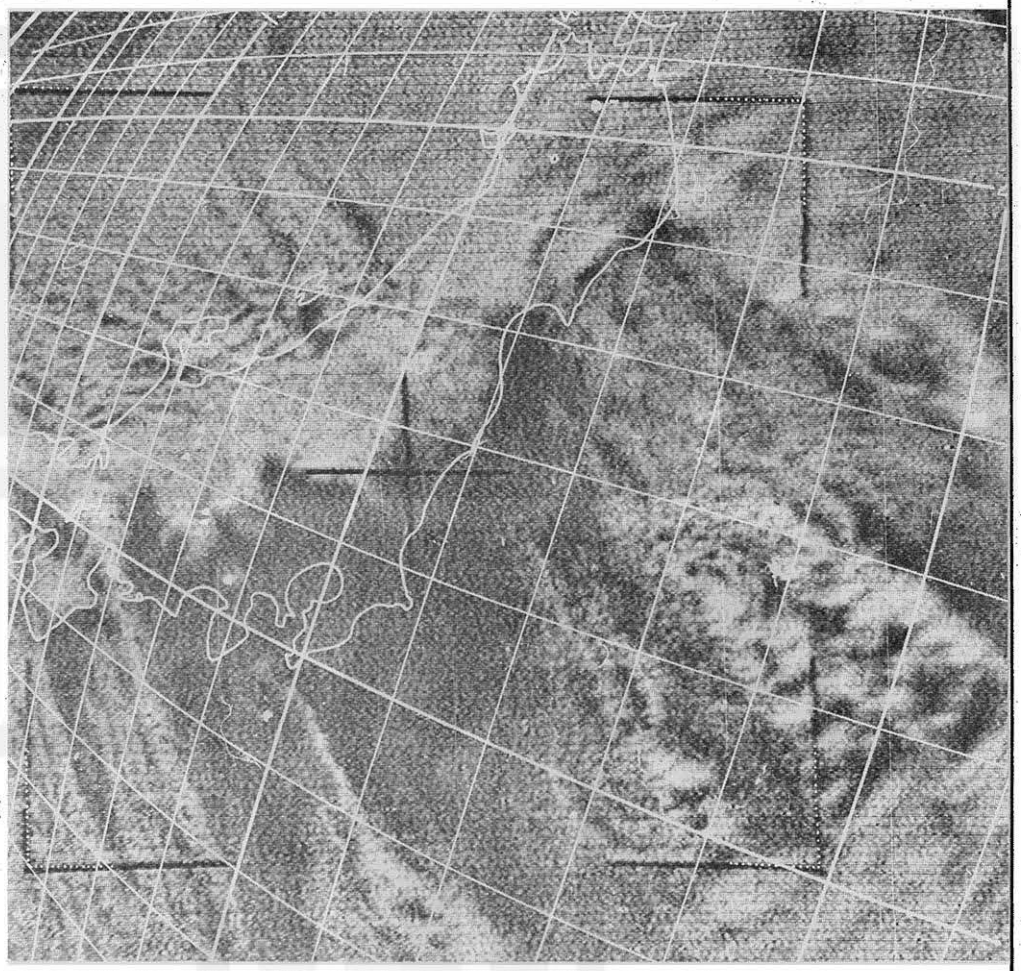

FRAME 14
t = 2337.5 Z
ϕ^{TSP} = 36.7 N
θ^{TSP} = 144.2 E
H = 639 km
τ = 27.9°
α^{PL} = 270.9°

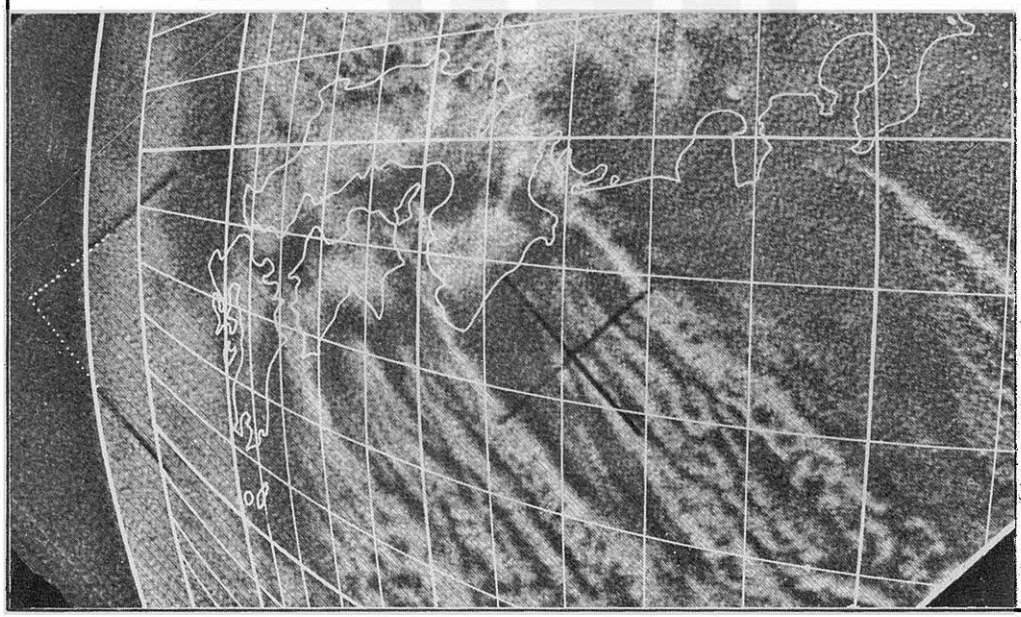

FRAME 16
t = 2336.5 Z
ϕ^{TSP} = 33.9 N
θ^{TSP} = 141.6 E
H = 638 km
τ = 30.3°
α^{PL} = 264.4°

SMRP, University of Chicago

Qb2

CLOUD TRANSFER MAP

2335.5—2336.5 GMT JAN 19, 1964

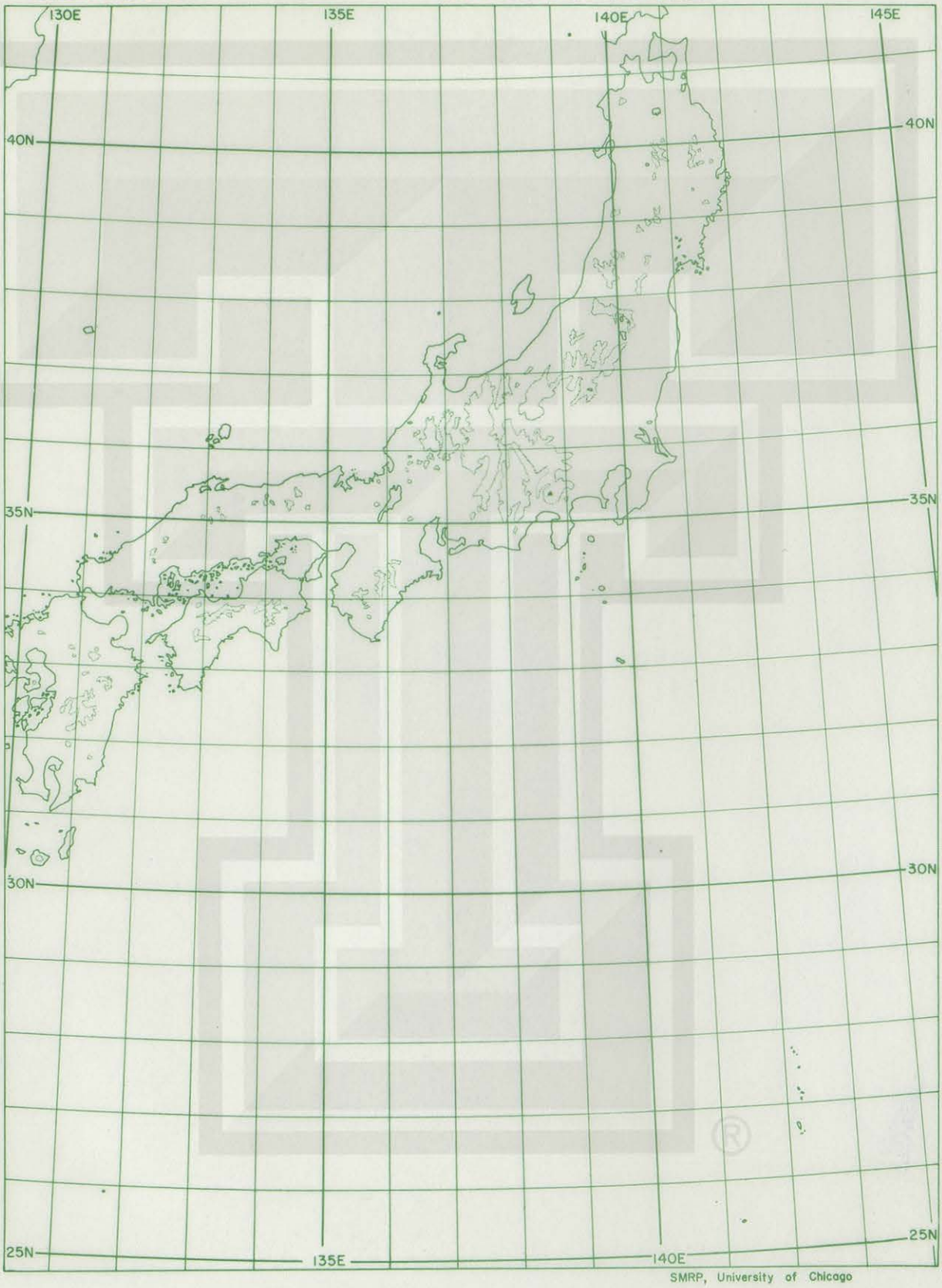

SMRP, University of Chicago

CLOUD CHART 2335-2337 Z JAN 20, 1964

Qb 3

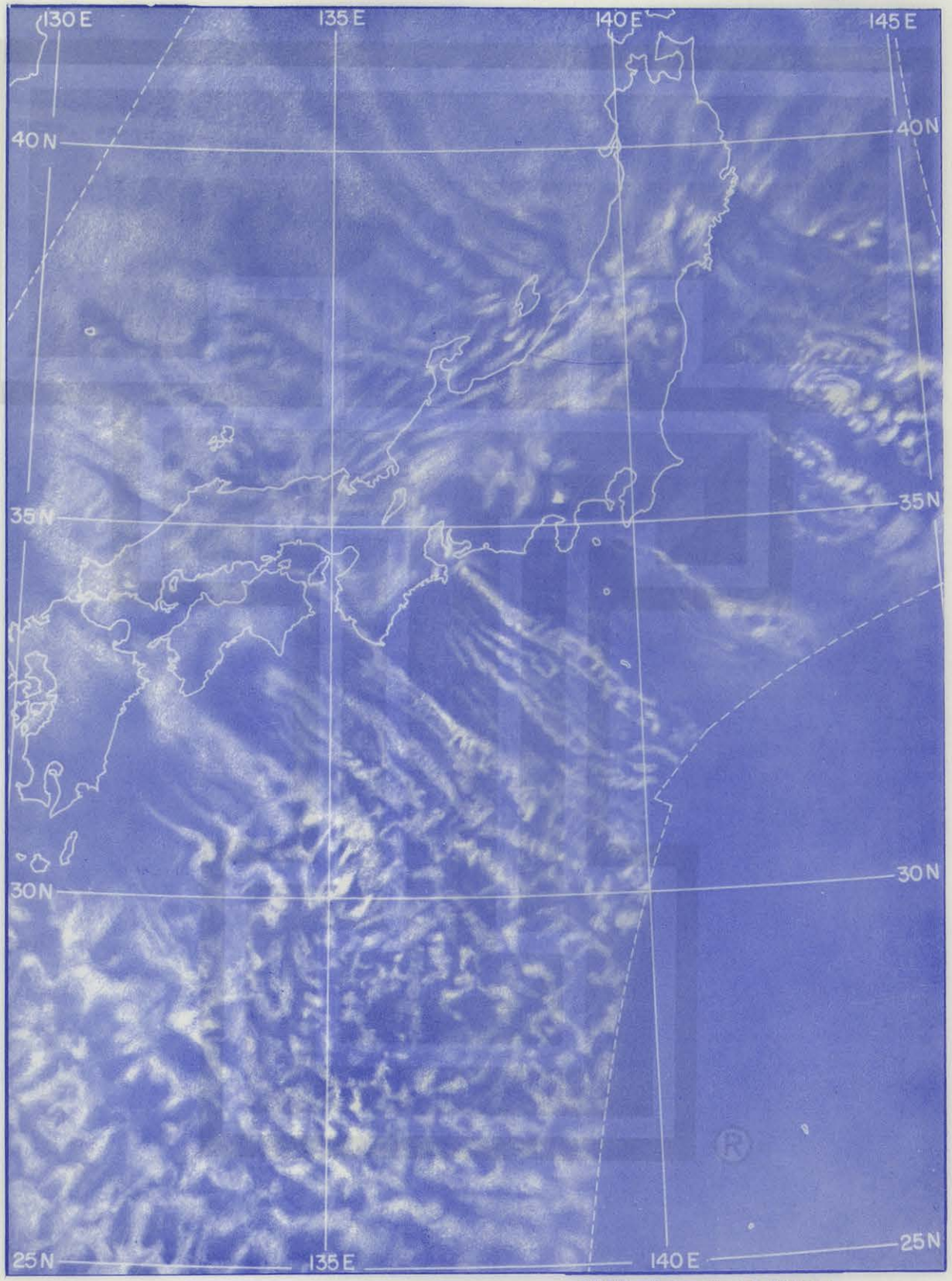

SMRP, University of Chicago

Qb 4

PLOTTED SURFACE DATA

0000 GMT JAN 20, 1964

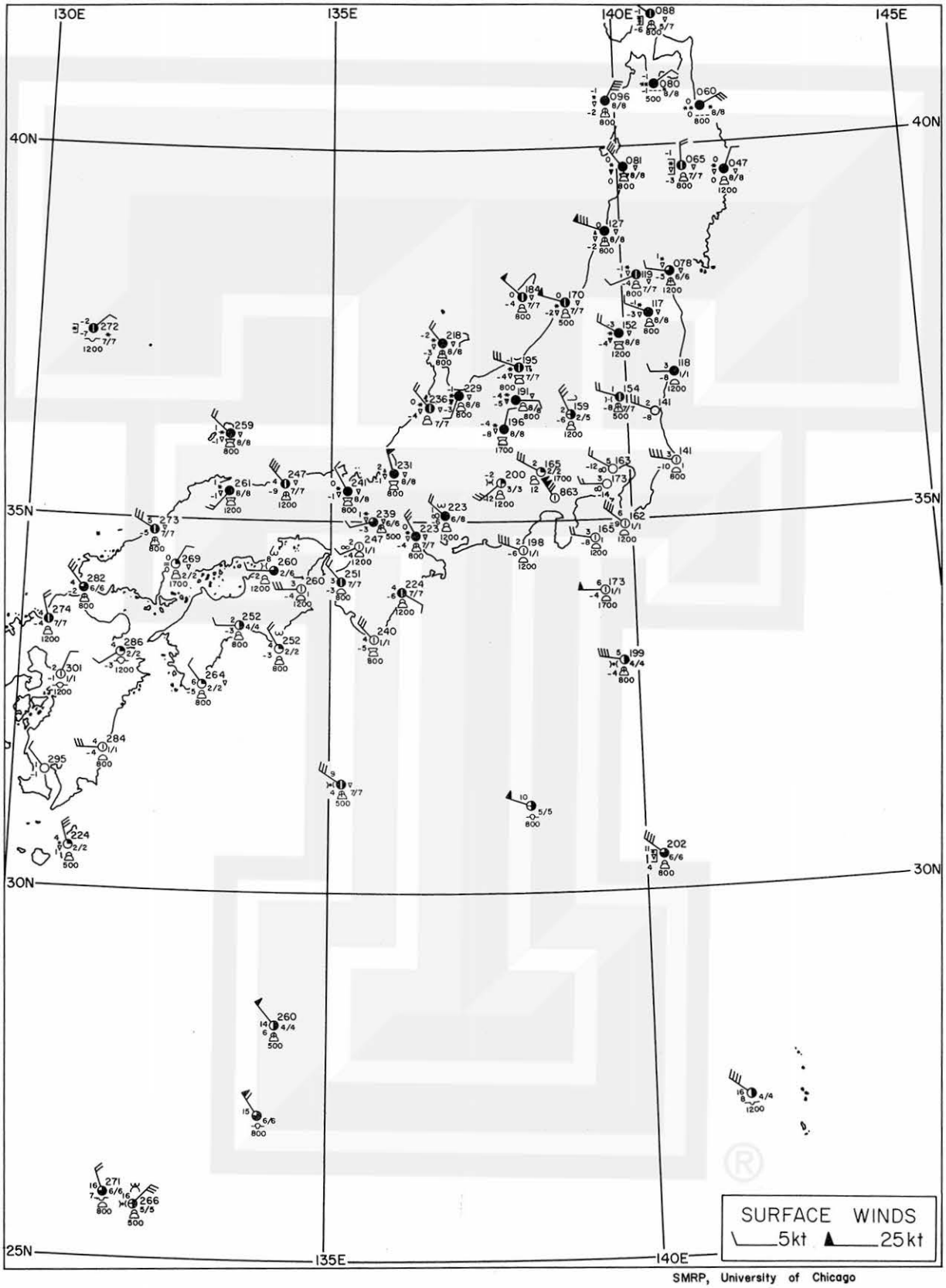

SMRP, University of Chicago

Qb 5

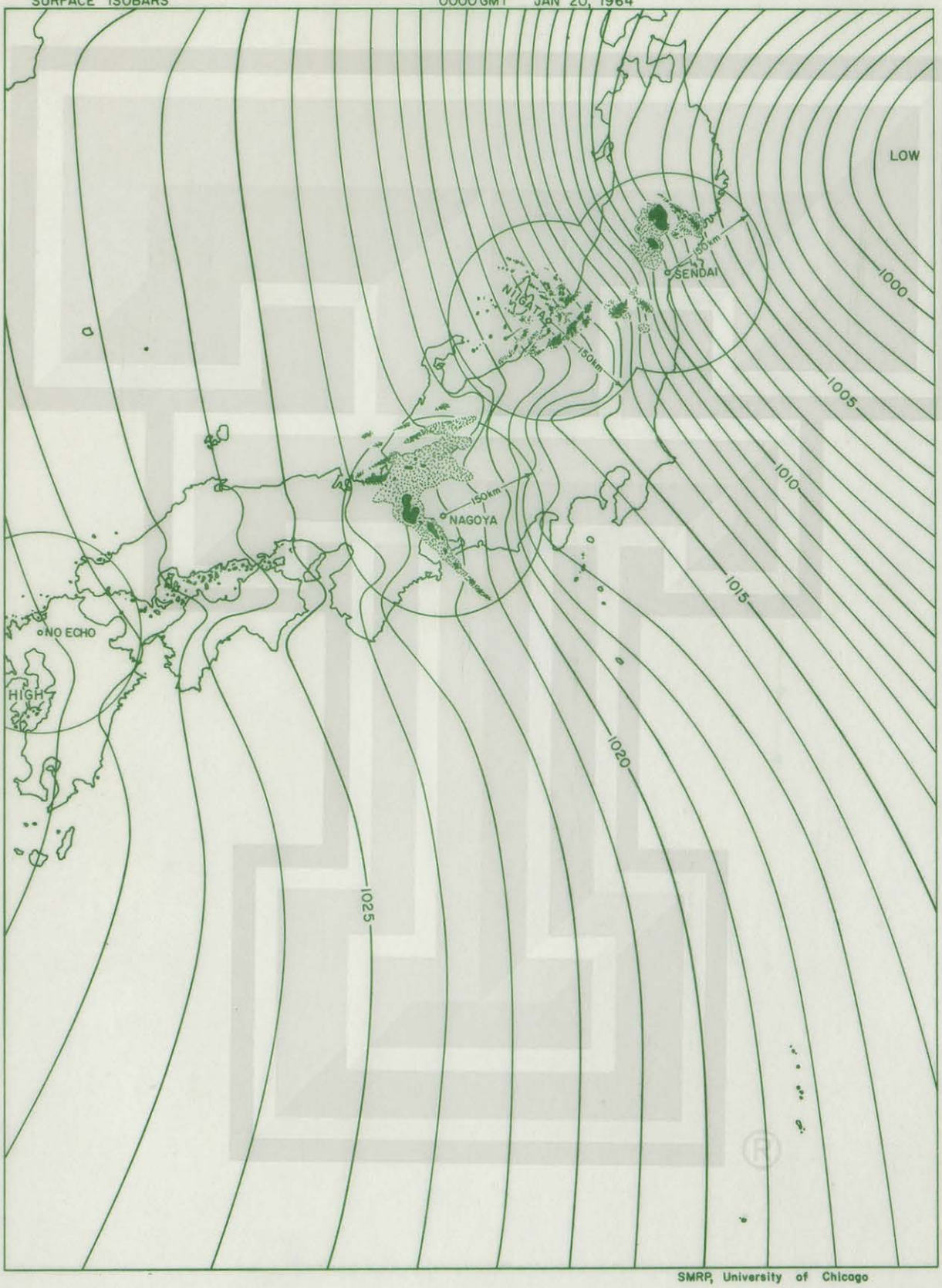

SMRP, University of Chicago

ISOTHERMS 0000 GMT JAN 20, 1964 Qb6

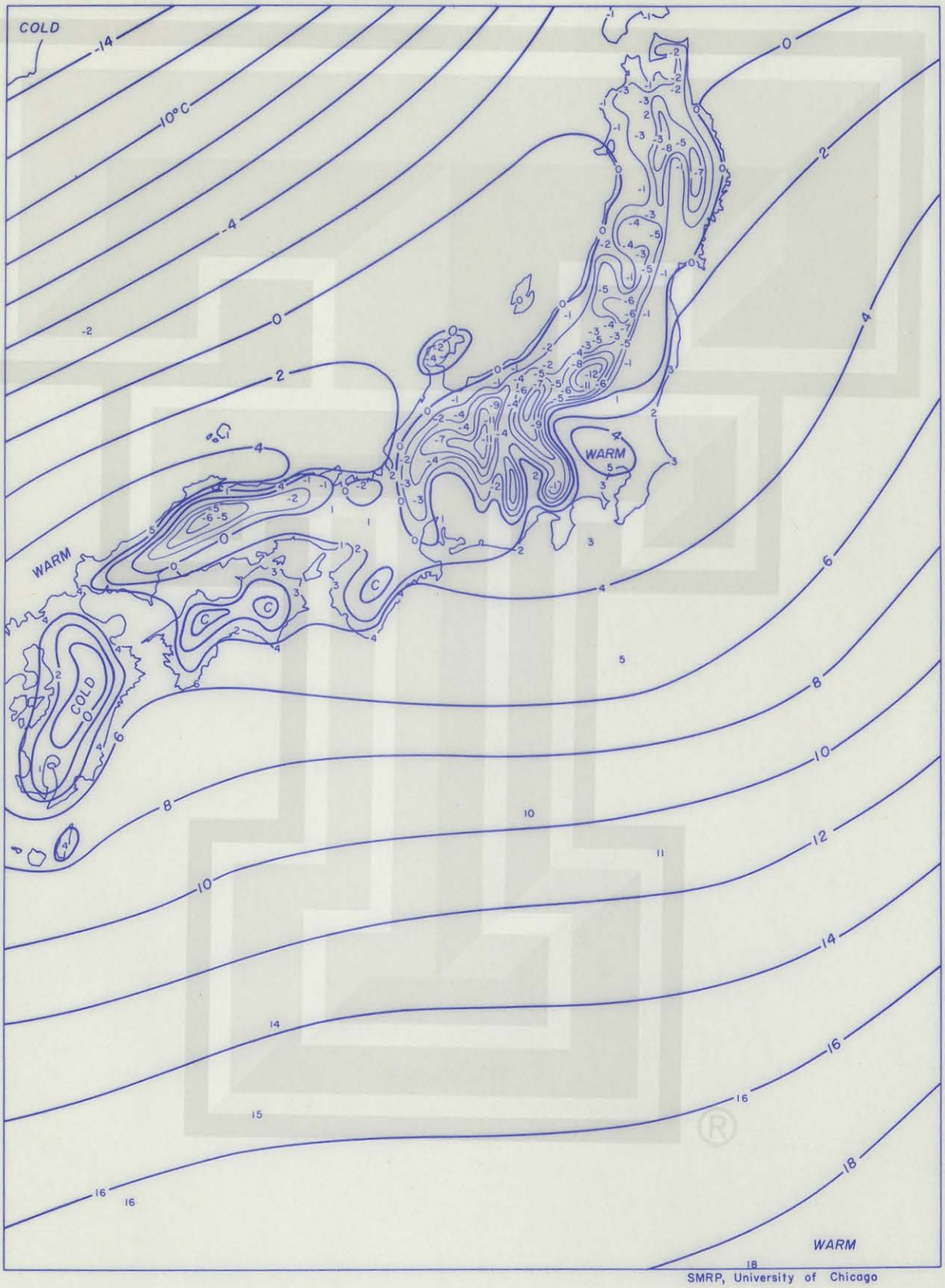

SMRP, University of Chicago

Qb7

ISODROSOTHERMS 0000 GMT JAN. 20, 1964

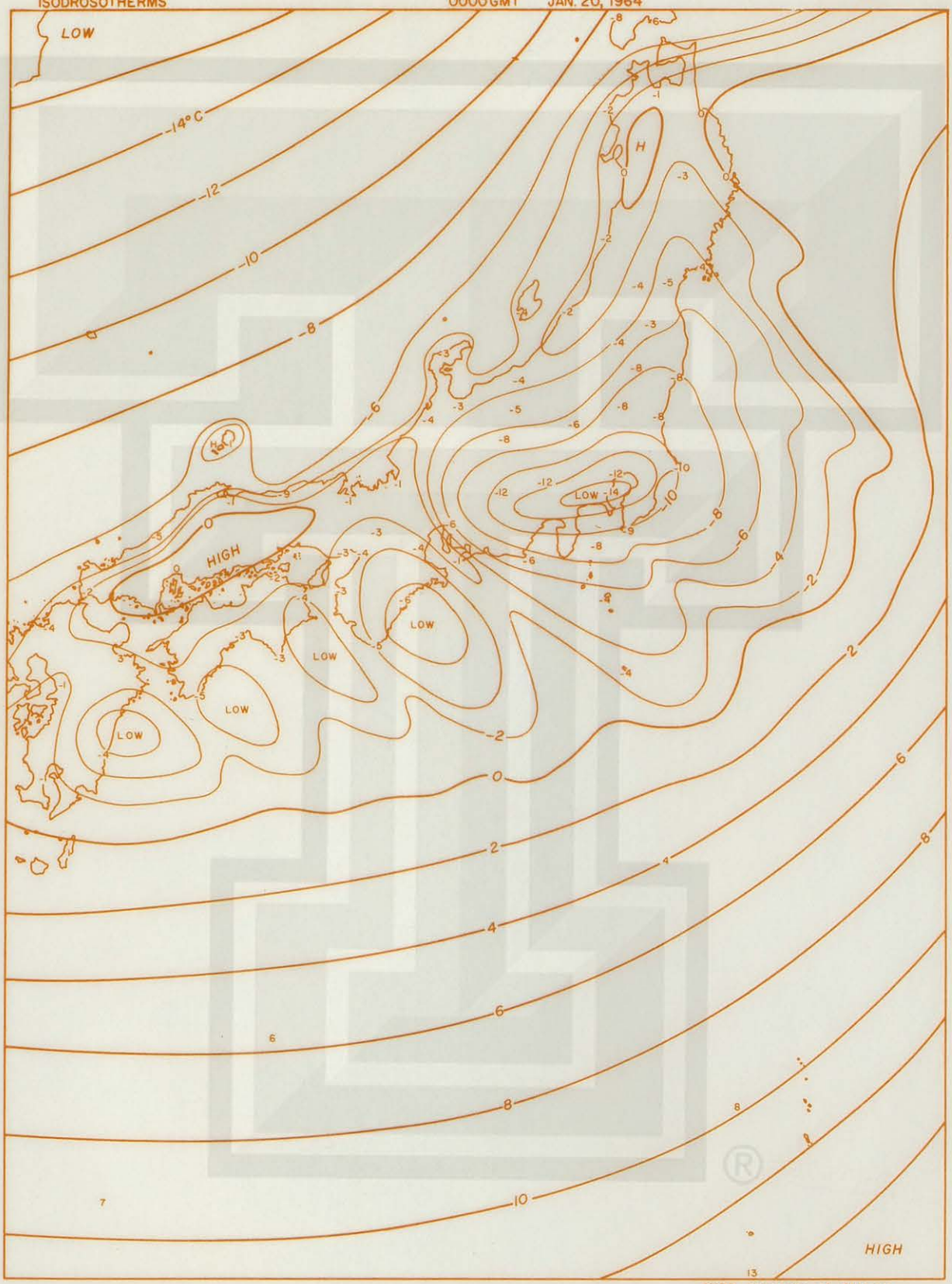

SMRP, University of Chicago

Qb 8

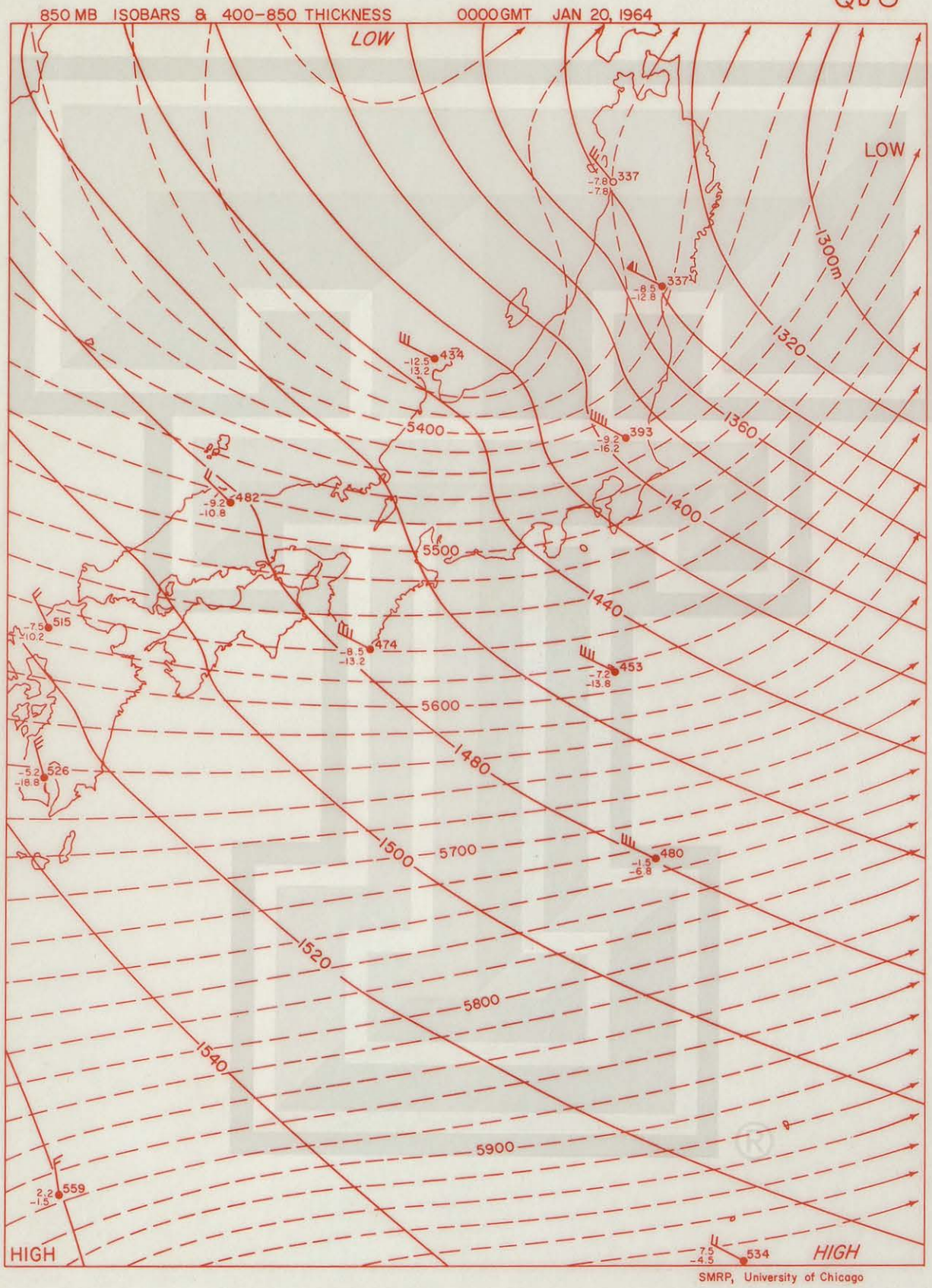

SMRP, University of Chicago

Qb 9

SNOW DEPTH AND WEATHER 0000 GMT JAN 20, 1964

SMRP, University of Chicago

RADIATION MAP 2335-2336Z JAN 19, 1964 Qb 10

SMRP, University of Chicago

Qb 11

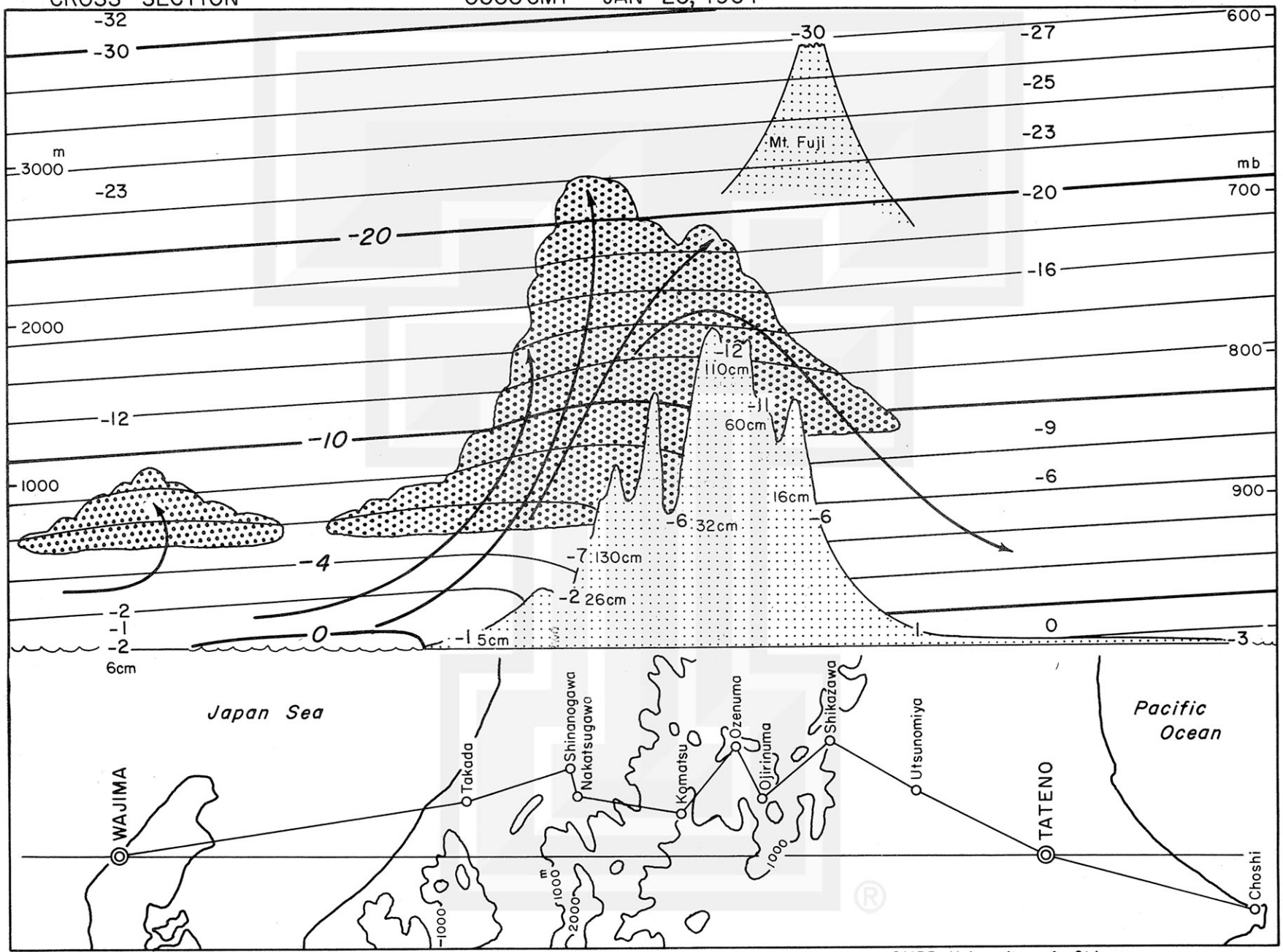

SMRP, University of Chicago